

**Linking Porphyry Deposit Geology to Geophysics via
Physical Properties:
Adding Value to Geoscience BC Geophysical Data**

D.E. Mitchinson, R.J. Enkin, and C.J.R. Hart

December, 2013

Geoscience BC Report 2013-14

Table of Contents

1. Introduction.....	6
1.1. Objectives	6
1.2. Location and General Geologic Setting.....	7
1.3. Report Content and Organization	9
2. Methods and Data	9
2.1. Physical Rock Properties and Measurement Methods.....	9
2.2. Mineral Abundance Analyses	13
2.3. Geophysical Survey Data.....	14
3. Summary of Findings.....	14
4. Acknowledgements.....	18
5. References.....	19
Appendix 1. Mount Milligan	22
1.1. Regional Geology and Magnetic Data.....	22
1.1.1. Regional Geologic Setting	22
1.1.2. Regional Magnetic Data.....	22
1.2. Deposit Geology	25
1.3. Physical Properties of Rocks from the Mount Milligan Deposit	27
1.3.1. Sample Suite	27
1.3.2. Magnetic Susceptibility and Deposit Scale Magnetic Data	27
1.3.3. Density and Porosity	29
1.3.4. Resistivity Data and Deposit Scale Conductivity	31
1.4. References.....	36
Appendix 2. Endako.....	38
2.1. Regional Geology and Magnetic Data.....	38
2.1.1. Regional Geologic Setting	38

2.1.2. Regional Magnetic Data.....	41
2.2. Deposit Geology	41
2.3. Physical Properties of Rocks from the Endako Deposit	43
2.3.1. Sample Suite	43
2.3.2. Magnetic Susceptibility and Deposit Scale Magnetic Data	43
2.3.3. Density and Porosity	45
2.3.4. Resistivity Data and Deposit Scale Conductivity Data.....	47
2.4. References.....	51
Appendix 3. Huckleberry.....	52
3.1. Regional Geology and Magnetic Data.....	52
3.1.1. Regional Geologic Setting.....	52
3.1.2. Regional Magnetic Data.....	54
3.2. Deposit Geology	54
3.3. Physical Properties of Rocks from the Huckleberry Deposit.....	56
3.3.1. Sample Suite	56
3.3.2. Magnetic Susceptibility and Deposit Scale Magnetic Data	57
3.3.3. Density and Porosity	59
3.3.4. Resistivity Data and Deposit Scale Conductivity	60
3.4. References.....	63
Appendix 4. Bell.....	65
4.1. Regional Geology and Magnetic Data.....	65
4.1.1. Regional Geologic Setting.....	65
4.1.2. Regional Magnetic Data.....	65
4.2. Deposit Geology	65
4.2. Physical Properties of Rocks from the Bell Deposit.....	70
4.2.1. Sample Suite	70

4.2.2. Magnetic Susceptibility and Deposit Scale Magnetic Data	71
4.2.3. Density and Porosity	72
4.2.4. Resistivity Data and Deposit Scale Conductivity Data	74
4.4. References	78
Appendix 5. Granisle	79
5.1. Regional Geology and Magnetic Data	79
5.1.1. Regional Geologic Setting	79
5.1.2. Regional Magnetic Data	82
5.2. Deposit Geology	82
5.2. Physical Properties of Rocks from the Granisle Deposit	83
5.2.1. Sample Suite	83
5.2.2. Magnetic Susceptibility and Deposit Scale Magnetic Data	83
5.2.3. Density and Porosity	85
5.2.4. Resistivity Data and Deposit Scale Conductivity	86
5.4. References	89
Appendix 6. Morrison	91
6.1. Regional Geology and Magnetic Data	91
6.1.1. Regional Geologic Setting	91
6.1.2. Regional Magnetic Data	94
6.2. Deposit Geology	94
6.2. Physical Properties of Rocks from the Morrison Deposit	95
6.2.1. Sample Suite	95
6.2.2. Magnetic Susceptibility and Deposit Scale Magnetic Data	96
6.2.3. Density and Porosity	97
6.2.4. Resistivity Data and Deposit Scale Conductivity	98
6.4. References	102

Appendix 7. Deposit-scale Relationships between Metallic Minerals and Electrical Properties	104
7.1. Controls on Electrical Resistivity/Conductivity - Sulphide Abundance vs. Porosity	104
7.2. Controls on Electrical Resistivity/Conductivity - Sulphide Distribution.....	108
7.3. Controls on Chargeability - Sulphide Abundance and Distribution	110
7.4. Summary of Resistivity and Chargeability Trends for BC Porphyry Case Study Sites.....	114
7.5. References.....	114
Appendix 8. Physical Property Data.....	116
Appendix 9. XRD Mineral Data	116
Appendix 10. Geochemistry	116

1. Introduction

In an effort to gain insight into subsurface geology, and to stimulate mineral exploration in till-covered regions of British Columbia, Geoscience BC carried out a series of regional and local magnetic and electromagnetic geophysical surveys in collaboration with the mineral exploration industry. As part of the QUEST and QUEST-West project geophysical initiatives (Kowalczyk, 2009), localized geophysical surveys focused on six known porphyry deposits to attempt to identify characteristic geophysical footprints for these economically important deposit types. The deposits chosen for investigation include Mount Milligan, Endako, Huckleberry, Bell, Granisle, and Morrison (Figure 1).

Geophysical response is linked to the physical properties of the rocks at and within the Earth's subsurface. This report summarizes the results of a study initiated to investigate physical rock properties of the hosting and mineralized rocks associated with the porphyry deposits targeted for geophysical surveys as part of the QUEST and QUEST-West projects. This research was conducted as part of a Geoscience BC-supported post-doctoral study at the University of British Columbia's Mineral Deposit Research Unit (MDRU). The resulting physical property data compilation has obvious implications for improving interpretations of geophysical data from porphyry deposits. This work will additionally serve to enhance geophysics-based mineral exploration in several other ways. Understanding how and why physical rock properties vary within the Earth's subsurface ensures that appropriate geophysical exploration methods can be chosen, and allows for more efficient and effective surveys to be designed. Physical property knowledge is also integral to geophysical modeling; measured data or values estimated based on geological understanding can be used to constrain forward and inversion models. Geophysical inversion modelling has become an increasingly common tool used within the mineral industry for generating 3D physical property models of the Earth to identify buried mineralization (Oldenburg and Pratt, 2007). These models are significantly improved through use of physical property constraints (Farquharson, et al., 2008, Fullagar et al., 2008, Williams, 2008).

1.1. Objectives

This report presents physical rock property data from a suite of six BC porphyry deposits, and discusses observed trends within the datasets in the context of available geophysical data, and mapped geology.

The primary objectives of the research were to:

- identify physical property data distributions and ranges for characteristic host rocks and their altered equivalents from the six porphyry deposit sites investigated;

- understand the causes of physical property variations by identifying correlations between physical properties and ore and alteration mineralogy, and by comparing data trends between different physical property datasets; and
- provide a synopsis of physical property criteria defining hydrothermally altered or mineralized rocks in BC porphyry settings which can be used for ranking mineral exploration targets, and minimizing exploration risk.

1.2. Location and General Geologic Setting

Regional airborne magnetic, electromagnetic (Geotech Limited, 2008, and Aeroquest Surveys, 2009), and gravity (Sander Geophysics Ltd., 2008a, 2008b) surveys were carried out over two areas as part of Geoscience BC's QUEST and QUEST-West projects (Figure 1). The QUEST project area focuses on the central Quesnel Terrane, a Late Triassic to Early Jurassic volcano-sedimentary arc. Rocks of the Quesnel Terrane are known to host economically important Cu-Au alkalic porphyry deposits. The QUEST-West project comprises a large area west of and adjacent to the QUEST project block. The QUEST-West block encompasses mainly Jurassic and Cretaceous volcanic and sedimentary rocks of the Stikine Terrane, and younger Eocene volcanic rocks. Like the QUEST project area, the region is economically prospective, with numerous known porphyry and epithermal deposits. Large expanses of both the QUEST and QUEST-West project areas are covered by glacial till, making exploration challenging in these regions.

Porphyry deposits surveyed during the QUEST and QUEST-West projects include Mount Milligan, Endako, Huckleberry, Bell, Granisle, and Morrison. Airborne magnetic and electromagnetic surveys (VTEM or AeroTEM) were conducted over each of these deposits. Additionally, a ZTEM (Z-axis tipper electromagnetic) survey was completed over the Mount Milligan deposit as a joint initiative between Geoscience BC and Terrane Metals Corp.

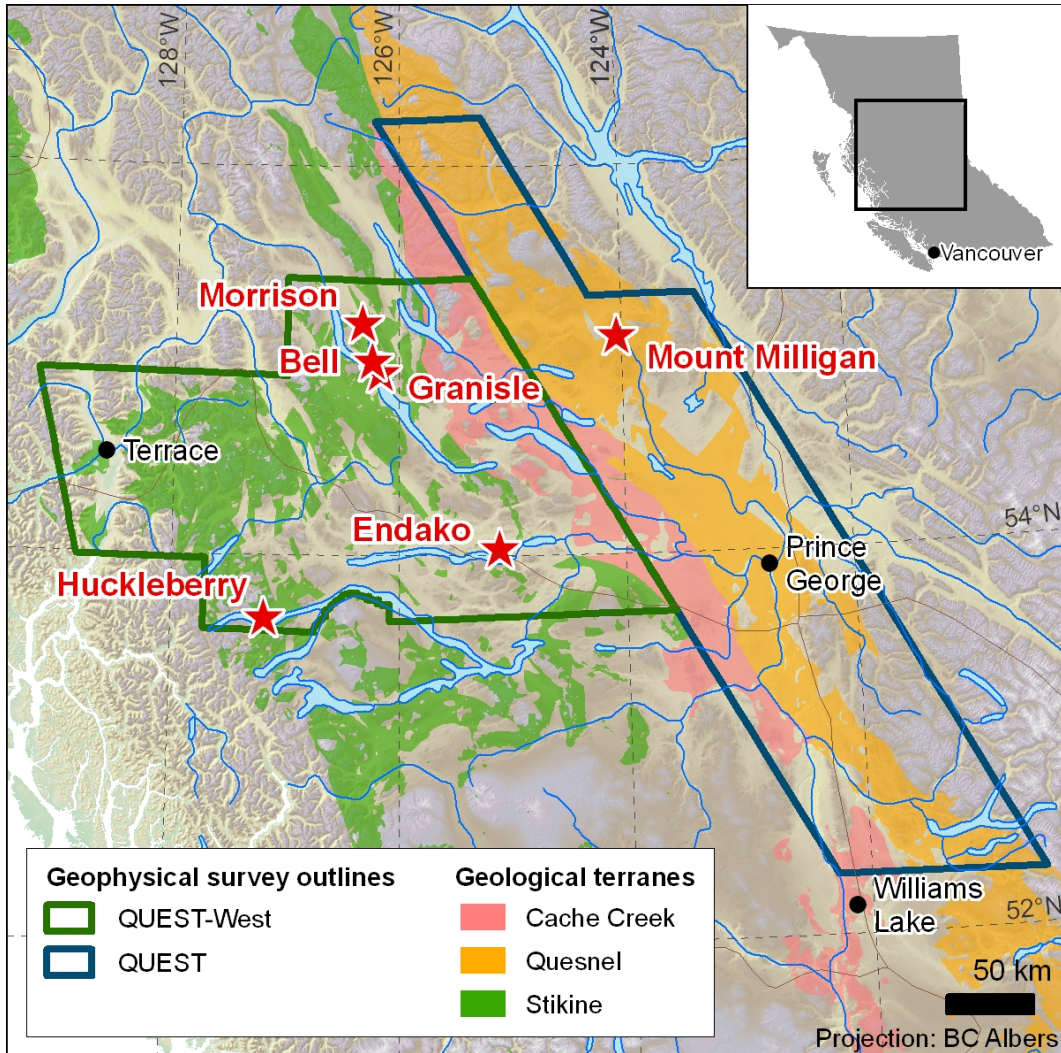


Figure 1. Areas covered by the Geoscience BC QUEST and QUEST-West airborne electromagnetic (EM) and magnetic geophysical surveys of central British Columbia. Locations of detailed infill surveys completed over six known porphyry deposits (the Mount Milligan, Endako, Huckleberry, Granisle, Bell and Morrison deposits are indicated). Base map data from Natural Resources Canada (1999), and digital elevation from GeoBase® (2004). Geology and deposit locations are from Massey et al. (2005) and MINFILE (BC Geological Survey, 2013), respectively.

A range of host rocks and alteration mineral assemblages characterize the porphyry deposits studied as part of this project. The deposits examined belong to two porphyry subtypes and represent four magmatic episodes. The Mount Milligan deposit is an alkalic porphyry Cu-Au deposit that is spatially related to Early Jurassic quartz monzonitic plugs in Takla Group volcanic rocks of the Quesnel Terrane. Endako, Huckleberry, Morrison, Bell and Granisle are calc-alkalic porphyry deposits in the Stikine Terrane.

Endako is linked to Late Jurassic magmatism, Huckleberry to Cretaceous magmatism and Granisle, Bell and Morrison to Eocene magmatism.

1.3. Report Content and Organization

Following the Introductory and Methods sections of this report (Sections 1 and 2, respectively), the Summary of Findings (Section 3) presents general conclusions from this research and summarizes similarities and differences between physical rock property trends characterizing each of the six porphyry deposits investigated.

Physical property data and discussion of physical property trends identified for each of the six porphyry deposits are detailed in separate appendices (Appendices 1-6). For each deposit, background geology and regional-scale airborne magnetic data maps are presented to outline a regional context for the local-scale mineral deposit setting. This is followed by a brief discussion of the local-scale geology, with emphasis on porphyry deposit structure, alteration, and mineralization. Physical property data (magnetic susceptibility, density, porosity, and resistivity) are presented as histograms for the six porphyry deposits, the choice of data presentation chosen to show the full range of data as well as the population distribution. Physical property trends are discussed in light of petrographic and mineralogical assessments, and through various data plots highlighting relationships between different physical properties.

As conductivity and chargeability are considered to be properties that may be linked directly to porphyry sulphide mineralization, Appendix 7 examines in more detail relationships between electrical properties, sulphide minerals, and other physical properties at the sample scale.

Tables compiling physical rock property data, mineral data, and geochemical data are presented in digital Appendices 8-10.

2. Methods and Data

2.1. Physical Rock Properties and Measurement Methods

The physical properties focused on for this study include magnetic susceptibility, density, porosity, electrical resistivity, and chargeability. Physical rock properties are generally controlled by lithology, but more specifically by the modal mineralogy of the rocks, and by mineral and rock textures. The following briefly outlines the dominant mineral and textural controls on the various physical properties measured

during this study, and outlines the methods of measurement, which are also detailed in Enkin et al. (2012). Physical property measurements collected during this study are tabulated in Appendix 8.

Magnetic Susceptibility

Magnetic susceptibility is most strongly controlled by mineralogy, specifically by the presence and abundance of iron-oxide and sulphide minerals. Magnetite is the predominant magnetic mineral in rocks sampled for this study. Magnetic susceptibility is also controlled by the size, shape, and microstructure of magnetic mineral grains, as well as by interactions between grains (Clark et al, 1997).

Most magnetic susceptibility measurements reported here were measured at the Geological Survey of Canada - Pacific using the Sapphire SI2B susceptibility meter, which is accurate to 10^{-7} SI. Magnetic susceptibility measurements are made on 2.2 cm long cylindrical cores that are 2.5 cm in diameter, drilled from larger core samples or from hand samples. Some measurements from outcrop were made using the KT-9 Kappameter hand susceptibility meter. Susceptibility data herein are presented in SI units equivalent to (A/m)/(A/m).

Magnetic remanence was also measured at the GSC-Pacific laboratories. Natural remanent magnetization (NRM) was measured using the AGICO JR5-A spinner magnetometer. Samples were not oriented and only the vector magnitude is reported. The Koenigsberger ratio (K_N), the ratio of remanent magnetization to induced magnetization, is calculated according to the equation:

$$K_N = \text{NRM} / (H_0 \chi_0)$$

where $H_0 \chi_0$ represents the induced magnetization in the geomagnetic field, H_0 is the magnetic field strength, and χ_0 is magnetic susceptibility. If K_N is observed to be > 1 , then magnetic remanence may be a concern during magnetic interpretation and modeling since magnetic survey anomalies are dominated by the remanence rather than the magnetic susceptibility of the rock being measured. Although not discussed in detail in this report, remanence data are included in accompanying physical rock property data tables.

Density and Porosity

Rock density is controlled primarily by mineralogy and porosity. Igneous rock densities generally decrease with increasing SiO_2 content (Telford et al., 1990). In non-porous or low porosity igneous rocks, density is a function of the relative proportions of mafic (Fe-Mg rich) and felsic (Fe-Mg poor) silicate minerals (Johnson and Olhoeft, 1984). Sulphide and oxide minerals are the densest minerals, and, when in

abundance, these significantly increase the density of a rock. In high porosity rocks, sedimentary or brecciated rocks for example, rock mass is decreased, subsequently lowering density.

Densities were measured on the same 2.2 cm long core samples using the buoyancy or hydrostatic method and calculations outlined by Johnson and Olhoeft (1984). For this method, dry and saturated mass measurements were made on samples in air, and suspended in water, and from these values densities and porosities were derived. Grain density was first calculated using:

$$\rho_G = \rho_w * W1 / (W1 - W2)$$

where ρ_G is grain density, $W1$ is the mass of the dry sample in air, and $W2$ is the mass of the sample submerged in water. ρ_w is the density of the water, 1 g/cm^3 . This calculation only accounts for the solid rock volume.

Dry bulk density (ρ_B) is calculated using:

$$\rho_B = \rho_w * W1 / (W3 - W2)$$

where $W3$ is the mass of the saturated sample weighed in air. To account for porosity, and consider the total volume of the rock, saturated bulk density (ρ_S) is calculated:

$$\rho_S = \rho_w * W3 / (W3 - W2)$$

The density calculated in this manner is more representative of the density of a rock as it occurs in situ, likely containing some amount of pore space, filled with groundwater or other fluid.

The densities discussed and plotted in this report represent saturated bulk density. Density is reported in g/cm^3 .

The ratio of dry bulk density to grain density is used to calculate porosity:

$$\phi = 100 * (1 - \rho_B / \rho_G)$$

Porosity is reported as %.

Electrical Resistivity/Conductivity

Resistivity (in Ohm-m) is the measure of the resistance a circuit presents to an electrical current.

Conductivity (in Siemens per meter, or S/m) is calculated as the inverse of resistivity. Most silicate and carbonate minerals are poor to intermediate electrical conductors (Telford et al., 1990), meaning most homogenous, non-porous igneous and volcanic rocks will be resistive. Conductivity increases when conductive metallic sulphide or oxide minerals are present, and especially when they form connected

pathways throughout the rock. Porosity also leads to higher rock conductivities; when pore fluids containing dissolved solutes are present, ion flow increases, and conductivity will consequently increase (Archie's Law, Archie, 1942). Conductivity increases considerably with increasing water content of rocks (examples in Telford et al., 1990).

The method used at the Geological Survey of Canada - Pacific's Paleomagnetism and Petrophysics Laboratory to collect resistivity/conductivity data for rock samples is outlined in Enkin et al. (2012). Prior to taking resistivity measurements, the 2.5 x 2.2 cm cylindrical core samples were vacuum-impregnated with distilled water and soaked for a minimum of 24 hours. This soaking allows solutes to dissolve from pore walls generating a solution approximating original groundwater. The samples were then placed in a clamp, using graphite discs at each sample end, acting to separate the sample from the stainless steel electrodes. Complex electrical impedance data are collected on samples using a Solartron 1260 Impedance Spectrum Analyser, based on the method of Katsube (2001). Impedance was measured at 5 frequencies per decade from 1 MHz to 0.1 Hz. The DC resistance is the real impedance extrapolated to zero frequency after removing the low frequency response of the sample contacts. Resistivity is then calculated from the resistance multiplied by a geometric factor:

$$\rho_x = R_x \times K_G$$

Where ρ_x is resistivity in Ohm-m, R_x is the resistance in Ohm, and K_G is the geometric factor (sample cross-section area divided by length in m).

Chargeability

Induced polarization (IP) surveys measure electrical chargeability within the ground. During IP surveys, an electrical current is applied. Metallic particles blocking pore space will cause ions to build-up. The current is turned off and measurements are made to determine how quickly the charge dissipates within the ground or sample. Mineral deposits characterized by disseminated sulphide mineralization are ideally suited for application of IP methods since chargeability is strongly influenced by surface area with larger surface areas leading to stronger polarizations (Telford, 1990). The presence of clay minerals can also cause a rock to be chargeable since the surfaces of these minerals are negatively charged, attracting positive ions, leading to a charge build-up.

Sample chargeability was determined by first removing the low frequency sample holder impedance spectrum from that of the sample. Then the complex impedance curve is converted from frequency domain to time domain by Fourier transform and convolution to yield an IP step-response decay curve.

The area beneath the curve is integrated to find the change in voltage over the Newmont Standard time window (430-1100 ms). The values for chargeability reported on here are in milliseconds (ms).

Physical rock property data limitations

A cautionary note regarding the representativeness of sample scale physical property measurements is required. Most physical property measurements were made on relatively small samples ranging from approximately 500 ml hand samples collected from outcrop down to 2.2 x 2.5 cm cylindrical core samples. As such, the physical property values may not be representative of the same rocks *in situ* within the ground. It is well known that, especially for resistivity/conductivity data, measurements made at small scales do not reflect outcrop scale or larger measurements, which also detect large scale fractures, faults, or anisotropies.

Physical property measurements do not test the exact portion of the sample that was examined in thin section, or analyzed using X-ray diffraction (XRD). Thin sections sample only a small fraction of the rock, and mineral modes visually estimated in this manner may not accurately represent the entire sample. XRD analyses were in most cases performed on bulk rock pulp from material remaining after samples were cored, or from an adjacent piece of rock.

Additionally, some sample suites are small. Attempts were made to collect multiple samples of the same rock type or alteration assemblages, but this was not possible in all cases due to time constraints and limited accessibility to drill core. Although measurements included in the report are limited for particular sample suites, there is good control on the rock type and mineralogy composing the sample, making interpretation of the data possible.

2.2. Mineral Abundance Analyses

Thin sections were cut for representative samples from each porphyry deposit and were examined to document mineralogy and rock textures. Physical properties are especially influenced by magnetic, dense, and metallic minerals. For quantitative comparisons between mineralogy and physical property data, X-ray diffraction (XRD) methods were employed to collect mineral abundance data. The XRD Rietveld refinement method (Rietveld, 1967, 1969) estimates mineral abundances from pulverized whole rock material. Rietveld refinement methods as used to determine bulk rock mineralogy are described in Raudsepp and Pani (2003). Accuracy and precision of Rietveld refinement methods as used to derive mineral abundances in multi-phase samples were examined in Raudsepp et al. (1999). Relative

uncertainty on mineral abundance sits around 1% when minerals are of high modal abundance (making up 30-99% of the sample). Uncertainty increases as mineral abundance decreases. XRD analyses for this study were conducted by E. Pani at The University of British Columbia.

2.3. Geophysical Survey Data

Geophysical survey data displayed in this report are from the Natural Resources Canada Geoscience Data Repository (Natural Resources Canada, 2004), and from the QUEST and QUEST-West geophysical survey projects. QUEST project area VTEM (versatile time domain electromagnetic) and magnetic data were collected by Geotech Limited (Geotech Limited, 2008). A detailed ZTEM (Z-axis tipper electromagnetic) survey over the Mount Milligan deposit was also carried out by Geotech (Geotech Limited, 2009). QUEST-West electromagnetic and magnetic data were collected by Aeroquest Limited (Aeroquest Surveys, 2009). Aeroquest Ltd. carried out detailed AeroTEM and magnetic surveys over the Endako, Huckleberry, Bell, Granisle, and Morrison deposits. For both QUEST and QUEST-West projects, regional airborne EM and magnetic survey data were acquired at line-spacings of 4 km. Detailed EM and magnetic surveys had line spacings of 200 m.

3. Summary of Findings

Table 1 schematically summarizes physical rock property contrasts between the six investigated central British Columbia porphyry deposits.

The individual BC porphyries studied have features typical of calc-alkalic and alkalic porphyry deposits (Figure 2). The deposits are generally characterized by an association with porphyritic intrusions, by overprinting propylitic, potassic, and phyllic alteration, by disseminated or fracture-controlled sulphides, and by metal zonation (Seedorff et al., 2005, Sillitoe, 2010). Despite these similarities, geophysical responses can vary from one porphyry deposit to another. Differences in geophysical response between calc-alkalic and alkalic porphyry systems are expected due to the slightly different alteration mineral assemblages characterizing the alteration zones which form in association with each type (Holliday and Cooke, 2007). The size of the physical and geochemical footprints of the systems may also differ between porphyry deposit types. In comparison to calc-alkalic porphyry deposits, alkalic porphyry deposits and their associated alteration footprints commonly have more narrow, pipe-like geometries (Chamberlain, 2013). This means the geophysical anomalies corresponding to alkalic porphyry deposits may be less pronounced.

Table 1. Summary of physical rock property contrasts between the six central BC porphyry deposits studied.

	Magnetics/Susceptibility			Gravity/Density			Porosity			Conductivity		
	Intrusives	Volcanics or Sediments	Mineralization /alteration	Intrusives	Volcanics or Sediments	Mineralization /alteration	Intrusives	Volcanics or Sediments	Mineralization /alteration	Intrusives	Volcanics or Sediments	Mineralization /alteration
Legend 												
Mount Milligan (alkalic)	High	Low	Potassic alteration	Low	High		Low	High		Low	Sulfide-rich zones	High
Endako (calc-alkalic)	High	n/a		Low	n/a		Low	n/a		Low	n/a	Phyllic-argillic alteration
Huckleberry (calc-alkalic)	High	High		Low	High	Hornfels Background volcanics	Low	High		Low	Background volcanics Hornfels	Sulfide-fractures
Granisle (calc-alkalic)	High	High	Potassic Phyllic	Low	High	Potassic Phyllic	Low	High		Low		Phyllic Potassic
Bell (calc-alkalic)	High	Low	Potassic Phyllic	Low	High	Potassic Phyllic	Low	Sedimentary rocks		Low		Phyllic Potassic
Morrison (calc-alkalic)	High	Low	Potassic Phyllic	Low	High	Potassic Phyllic	Low			Low		Phyllic Potassic

The dissimilarities in geophysical response between porphyry deposits of similar magmatic affinity are primarily caused by the existence of different host rocks at each site, and by variations in rock texture and overprinting structural fabrics. The extent of development of particular alteration phases, and the manifestation of alteration is dependent on host rock lithology and composition. Fractures, veins, brecciation, and faulting will increase porosity in host rocks which can modify physical property signatures. The degree to which porosity is annealed will affect resistivity and density. If void space remains open, resistivities and densities will be lowered relative to coherent rock. If later fluids infiltrate the rock and minerals like quartz or carbonate are formed, the rock will become more resistive and dense.

For successful interpretation of geophysical data from porphyry deposits, several factors should be considered:

- Is the porphyry system alkalic or calc-alkalic? It is essential to understand the characteristic system size, alteration mineralogy, and sulphide assemblages.
- What are the dominant host rock types and expected modal mineralogy? How will potassic, sodic-calcic, phyllic, and propylitic alteration be manifested within the host rocks?
- Are potassic alteration assemblages magnetite-bearing? If so, the core of the porphyry system could be associated with a strong magnetic response. Potassic alteration does not always generate magnetite, however, and it is just as likely that a porphyry deposit will lack a magnetic response. Is there evidence of a later overprinting phyllic or argillic alteration phase? This alteration will lead to destruction of any primary or secondary magnetite, reducing magnetic susceptibility. It may simultaneously enhance conductivity by increasing porosity, or if significant amounts of clays are formed.
- Are there significant overprinting fabrics or structures? These features will influence permeability and porosity, focusing groundwater or other fluids, which will alter adjacent wall rock and destroy primary mineralogy. Magnetic susceptibility, density, and resistivity will decrease.
- Have tectonic events caused the porphyry system to become tilted? How deep has the system been eroded? The orientation of the porphyry system and erosion levels will determine which part of the system sits nearest to the surface. This will influence which alteration zones are exposed, which will have an effect on geophysical responses.

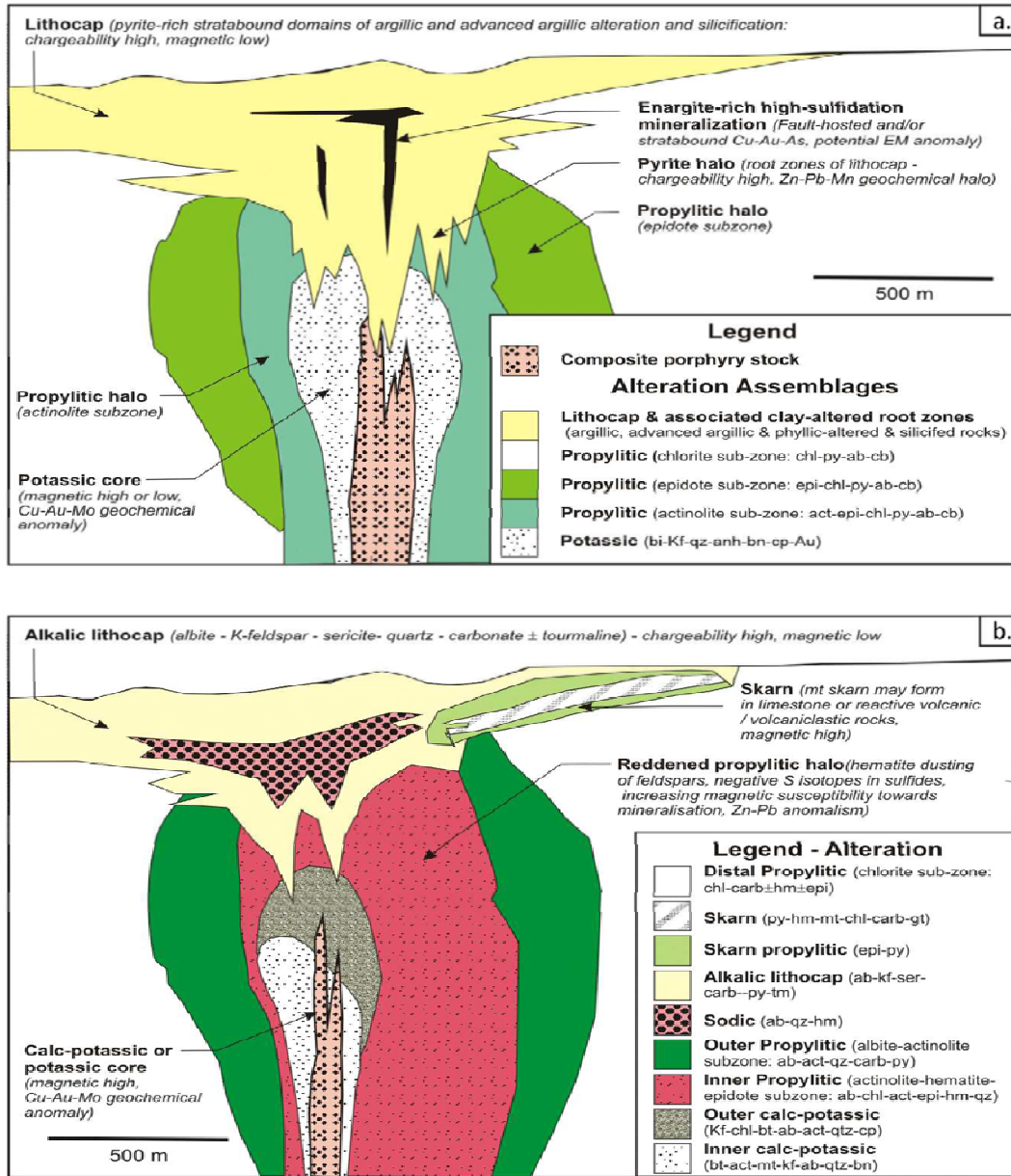


Figure 2. Schematic illustrations of a calc-alkalic porphyry system (like Endako, Huckleberry, Bell, Granisle, and Morrison), a) and an alkalic porphyry system (like Mount Milligan), b). Abbreviations: ab – albite; act – actinolite; anh – anhydrite; Au- gold; bi – biotite; bn – bornite; cb – carbonate; chl – chlorite; cp – chalcopyrite; epi – epidote; gt – garnet; hm – hematite; Kf – K-feldspar; lm – laumontite; mt – magnetite; pr – prehnite; py – pyrite; qz – quartz; ser – sericite; tm – tourmaline. Figure from Holliday and Cooke (2007).

- Has there been contact metamorphism associated with intrusion emplacement (or any other overprinting metamorphism), and what might the resulting mineralogy be? Hornfelsing related to the intrusion of granodiorite at Huckleberry added magnetite to the surrounding mafic volcanic rocks increasing susceptibility and masking the signature of magnetite-forming potassic alteration associated with mineralization.
- How are sulphides distributed within the rock? If sulphides are disseminated the rock may be chargeable, but not necessarily conductive. Connected networks of sulphides will enhance conductivities, but may not result in high chargeabilities. The variety of sulphide and oxide minerals which occur will also influence electrical rock properties, with some minerals being inherently more chargeable or conductive than others.

There is always some amount of information known about the geology of a given area, which allows physical rock property trends to be anticipated to some degree. A sense of the lithologies, alteration assemblages, sulphide distributions, and structural overprints can be acquired from historical data, public geoscience data, articles or reports on similar mineral deposits, and from conceptual mineral deposit models. The most effective means to building physical property knowledge prior to geophysical investigation remains collecting physical rock property measurements, ideally at different scales from hand sample to outcrop. The cost of rock property data collection is low, relative to the overall costs of running a mineral exploration program, and can provide an important framework for design of geophysical surveys, survey method selection, geophysical modelling, and data interpretation.

4. Acknowledgements

The authors gratefully acknowledge Geoscience BC and the Mineral Deposit Research Unit at The University of British Columbia for funding this project. T. Bissig, MDRU, initially proposed this research and provided valuable feedback and discussion throughout the course of the study. M. Thomas of the Geological Survey of Canada is thanked for his thorough review and suggestions for improvements to the report. Thanks are extended to the companies who supported this project by providing access to their properties and providing data, information, and assistance: Pacific Booker Minerals, Xstrata, Terrane Metals Corp., Endako Mines, Imperial Metals, and Huckleberry Mines Ltd. P. Ogryzlo is thanked for providing a geological tour of the Babine Lake area and for introductions to the geology of the Huckleberry, Morrison, Bell and Granisle deposits. A. Tkachyk and R. Raynor are acknowledged for assistance in the Geological Survey of Canada—Pacific Paleomagnetism and Petrophysics Laboratory; E.

Pani, J. Lai, and M. Raudsepp at UBC are thanked for X-ray diffraction analyses and interpretations. Additional acknowledgements go to W. Putt for help in the field and with sample preparation at UBC, and to N. Bueckert for data entry.

5. References

- Aeroquest Surveys (2009): Report on a helicopter-borne AeroTEM system electromagnetic & magnetic survey; Geoscience BC, Report 2009-6, 28 p.
- Archie, G.E. (1942): The electrical resistivity log as an aid in determining some reservoir characteristics; *Petroleum Transactions of AIME*, v. 146, p. 54–62.
- B.C. Geological Survey (2013): MINFILE BC mineral deposits database; B.C. Ministry of Energy and Mines, URL <<http://minfile.ca/>> [December 2013].
- Chamberlain, C. (2013): Undersaturated alkalic porphyry deposits of BC - field characteristics and exploration criteria (abstract); *Society of Economic Geologists - Whistler 2013:Geoscience for Discovery*, Whistler, BC, Abstract Volume, p. 14-15.
- Clark, D.A. (1997): Magnetic petrophysics and magnetic petrology: aids to geological interpretation of magnetic surveys; *Journal of Australian Geology and Geophysics*, v. 17, p. 83-103.
- Enkin, R.J., Cowan, D., Tigner J., Severide, A., Gilmour, D., Tkachyk, A., Kilduff, M., Vidal, B., and Baker, J. (2012): Physical property measurements at the GSC Paleomagnetism and Petrophysics Laboratory, including electric impedance spectrum methodology and analysis; *Geological Survey of Canada*, Open File 7227, 42 p.
- Farquharson, C.G, Ash, M.R., and Miller, H.G. (2008): Geologically constrained gravity inversion for the Voisey's Bay ovoid deposit; *The Leading Edge*, v. 27, p. 64-69.
- Fullagar, P.K., Pears, G.A., and McMonnies, B. (2008): Constrained inversion of geologic surfaces—pushing the boundaries; *The Leading Edge*, v.27, p. 98-105.
- GeoBase® (2004): Canadian digital elevation data, edition 2.0; Canadian Council on Geomatics, URL <<http://www.geobase.ca/geobase/en/data/cded/description.html>> [November 2012].
- Geotech Limited (2008): Report on a helicopter-borne versatile time domain electromagnetic (VTEM) geophysical survey: QUEST Project, central British Columbia (NTS 93A, B, G, H, J, K, N, O & 94C, D); *Geoscience BC*, Report 2008-4, 35 p.

- Geotech Limited (2009): Helicopter-borne Z-Axis Tipper Electromagnetic (ZTEM) and Aeromagnetic Survey, Mt. Milligan Test Block; Geoscience BC, Report 2009-7, 51 p.
- Holliday, J.R. and Cooke, D.R. (2007): Advances in geological models and exploration methods for copper ± gold porphyry deposits; *in*: Proceedings of Exploration 07: Fifth Decennial International Conference on Mineral Exploration, B. Milkereit (ed), p. 791–809.
- Johnson, G.R., and Olhoeft G.R. (1984): Density of rocks and minerals; *in* Carmichael, R.S., ed., Handbook of physical properties of rocks; Volume III, CRC Press, Florida, p. 1-38.
- Katsube, T.J. (2001): An analytical procedure for determining spectral induced polarization characteristics of anisotropic rocks, Yellowknife mining district, Northwest Territories; Geological Survey of Canada, Current Research 2001-E3, 29 p.
- Kowalczyk, P.K (2009): QUEST-West geophysics in central British Columbia (NTS 093E, F, G, K, L, M, N, 103I): new regional gravity and helicopter time-domain electromagnetic data; in Geoscience BC Summary of Activities 2008, Geoscience BC, Report 2009-1, p. 1–6.
- Massey, N.W.D, MacIntyre, D.G., Desjardins, P.J. and Cooney, R.T. (2005): Digital geology map of British Columbia: whole province; B.C. Ministry of Energy and Mines, Geofile 2005-1, URL <<http://www.empr.gov.bc.ca/Mining/Geoscience/PublicationsCatalogue/GeoFiles/Pages/2005-1.aspx>> [November 2007].
- Natural Resources Canada (1999): Atlas of Canada base maps; Natural Resources Canada, Earth Sciences Sector, URL <<http://geogratis.gc.ca/api/en/nrcan-rncan/ess-sst/501ca077-c481-55b3-930b-f5e97fb1908c.html>> [July 2009].
- Natural Resources Canada (2004): Canadian aeromagnetic data base, Continental Geoscience Division, Geological Survey of Canada, Earth Sciences Sector, Natural Resources Canada, Geoscience Data Repository, URL <<http://gdrdap.agg.nrcan.gc.ca/geodap/home/Default.aspx?lang=e>> [March 2013].
- Oldenburg, D.W., Li, Y. and Ellis, R.G. (1997): Inversion of geophysical data over a copper gold porphyry deposit: a case history for Mt. Milligan; Geophysics, v. 62, p. 1419–1431.
- Oldenburg, D.W., and Pratt, D.A. (2007): Geophysical inversion for mineral exploration: A decade of progress in theory and practice; *in*: Proceedings of Exploration 07: Fifth Decennial International Conference on Mineral Exploration, B. Milkereit (ed), p. 61–95.
- Raudsepp, M., Pani., E., and Dipple, G.M. (1999): Measuring mineral abundance in Skarn I: the Rietveld method using X-ray powder diffraction data, Canadian Mineralogist, v.37, p.1-15.

- Raudsepp, M. and Pani, E. (2003): Application of Rietveld analysis to environmental mineralogy; Chapter 8 *in* Environmental Aspects of Mine Wastes, J.L. Jambor, D.W. Blowes and A.I.M. Ritchie (ed.), Mineralogical Association of Canada, Short Course Series, v. 31, p. 165–180.
- Rietveld, H.M. (1967): Line profiles of neutron powder-diffraction peaks for structure refinement, *Acta Crystallographica*, v.22, p.151-152.
- Rietveld, H.M. (1969): A profile refinement method for nuclear and magnetic structures, *Journal of Applied Crystallography*, v. 2, p.65-71.
- Sander Geophysics Limited (2008a): Airborne gravity survey, Quesnellia Region, British Columbia; Geoscience BC, Report 2008-8, 121 p.
- Sander Geophysics Limited (2008b): Airborne gravity survey, QUEST West, British Columbia - 2008; Geoscience BC, Report 2008-10, 129 p.
- Seedorff, E., Dilles, J.H., Proffett, J.M., Jr., Einaudi, M.T., Zurcher, L., Stavast, W.J.A., Johnson, D.A., and Barton, M.D. (2005): Porphyry deposits: Characteristics and origin of hypogene features; *Economic Geology*, 100th Anniversary Volume, v. 100, p. 251–298.
- Sillitoe, R.H. (2010): Porphyry copper systems; *Economic Geology*, v. 105, p. 3-41.
- Telford, W.M., Geldart, L.P. and Sheriff, R.E. (1990): *Applied Geophysics*, Second Edition; Cambridge University Press, 770 p.
- Williams, N.C. (2008): Geologically-constrained UBC—GIF gravity and magnetic inversions with examples from the Agnew-Wiluna greenstone belt, Western Australia; Unpublished Ph.D. Thesis, The University of British Columbia, 479 p.

Appendix 1. Mount Milligan

1.1. Regional Geology and Magnetic Data

1.1.1. Regional Geologic Setting

The Mount Milligan deposit occurs within the Mesozoic Quesnel Terrane, an oceanic island arc terrane forming part of the Intermontane Belt of the northwest Canadian Cordillera. The Quesnel Terrane's volcanic, volcano-sedimentary, and intrusive rocks are recognized globally as important hosts to several economically significant gold-rich alkalic porphyry deposits, including Mount Polley, Copper Mountain and New Afton.

Geology in the Mount Milligan deposit area is dominated by augite-phyric basaltic and sedimentary rocks of the Late Triassic to Early Jurassic Takla Group (Figure 1.1), which are intruded by Early Jurassic monzonitic intrusions. (Nelson and Bellefontaine, 1996). Two episodes of alkalic plutonism are recorded in the Cordillera, dated 210-200 Ma and 190-180 Ma (Mortensen et al., 1995). Monzonite intrusions linked to mineralization at Mount Milligan belong to the second episode, yielding an age gap of approximately 20 Ma between hosting volcanic rocks and intrusive rocks. Regional magnetic and structural trends suggest the monzonitic intrusions at Mount Milligan, and the Mount Milligan pluton mapped 7 km north of the deposit are related to the large Hogem batholith paralleling the western margin of the Quesnel Terrane. The linear trend of these intrusive bodies indicate regional structural control on their emplacement (Nelson and Bellefontaine, 1996).

1.1.2. Regional Magnetic Data

Natural Resources Canada regional magnetic data reveal Takla Group volcanic and volcanoclastic rocks in the Mount Milligan district have a weak magnetic response (Figure 1.1). In contrast, Jurassic monzonitic intrusions on the Mount Milligan property, and an intrusion mapped directly to the north of Mount Milligan are magnetic. Other regional magnetic highs are associated with paragneissic metamorphic rocks of the Wolverine Metamorphic Complex mapped 20 km to the southeast of the Mount Milligan deposit, and to Triassic and Cretaceous intrusions. Regional magnetic data show that sedimentary rock units yield relatively weak magnetic responses.

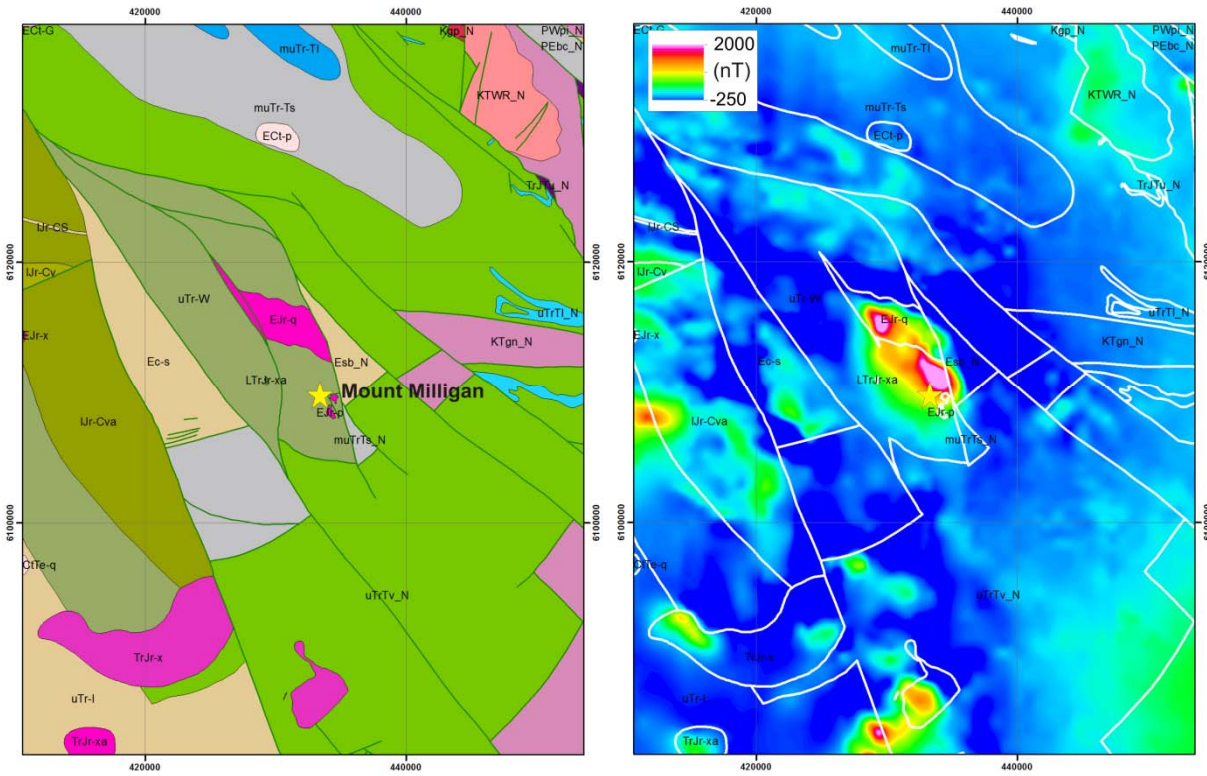




Figure 1.1. Regional geological setting for the Mount Milligan porphyry deposit (Massey et al., 2005), and regional residual total field magnetic data from Natural Resources Canada's Geoscience Data Repository (Natural Resources Canada, 2004).

Regional Geology of the Mount Milligan Deposit

Legend




Eocene

-  EOIEs - Nechako Plateau Group undivided sedimentary rocks
-  Esb_N - Unnamed undivided sedimentary rocks

Eocene Intrusive Rocks




-  ECt-G - Germansen Batholith granite, alkali feldspar granite intrusive rocks
-  ECt-p - Unnamed feldspar porphyritic intrusive rocks

Cretaceous to Tertiary Intrusive Rocks

-  CtTe-q - Unnamed granite, alkali feldspar granite intrusive rocks
-  KTWR_N - Wolverine Range Plutonic Suite granodioritic intrusive rocks
-  Kgp_N - Wolverine Range Plutonic Suite pegmatitic intrusive rocks







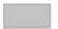
Lower Jurassic

Chuchi Lake Succession








-  IJr-Cva - Chuchi Lake Succession coarse volcanoclastic and pyroclastic volcanic rocks
-  IJr-CS - Chuchi Lake Succession undivided sedimentary rocks
-  IJr-Cv - Chuchi Lake Succession undivided volcanic rocks

Upper Triassic

Takla Group

-  uTrTI_N - Takla Group limestone bioherm/reef
-  uTrTv_N - Takla Group calc-alkaline volcanic rocks
-  uTr-W - Takla Group - Witch Lake Formation volcanoclastic rocks
-  uTr-I - Takla Group - Inzana Lake Formation undivided sedimentary rocks
-  muTr-TI - Takla Group limestone, marble, calcareous sedimentary rocks
-  muTrTs_N - Takla Group mudstone, siltstone, shale fine clastic sedimentary rocks
-  muTr-Ts - Takla Group mudstone, siltstone, shale fine clastic sedimentary rocks



Triassic to Jurassic Intrusive Rocks

-  TrJTU_N - Unnamed ultramafic rocks
-  TrJr-xa - Unnamed syenitic to monzonitic intrusive rocks
-  TrJr-x - Unnamed dioritic intrusive rocks
-  LTrJr-xa - Unnamed dioritic intrusive rocks
-  EJr-x - Unnamed dioritic intrusive rocks
-  EJr-p - Unnamed syenitic to monzonitic intrusive rocks
-  EJr-q - Unnamed syenitic to monzonitic intrusive rocks

Paleozoic

-  PEbc_N - Earn Group mudstone, siltstone, shale fine clastic sedimentary rocks

Late Proterozoic to Late Paleozoic

-  KTgn_N - Wolverine Metamorphic Complex paragneiss metamorphic rocks
-  PWpi_N - Unnamed paragneiss metamorphic rocks

1.2. Deposit Geology

Mineralization at Mount Milligan is spatially associated with two, silica-saturated alkalic plagioclase porphyritic monzonite stocks (Sketchley et al., 1995; Jago, 2008) but occurs predominantly within the hosting basaltic volcanoclastic Takla Group rocks (Figure 1.2). Four mineralized zones are related to the northern MBX stock, the DWBX, WBX, MBX and 66 zones. The highest grades occur within the MBX zone, where mineralization is found in brecciated and altered rocks between the MBX stock and the Rainbow Dike (Figure 1.3). To the south, mineralization is related to the faulted Southern Star stock. Ore-related sulphide minerals are predominantly disseminated, as well as hosted within veins, veinlets, and brecciated zones. A cross section through the northern mineralized zones shows the position of the MBX stock within the volcanic rocks (Figure 1.3), and shows the locations of the DWBX, WBX, MBX and 66 zones. East-dipping trachyte beds indicate that the volcanic package and the MBX monzonite stock are tilted.

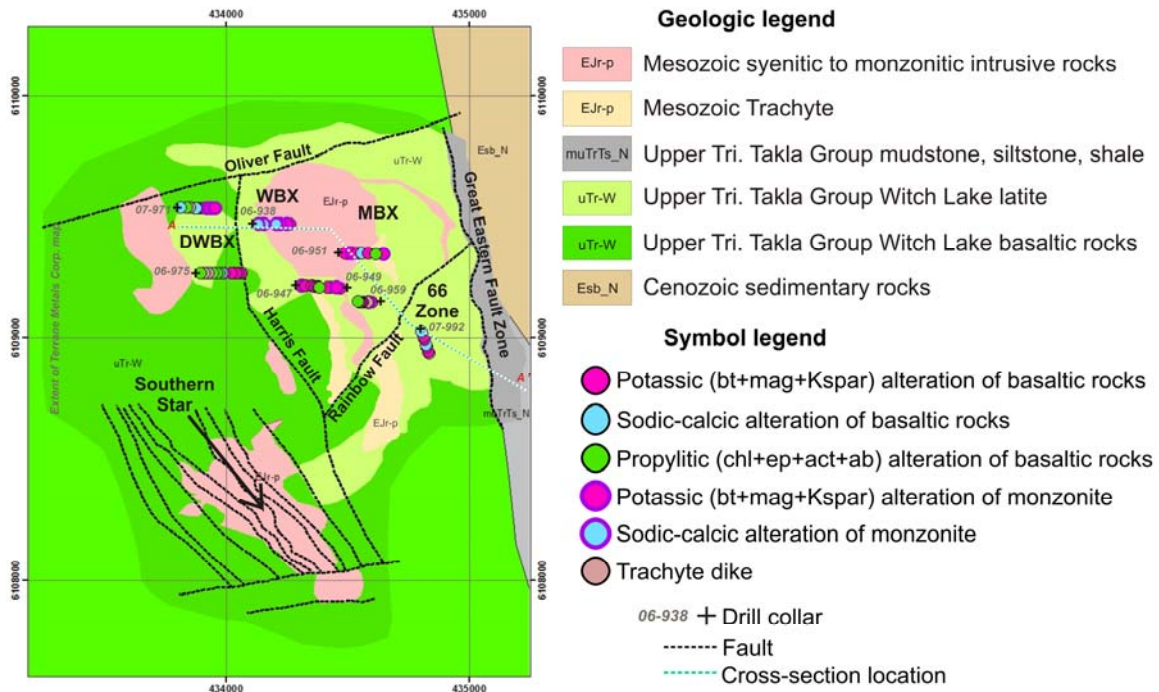


Figure 1.2. Geology of the Mount Milligan porphyry deposit, showing the location of the five mineralized areas, as well as the locations of drill core samples collected for this study, which have been projected to surface in this image. Samples are colored to reflect alteration. Mount Milligan base map files provided by Terrane Metals Corp. Abbreviations: ab=albite, act=actinolite, bt=biotite, chl=chlorite, ep=epidote, Kspar=K-feldspar, mag=magnetite.

Hydrothermal alteration of the hosting intrusions and volcanic rocks forms near-concentric zones centered around mineralized areas (Figure 1.3; Jago, 2008). Potassic alteration, manifested as biotite+K-feldspar±magnetite, occurs centrally, passing outward into albite+actinolite+epidote alteration (sodic-calcic zone of Jago, 2008), and then into a propylitic alteration assemblage of epidote+albite+chlorite+actinolite+calcite+pyrite.

Phyllic and argillic alteration mineral assemblages common to calc-alkalic porphyry settings are generally poorly represented in alkalic systems (Holliday and Cooke, 2007), however, a zone of quartz+sericite+carbonate alteration occurs in the 66 Zone at Mount Milligan (Jago, 2008).

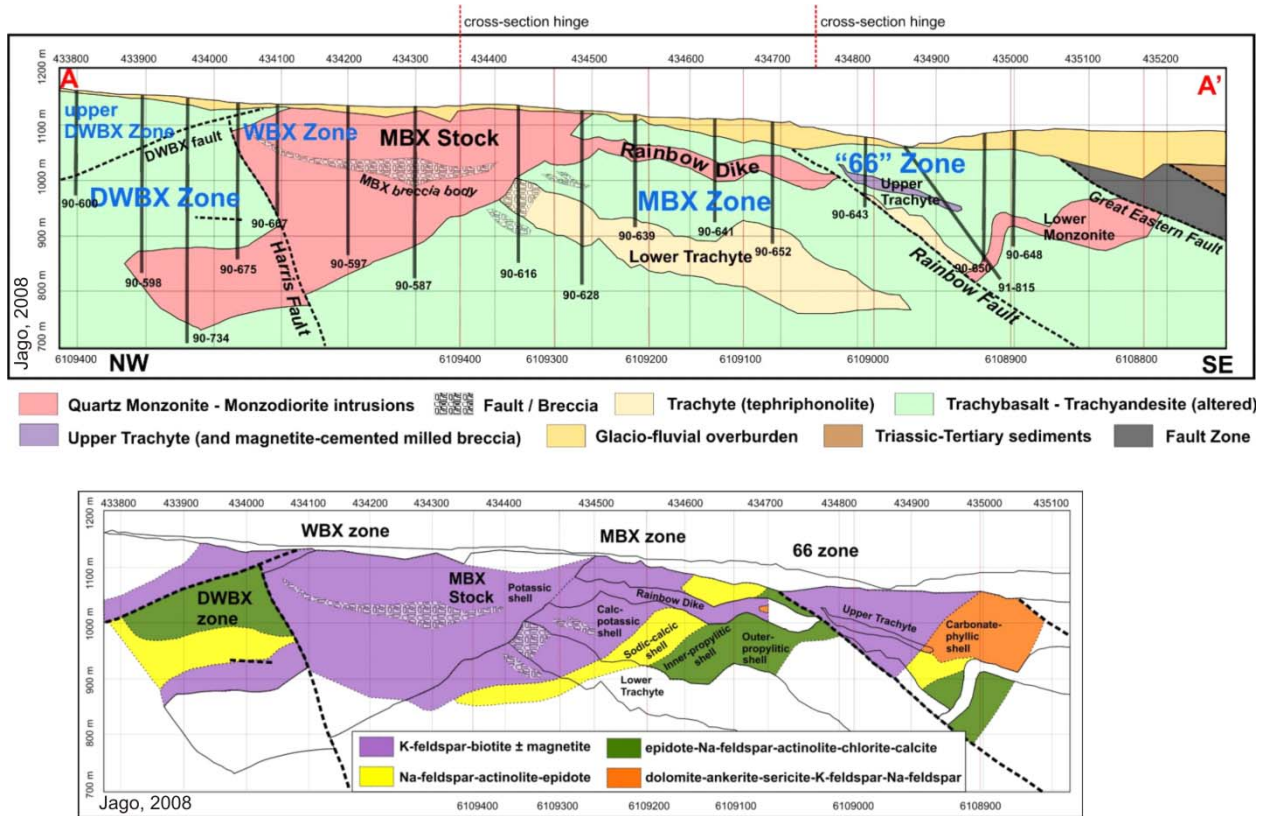


Figure 1.3. Cross-section through geology and alteration zones at Mount Milligan from Jago (2008).

1.3. Physical Properties of Rocks from the Mount Milligan Deposit

1.3.1. Sample Suite

Seventy-two samples were collected from nine representative drillholes from the MBX stock area (Figure 1.2). One hand sample was collected from outcrop. Ten hand samples were collected by T. Bissig (Bissig et al., 2010) from outcrops outside of the deposit area and represent weakly propylitically-altered background basaltic rocks. For presentation in graphs and plots in this report, rocks are grouped into subsuites based on alteration. Some samples were omitted from plots if they did not fall into one of the primary lithological or alteration subsuites. Physical property data are tabulated in Appendix 8.

1.3.2. Magnetic Susceptibility and Deposit Scale Magnetic Data

Magnetic susceptibility data collected from Mount Milligan samples is shown in Figure 1.4. Least-altered basalt samples from outside the deposit area generally have low magnetic susceptibilities, with most samples measured at $< 2 \times 10^{-3}$ SI units, reflecting a composition lacking significant magnetite (Vaca et al., 2011). The highest measurement for background basalt was 36×10^{-3} SI units. Petrography on this sample indicates that magnetite is an overprinting phase, and is possibly alteration-related.

Potassically-altered (biotite+magnetite+K-feldspar) basalt samples range in susceptibility up to 277×10^{-3} SI units, with the highest susceptibilities derived from samples containing magnetite veins. Propylitic and sodic-calcic-altered basalt usually do not exhibit the very high susceptibilities seen in the potassically-altered sample suite, and most samples have susceptibilities $< 10 \times 10^{-3}$ SI units.

Most monzonite samples contain primary magnetite at various stages of destruction or alteration to hematite, in addition to secondary magnetite. Potassically-altered monzonite therefore typically has moderate to high susceptibilities. Sodic-calcic alteration of monzonite appears to cause magnetite destruction.

The MBX and Southern Star monzonite stocks are not distinguishable within regional Natural Resources Canada airborne magnetic survey data due to the influence of the large highly magnetic plutons which occur north of the Mount Milligan deposit (Figure 1.1).

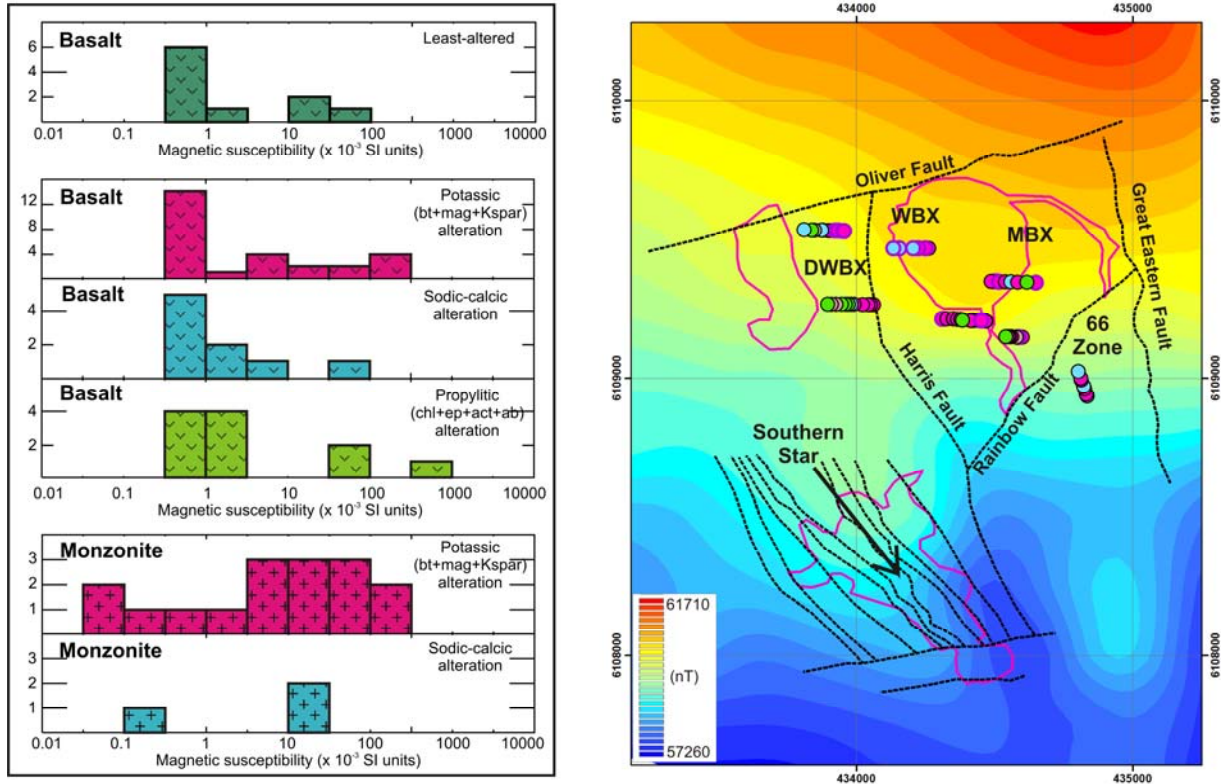


Figure 1.4. Magnetic susceptibility data from the Mount Milligan deposit, and local-scale airborne magnetic data (total magnetic intensity, Geotech Limited, 2009). Abbreviations: ab=albite, act=actinolite, bt=biotite, chl=chlorite, ep=epidote, Kspar=K-feldspar, mag=magnetite.

With a decrease in survey line spacing, magnetic data become more effective in detecting localized magnetite-rich intrusive rocks and alteration zones. In the 200 m line spacing airborne magnetic data collected over Mount Milligan (Figure 1.4), the Southern Star monzonite and the MBX stock appear as superimposed positive anomalies on the regional gradient. Using ground magnetic data, local potassically-altered mineralized zones become detectable. Oldenburg et al. (1997) inverted Mount Milligan ground magnetic data and a horizontal slice through the inversion model at 80 m depth shows the strongest magnetic susceptibility anomalies are coincident with the locations of the potassically-altered WBX, MBX, and 66 zones (Figure 1.5).

The close spatial relationship between magnetite, biotite and copper mineralization at Mount Milligan has been documented by several researchers (Sketchley et al., 1995; Jago, 2008). The data from this work indicates that high-susceptibility rocks greater than approximately 15×10^{-3} SI units are potassically-altered basalt, or else primary or secondary magnetite-bearing monzonite. Low susceptibility propylitically-altered areas can consequently be easily ruled out as less favourable host rocks.

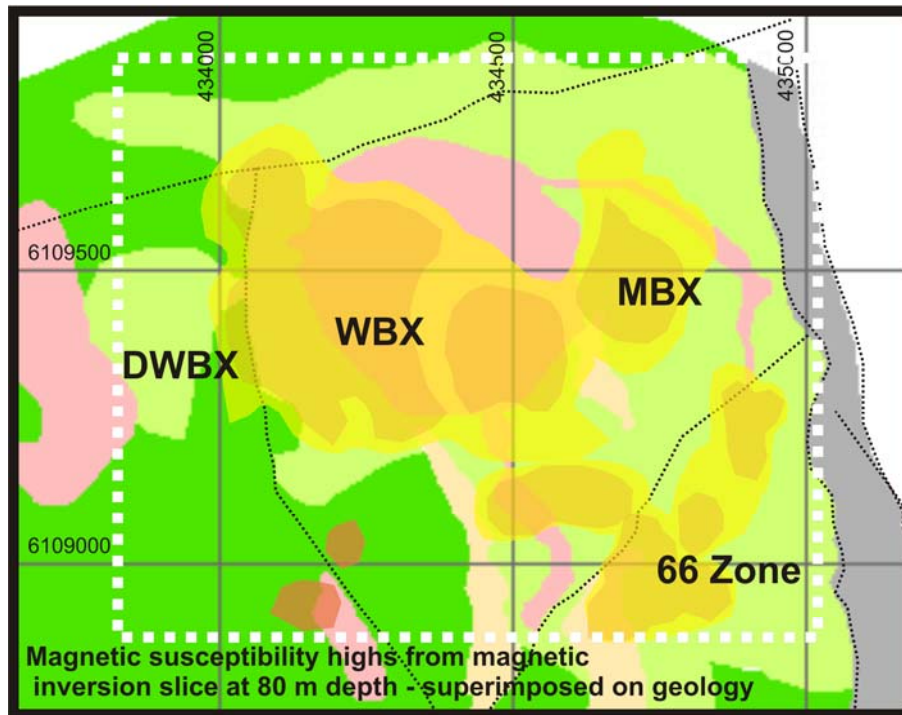


Figure 1.5. Polygons (orange and yellow color) digitized onto the Mount Milligan surface geological map (same as Figure 1.2) represent magnetic susceptibility anomalies at 80 m depth from a plan-view slice through a magnetic inversion over the Mount Milligan MBX stock (Oldenburg et al., 1997). Magnetic data used in the inversion were collected in 1984–1985 by BP Minerals. The dotted line represents the extents of the magnetic inversion model.

1.3.3. Density and Porosity

The variations in density measured in the Mount Milligan samples are explained largely by mineralogy. The sample suites with the highest average densities are the distal background basalt sample suite, and the propylitically-altered basalt suite (Figure 1.6), with average densities of 2.93 g/cm³ and 3.03 g/cm³, respectively. These samples have the greatest abundance of mafic, or Fe-Mg-rich minerals, such as clinopyroxene (augite) and actinolite (3.30 and 3.20 g/cm³, respectively, Johnson and Olhoeft, 1984). Altered basaltic rocks proximal to, or hosting mineralization are lower in density due to increased abundance of felsic alteration minerals. The lowest density samples are monzonite samples (2.60-2.85 g/cm³) which are dominated by the low-density minerals albite and microcline (2.62 and 2.56 g/cm³, respectively, Johnson and Olhoeft, 1984).

Porosities are generally low for Mount Milligan samples, with the majority of the samples having < 1% porosity. A few brecciated andesitic and monzonitic samples have slightly higher porosities. Compared to

other porphyry sample suites from this study where high porosities correspond to decreases in density, there is no significant trend between density and porosity for Mount Milligan samples (Figure 1.7).

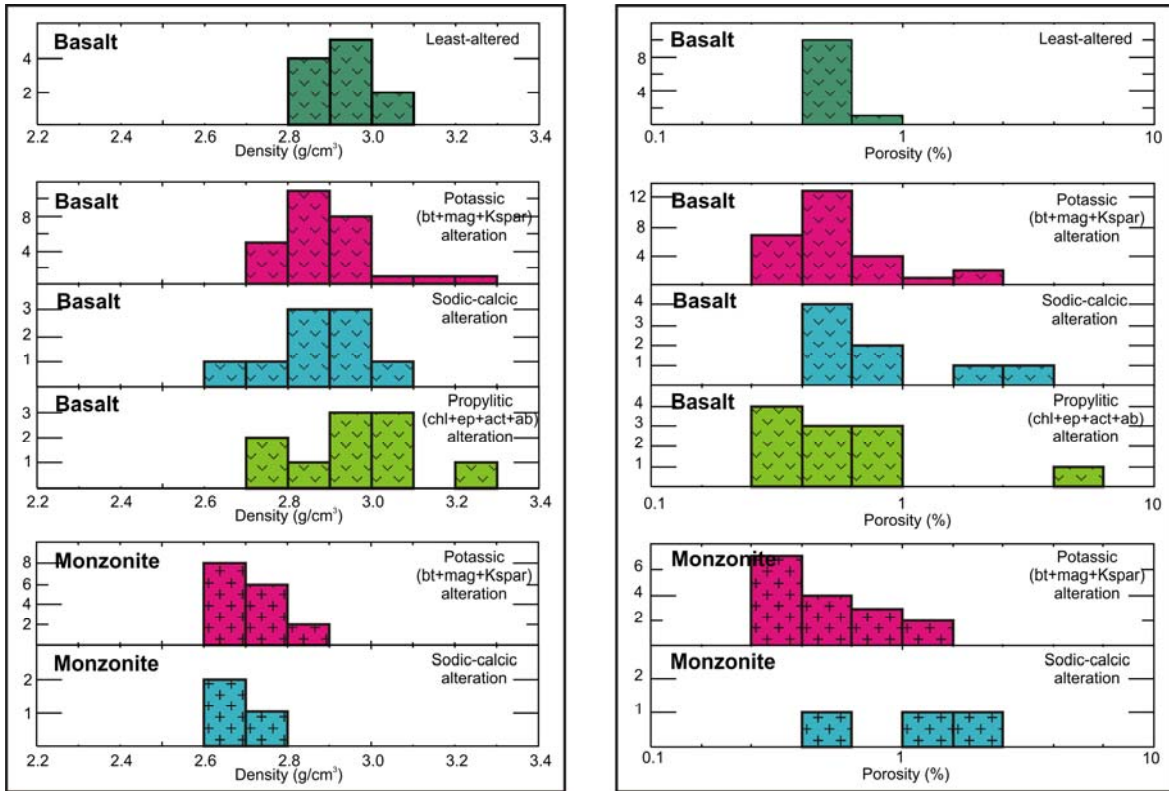


Figure 1.6. Density and porosity data from the Mount Milligan deposit. Abbreviations: ab=albite, act=actinolite, bt=biotite, chl=chlorite, ep=epidote, Kspar=K-feldspar, mag=magnetite.

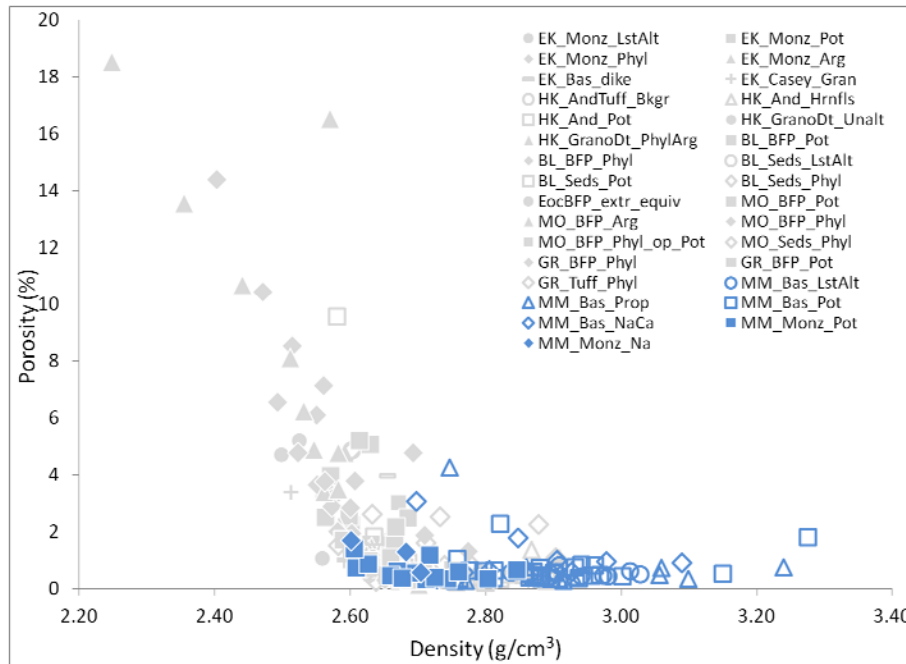


Figure 1.7. Density versus porosity data for all porphyry samples from this study. Mount Milligan samples are highlighted in blue. Relative to other samples, Mount Milligan samples are low porosity. Deposit abbreviations: BL=Bell, EK=Endako, GR=Granisle, HK=Huckleberry, MM=Mount Milligan, MO=Morrison. Rock type abbreviations: And=Andesite, Bas=basalt, BFP=biotite-feldspar porphyry, EocBFP Extr_equiv=Eocene biotite-feldspar porphyry extrusive equivalent, Gran=granite, GranoDt=granodiorite, Monz=monzonite, Seds=sedimentary rocks. Alteration assemblage abbreviations: Arg=argillic, Bkgr=background, Hrnfls=hornfels, LstAlt=least-altered, Na=sodic, NaCa=sodic-calcic, Phyl=phyllic, Phyl_op_Pot=potassic with overprinting phyllic alteration, Pot=potassic, Prop=propylitic, Unalt=unaltered.

1.3.4. Resistivity Data and Deposit Scale Conductivity

Propylitic and sodic-calcic-altered basalt from Mount Milligan have lower average resistivities (higher conductivities) than least-altered and potassically-altered basalt (Figure 1.8). Propylitic and sodic-calcic-altered rocks are in fact among the most conductive of the QUEST and QUEST-West porphyry sample collection. These peripheral alteration facies are correlative with high abundances of sulphides, specifically pyrite (Jago, 2008), which contribute to reducing basalt sample resistivity. Samples collected from the DWBX zone in particular contain a significantly high abundance of coarse-grained pyrite. This zone correlates with a high Total Divergence (Figure 1.8). Total Divergence is a parameter derived from ZTEM in-phase data which directly relates to the conductive properties of the subsurface (Geotech Limited, 2009); a high Total Divergence represents high conductivity. X-ray diffraction mineral abundance data confirms that high sulphide abundances correlate with lowered resistivities (Figure 1.9).

Monzonite rocks at Mount Milligan are generally resistive and have higher resistivity ranges similar to the least-altered and potassically-altered basalt sample suites.

Sulphide abundance is one of several factors expected to control resistivity. The distribution of sulphides within a rock also constitutes a factor in determining how resistive or conductive a rock will be. Sulphide minerals that are connected via a fracture network will have a greater impact on lowering rock resistivity than sulphides that are disseminated and disconnected within the rock. A more thorough discussion of the influence of sulphide abundance and distribution on resistivity, with plots generated from data from the entire porphyry sample suite, is presented in Appendix 7.

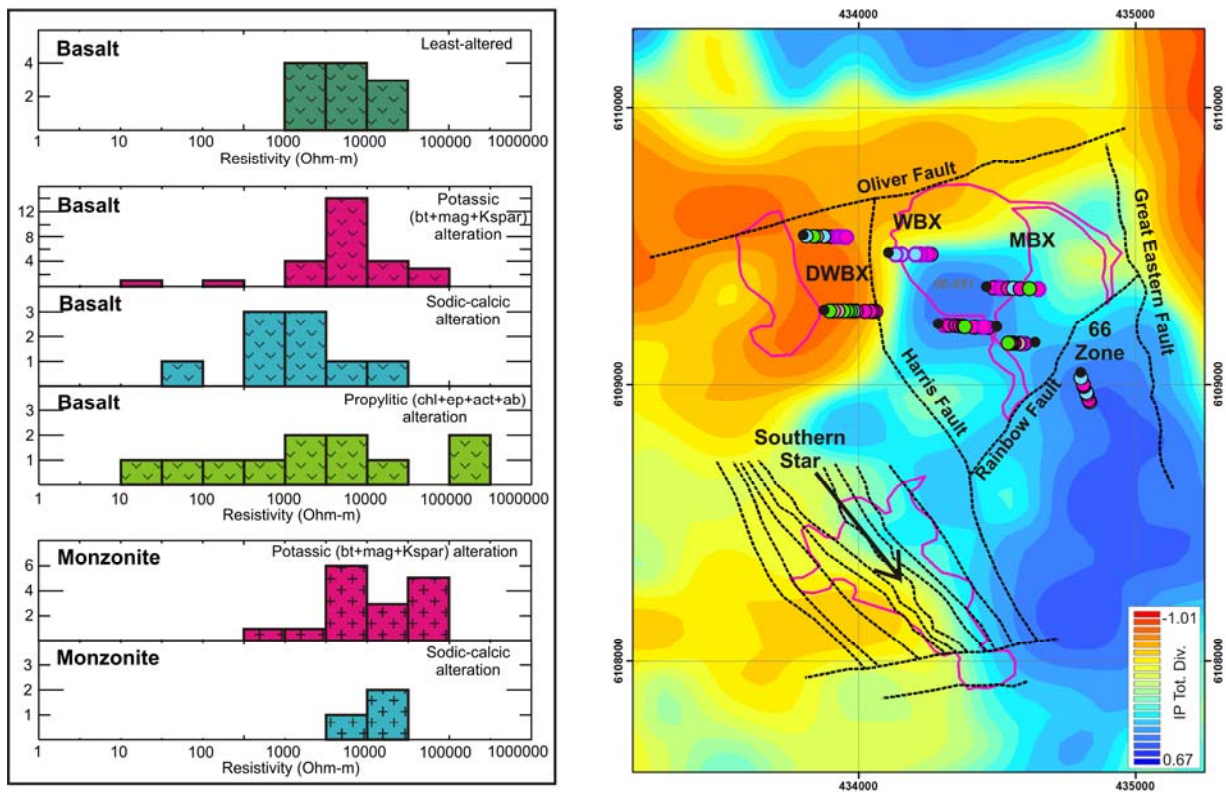


Figure 1.8. Resistivity data from the Mount Milligan deposit, and ZTEM data collected over the Mount Milligan deposit by Geotech Ltd. (ZTEM, 180 Hz, In-Phase Total Divergence grid, Geotech Limited, 2009). Abbreviations: ab=albite, act=actinolite, bt=biotite, chl=chlorite, ep=epidote, kspar=K-feldspar, mag=magnetite.

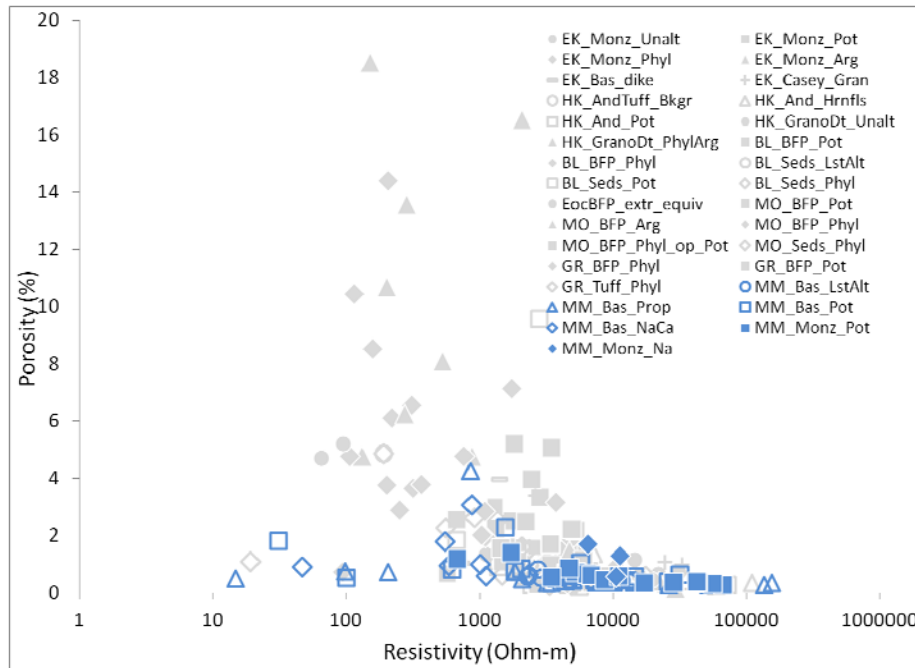


Figure 1.10. Resistivity versus porosity data for all porphyry samples from this study. Mount Milligan samples are highlighted in blue. Deposit abbreviations: BL=Bell, EK=Endako, GR=Granisle, HK=Huckleberry, MM=Mount Milligan, MO=Morrison. Rock type abbreviations: And=Andesite, Bas=basalt, BFP=biotite-feldspar porphyry, EocBFP Extr= Eocene biotite-feldspar porphyry extrusive equivalent, Gran=granite, GranoDt=granodiorite, Monz=monzonite, Sed=sedimentary rocks. Alteration assemblage abbreviations: Arg=argillic, Bkgr=background, Hrnfls=hornfels, LstAlt=least-altered, Na=sodic, NaCa=sodic-calcic, Phyl=phyllic, Phyl_op_Pot=potassic with overprinting phyllic alteration, Pot=potassic, Prop=propylitic, Unalt=unaltered.

As discussed in Section 1 of this report it is important to consider the scale of measurement when interpreting resistivity/conductivity data. Hand sample or drill core electrical measurements likely will not reflect measurements made at the outcrop scale or over larger areas, where macro-scale structural fabrics or fractures and the presence of groundwater will influence measurements. The control on conductivity by larger-scale structural features may be seen in geophysical inversions of DC resistivity data from Mount Milligan (Oldenburg et al., 1997). The conductivity anomalies appear spatially correlated with mapped local faults (Figure 1.11). Since these faults coincide in part with the distribution of peripheral sulphide-rich sodic-calcic and propylitic alteration assemblages, it is difficult to separate the respective influence of each in lowering resistivities.

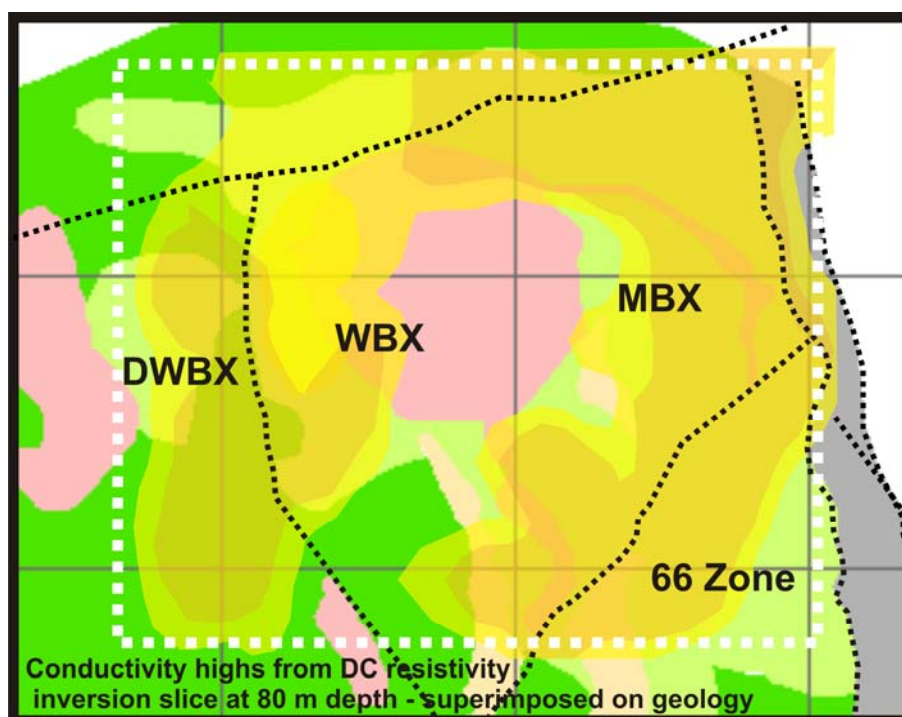


Figure 1.11. Polygons (orange and yellow color) digitized onto the Mount Milligan geological map represent conductivity anomalies at 80 m depth from a plan-view slice through a DC resistivity inversion over the Mount Milligan MBX stock (Oldenburg et al., 1997). Black dotted lines represent mapped faults, which show a broad spatial correlation with conductivity highs depicted in orange and yellow colors. DC resistivity data used in the inversion was collected in 1984–1985 by BP Minerals. The dotted white line represents extents of the inversion model.

Mount Milligan samples deviate from the resistivity versus density trend that is defined by other porphyry deposit samples. For the majority of rocks sampled for this study, decreases in both density and resistivity are correlated to increased porosities (Figure 1.12). Mount Milligan basaltic rocks are an exception where resistivity can be low while density remains high due to abundances (up to 20%) of conductive and dense sulphides. Figure 1.12 shows this trend.

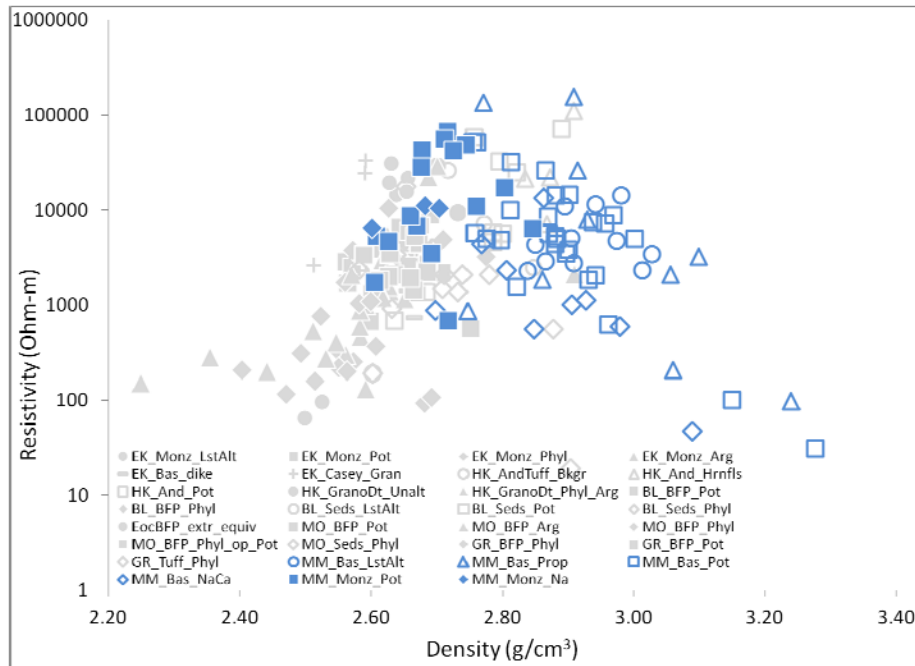


Figure 1.12. Resistivity versus density data for all porphyry samples from this study. Mount Milligan samples are highlighted in blue. Deposit abbreviations: BL=Bell, EK=Endako, GR=Granisle, HK=Huckleberry, MM=Mount Milligan, MO=Morrison. Rock type abbreviations: And=Andesite, Bas=basalt, BFP=biotite-feldspar porphyry, EocBFP Extr_equiv=Eocene biotite-feldspar porphyry extrusive equivalent, Gran=granite, GranoDt=granodiorite, Monz=monzonite, Seds=sedimentary rocks. Alteration assemblage abbreviations: Arg=argillic, Bkgr=background, Hrnfls=hornfels, LstAlt=least-altered, Na=sodic, NaCa=sodic-calcic, Phyl=phyllic, Phyl_op_Pot=potassic with overprinting phyllic alteration, Pot=potassic, Prop=propylitic, Unalt=unaltered.

1.4. References

- Bissig, T., Vaca, S., Schiarizza, P. and Hart, C. (2010): Geochemical and physical variations in the Late Triassic Nicola Arc and metallogenetic implications, central British Columbia (NTS 092P, 093A, N): preliminary results; *in* Geoscience BC Summary of Activities 2009, Geoscience BC, Report 2010-1, p. 49–52.
- Geotech Limited (2009): Helicopter-borne Z-Axis Tipper Electromagnetic (ZTEM) and Aeromagnetic Survey, Mt. Milligan Test Block; Geoscience BC, Report 2009-7, 51 p.
- Holliday, J.R. and Cooke, D.R. (2007): Advances in geological models and exploration methods for copper ± gold porphyry deposits; *in*: Proceedings of Exploration 07: Fifth Decennial International Conference on Mineral Exploration, B. Milkereit (ed), p. 791–809.

- Jago, C.P. (2008): Metal and alteration-zoning and hydrothermal flow paths at the moderately-tilted, silica-saturated Mount Milligan Cu-Au alkalic porphyry deposit; M.Sc. thesis, The University of British Columbia, 210 p.
- Johnson, G.R., and Olhoeft G.R. (1984): Density of rocks and minerals; *in* Carmichael, R.S., ed., Handbook of physical properties of rocks; Volume III, CRC Press, Florida, p. 1-38.
- Massey, N.W.D, MacIntyre, D.G., Desjardins, P.J. and Cooney, R.T. (2005): Digital geology map of British Columbia: whole province; B.C. Ministry of Energy and Mines, Geofile 2005-1, URL <<http://www.empr.gov.bc.ca/Mining/Geoscience/PublicationsCatalogue/GeoFiles/Pages/2005-1.aspx>> [November 2007].
- Mortensen, J.K., Ghosh, D.K. and Ferri, F. (1995): U-Pb geochronology of intrusive rocks associated with copper-gold porphyry deposits in the Canadian Cordillera; *in* Porphyry Deposits of the Northwestern Cordillera of North America, T.G. Schroeter (ed.), Canadian Institute of Mining, Metallurgy and Petroleum, Special Volume 46, p. 142–158.
- Natural Resources Canada (2004): Canadian aeromagnetic data base, Continental Geoscience Division, Geological Survey of Canada, Earth Sciences Sector, Natural Resources Canada, Geoscience Data Repository, URL <<http://gdrdap.agg.nrcan.gc.ca/geodap/home/Default.aspx?lang=e>> [March 2011].
- Nelson, J. L. and Bellefontaine, K.A. (1996): The geology and mineral deposits of north-central Quesnellia, Tezzeron Lake to Discovery Creek, central British Columbia; BC Ministry of Energy, Mines and Petroleum Resources, Bulletin 99, 112 p.
- Oldenburg, D.W., Li, Y. and Ellis, R.G. (1997): Inversion of geophysical data over a copper gold porphyry deposit: a case history for Mt. Milligan; *Geophysics*, v. 62, p. 1419–1431.
- Sketchley, D.A., Rebagliati, C.M. and DeLong, C. (1995): Geology, alteration, and zoning patterns of Mount Milligan copper-gold deposits; *in* Porphyry Deposits of the Northwestern Cordillera of North America, T.G. Schroeter (ed.), Canadian Institute of Mining and Metallurgy, Special Volume 46, p. 650–665.
- Telford, W.M., Geldart, L.P. and Sheriff, R.E. (1990): Applied Geophysics, Second Edition; Cambridge University Press, 770 p.
- Vaca, S., Bissig, T., Mitchinson, D.E., Barker, S. and Hart, C.J.R. (2011): Variability in the basaltic rocks hosting copper-gold porphyry mineralization in the Quesnel Terrane, south-central British Columbia (NTS 092, 093): geochemistry, stable isotopes and physical properties; *in* Geoscience BC Summary of Activities 2010, Geoscience BC, Report 2011-1, p. 123–132.

Appendix 2. Endako

2.1. Regional Geology and Magnetic Data

2.1.1. Regional Geologic Setting

The Endako molybdenum deposit is hosted within the calc-alkaline Jurassic Francois Lake plutonic suite of the Endako batholith. (Figure 2.1), a composite batholith situated within volcanic and sedimentary rocks of the Stikine Terrane of north-central British Columbia (Villeneuve et al., 1995). The Stikine rocks hosting the Endako batholith are predominantly early to mid-Jurassic Hazelton Group volcanic rocks and late Cretaceous Kasalka Group sedimentary rocks. Triassic to Cretaceous assemblages within the Endako deposit area are overlain in places by Eocene volcanic rocks (Massey et al., 2005).

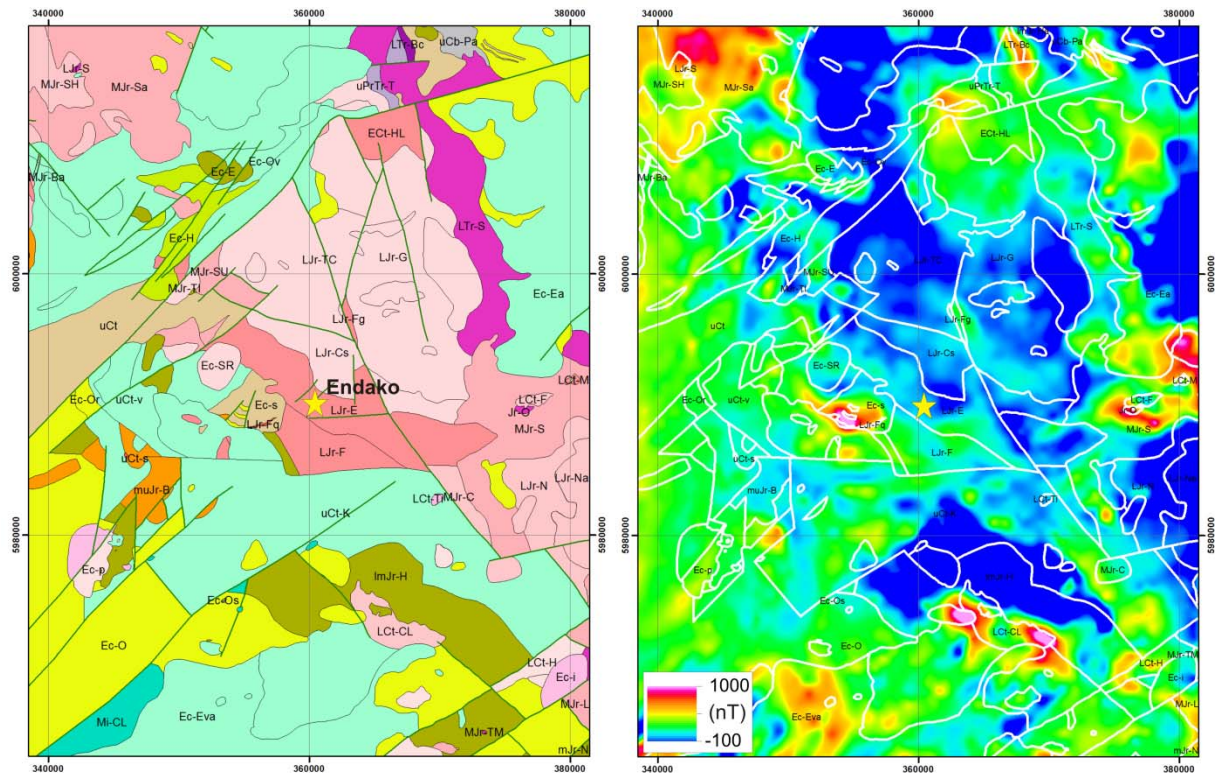


Figure 2.1. Regional geological setting for the Endako porphyry molybdenum deposit (Massey et al., 2005), and regional residual total field magnetic data from Natural Resources Canada's Geoscience Data Repository (Natural Resources Canada, 2004).

Regional Geology of the Endako Deposit

Legend

Miocene

- Mi-CL - Chilcotin Group - Cheslatta Lake Complex alkaline volcanic rocks

Eocene

- Ec-H - Nechako Plateau Group - Ootsa Lake Formation - Hicks Hill Dacite dacitic volcanic rocks
- Ec-O - Nechako Plateau Group - Ootsa Lake Formation rhyolite, felsic volcanic rocks
- Ec-Or - Nechako Plateau Group - Ootsa Lake Formation rhyolite, felsic volcanic rocks
- Ec-Ov - Nechako Plateau Group - Ootsa Lake Formation andesitic volcanic rocks
- Ec-Os - Nechako Plateau Group volcaniclastic rocks
- Ec-Eva - Nechako Plateau Group - Endako Formation andesitic volcanic rocks
- Ec-Ea - Nechako Plateau Group - Endako Formation andesitic volcanic rocks
- Ec-E - Nechako Plateau Group - Endako Formation undivided volcanic rocks
- Ec-s - Nechako Plateau Group undivided sedimentary rocks

Eocene Intrusive Rocks

- Ec-SR - Sam Ross Creek Pluton granite, alkali feldspar granite intrusive rocks
- Ec-p - Unnamed feldspar porphyritic intrusive rocks
- Ec-i - Unnamed intrusive rocks, undivided

Late Cretaceous

- uCt - Unnamed undivided sedimentary rocks
- uCt-v - Unnamed andesitic volcanic rocks

Kasalka Group

- uCt-K - Kasalka Group andesitic volcanic rocks
- uCt-s - Kasalka Group coarse clastic sedimentary rocks

Cretaceous Intrusive Rocks

- LCt-Ti - Unnamed intrusive rocks, undivided
- LCt-H - Holy Cross Pluton feldspar porphyritic intrusive rocks
- LCt-CL - Cabin Lake Pluton quartz monzonitic to monzogranitic intrusive rocks
- LCt-F - Endako Batholith - Fraser Lake Suite - Fraser Phase quartz monzonitic to monzogranitic intrusive rocks
- LCt-M - Endako Batholith - Fraser Lake Suite - Mouse Phase granodioritic intrusive rocks
- ECt-HL - Endako Batholith - Hanson Lake Phase granodioritic intrusive rocks

Middle and Late Jurassic

Bowser Lake Group

- muJr-B - Bowser Lake Group coarse clastic sedimentary rocks

Lower to Middle Jurassic

Hazelton Group

- ImJr-H - Hazelton Group undivided volcanic rocks
- mJr-N - Hazelton Group - Naglico Formation undivided volcanic rocks

Jurassic

Endako Batholith

- LJr-S - Slug Lake Phase dioritic intrusive rocks
- LJr-Fq - Francois Lake Suite high level quartz phyric, felsitic intrusive rocks
- LJr-Fg - Francois Lake Suite - Endako Subsuite granodioritic intrusive rocks
- LJr-F - Francois Lake Suite - Endako Subsuite - Francois Subphase granodioritic intrusive rocks
- LJr-E - Francois Lake Suite - Endako Subsuite - Endako Phase granodioritic intrusive rocks
- LJr-Cs - Francois Lake Suite - Endako Subsuite - Casey Phase granite, alkali feldspar granite intrusive rocks
- LJr-N - Francois Lake Suite - Glenannan Subsuite - Nithi Phase quartz monzonitic to monzogranitic intrusive rocks
- LJr-Na - Francois Lake Suite - Glenannan Subsuite - Nithi Phase quartz monzonitic to monzogranitic intrusive rocks
- LJr-TC - Francois Lake Suite - Glenannan Subsuite - Tatin Lake Subphase granite, alkali feldspar granite intrusive rocks
- LJr-G - Francois Lake Suite - Glenannan Subsuite - Glenannan Phase granite, alkali feldspar granite intrusive rocks
- Jr-O - Stag Lake Plutonic Suite - Overlander Phase dioritic intrusive rocks
- MJr-Sa - Stag Lake Plutonic Suite quartz dioritic intrusive rocks
- MJr-S - Stag Lake Plutonic Suite - Stellako Phase quartz dioritic intrusive rocks
- MJr-TI - Stag Lake Plutonic Suite - Tintagel Phase granite, alkali feldspar granite intrusive rocks
- MJr-SH - Stag Lake Plutonic Suite - Sheraton Phase quartz monzonitic to monzogranitic intrusive rocks
- MJr-Ba - Stag Lake Plutonic Suite - Boer Phase quartz dioritic intrusive rocks
- MJr-SU - Stag Lake Plutonic Suite - McKnab Phase - Sutherland Subphase quartz dioritic intrusive rocks
- MJr-C - Stag Lake Plutonic Suite - Caledonia Phase quartz monzonitic to monzogranitic intrusive rocks
- MJr-TM - Stag Lake Plutonic Suite - Twenty-Six Mile Phase dioritic intrusive rocks
- MJr-L - Stag Lake Plutonic Suite - Limit Lake Phase quartz dioritic intrusive rocks

Triassic to Jurassic

- uPrTr-T - Taltapin Metamorphic Complex lower amphibolite/kyanite grade metamorphic rocks

Triassic Intrusive rocks

- LTr-S - Stern Creek Plutonic Suite - Stern Creek Phase dioritic intrusive rocks
- LTr-Bc - Butterfield Lake Intrusive Complex serpentinite ultramafic rocks

Lower Permian

- uCb-P - Cache Creek Complex - Pope Succession basaltic volcanic rocks
- uCb-Pa - Asitka Group mudstone, siltstone, shale fine clastic sedimentary rocks

Late Proterozoic to Late Paleozoic

- KTgn_N - Wolverine Metamorphic Complex paragneiss metamorphic rocks

2.1.2. Regional Magnetic Data

Regional magnetic data (Figure 2.1) indicate that most intrusive phases related to the Late Jurassic Francois Lake plutonic suite are weakly magnetic to non-magnetic. The Endako deposit is situated in a magnetic low occurring within the otherwise magnetic Endako quartz monzonite subsuite of the Francois Lake Intrusive Suite. Dioritic rocks from the Late Triassic Stern Creek plutonic suite to the northeast are strongly magnetic, as are Middle Jurassic Stag Lake plutonic suite rocks in the northwest. Eocene Endako Formation and Cretaceous Kasalka Group andesitic rocks surround the major intrusive units. These volcanic rocks appear to be moderately to strongly magnetic throughout most of this region. Mapped Eocene Ootsa Lake Formation volcanic rocks are also characterized by a moderate magnetic response.

2.2. Deposit Geology

The Endako quartz monzonite (EQM), a subsuite of the Francois Lake plutonic suite, is the direct host of the Endako molybdenum deposit (Figure 2.2). Bounding granitic intrusive rocks, the Francois Lake granite and the Casey granite, are younger than, and intrude, the EQM (Bysouth and Wong, 1995). The Casey granite has been dated at an age similar to that of late-stage molybdenite mineralization at Endako (ca. 145 Ma; Villeneuve et al., 2001), thus mineralization is considered to be genetically related to its intrusion. Within the EQM, molybdenite occurs with quartz in a series of east-northeast-striking vein systems distributed along a northwesterly trend, parallel to the contact between the EQM and the Casey granite.

Mineralization-proximal alteration phases include a potassic phase and a phyllic phase. The potassic phase is characterized by pink K-feldspar, and the phyllic phase by quartz+sericite+pyrite fracture and vein selvages of varying widths (Kimura et al., 1976). Phyllic alteration is documented to be the phase most consistently related to molybdenite mineralization (Selby et al., 2000). Pervasive argillic (kaolinite-bearing) alteration overprints all other alteration phases and is considered to be a late, post-mineral alteration stage (Selby et al., 2000). In argillic zones, kaolinite forms after plagioclase, causing the rock to become friable where intensely altered. Figure 2.3 shows the mine scale distribution of alteration assemblages at Endako. The southeast end of the mineralized area exhibits the strongest potassic alteration (with lesser sericite and kaolinite present). More intense sericite and kaolinite alteration generally surrounds this potassic core. Mineralization and alteration in the southeasterly region of the deposit is flanked to the north and south by a pyrite halo. To the northwest, sericite and kaolinite alteration is dominant.

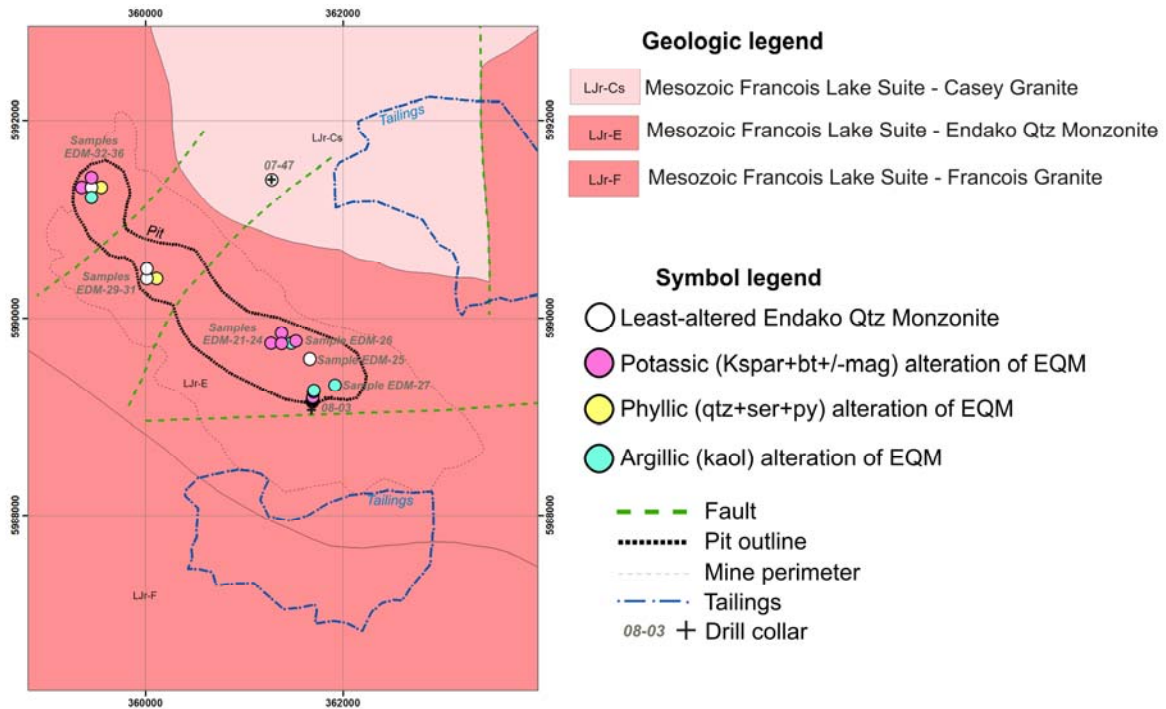


Figure 2.2. Plan-view of geology in the area of the Endako molybdenum deposit (Massey et al., 2005). The heavy black line indicates the extent of the open pit. The thin grey dashed line represents the outer margins of the mined area, and the blue dotted and dashed lines represent the tailings ponds. Drill core sample locations are projected to surface from depth. Drill core and hand sample symbols are colored based on alteration. Three of the drillholes sampled are located beyond the extents of the presented map and are thus not indicated. Abbreviations: bt=biotite, EQM=Endako Quartz Monzonite, kaol=kaolinite, Kspar=K-feldspar, mag=magnetite, monz=monzonite, py=pyrite, qtz=quartz, ser=sericite.

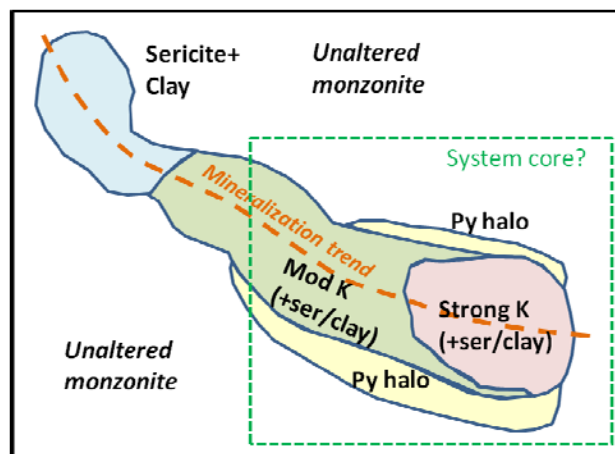


Figure 2.3. Schematic plan-view map of alteration affecting Endako quartz monzonite at the Endako mine. Map modified after Selby et al. (2000). Abbreviations: K=potassium, py=pyrite, ser=sericite.

2.3. Physical Properties of Rocks from the Endako Deposit

2.3.1. Sample Suite

Forty drill core samples were collected from four drillholes. Sixteen hand samples were collected from the Endako open pits. An effort was made to sample the range of alteration assemblages represented within the Casey granite and Endako quartz monzonite rocks, and to sample the least-altered protoliths. For presentation in graphs and plots in this report, rocks are grouped into sub-suites based on lithology and alteration. Some samples were omitted from plots if they did not fall into one of the primary lithological or alteration sub-suites. Sample descriptions and physical property data are tabulated in Appendix 8.

2.3.2. Magnetic Susceptibility and Deposit Scale Magnetic Data

Least-altered Endako quartz monzonite (EQM) was sampled from the shallow depths of drillhole 08-35. Magnetic susceptibility values were relatively consistent along the core, with values around 25×10^{-3} SI units, reflecting the presence of accessory magnetite (Figure 2.4)

In order to compare the magnetic susceptibility measurements of altered EQM samples, they were grouped based on the predominant or latest apparent alteration phase. Altered EQM, regardless of alteration assemblage, is characterized by consistently low susceptibilities (Figure 2.4), indicating that accessory magnetite is destroyed in association with one or more of the hydrothermal alteration events overprinting it. Even very weak overprinting argillic alteration causes magnetite destruction. Figure 2.5 compares a relatively fresh EQM sample with a kaolinite-altered EQM sample, the associated susceptibility values dropping significantly from 19×10^{-3} to 0.27×10^{-3} SI units. Magnetic susceptibility thus represents a useful measure for recognizing subtle alteration.

Airborne magnetic data reflects sample-scale trends; a magnetic low is indicated in the AeroTEM survey magnetic data in the area underlying the Endako pits, contrasting with surrounding highs representing unaltered EQM.

The Casey granite does not contain primary magnetite and therefore is associated with low susceptibilities. This unit is spatially correlated with a low within the Endako magnetic data (Figure 2.4). Post-mineral basalt dike samples from the deposit area are associated with high susceptibilities.

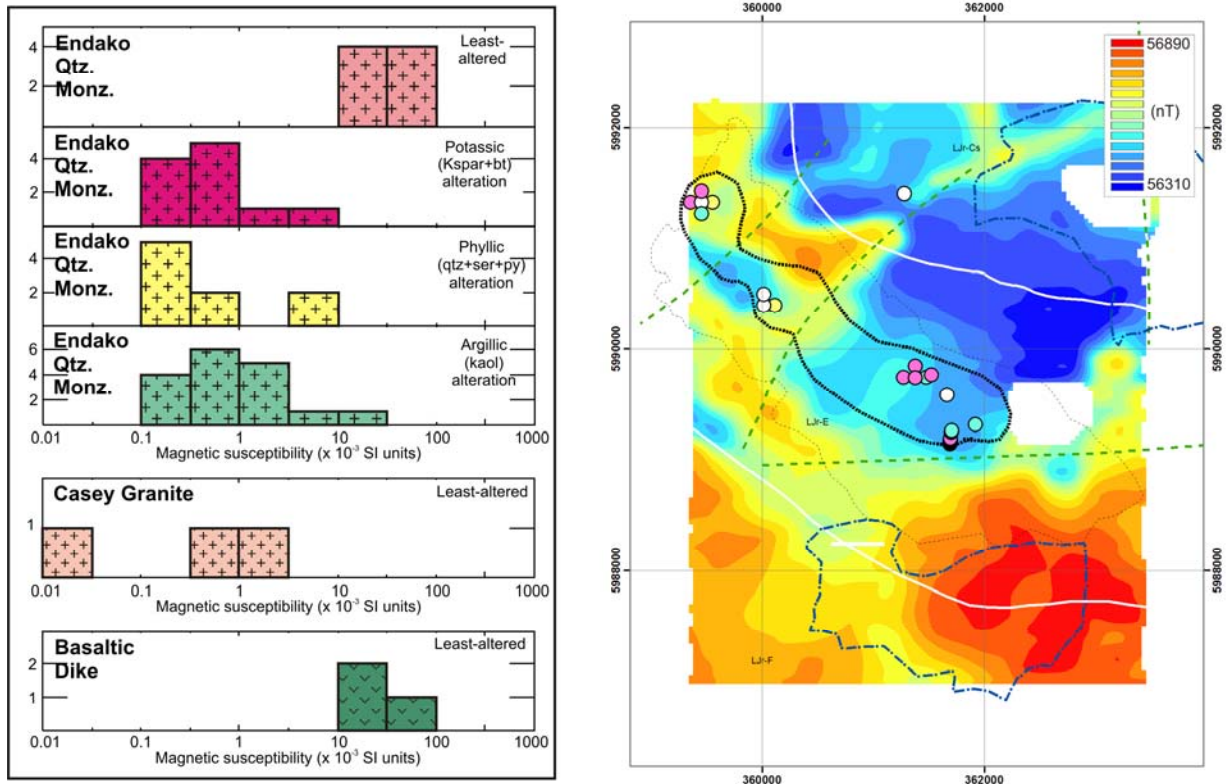


Figure 2.4. Magnetic susceptibility data from Endako quartz monzonite, Casey granite and basalt dike samples, and total magnetic intensity data (Aeroquest Surveys, 2009) from the Endako molybdenum deposit. Abbreviations: bt=biotite, kaol=kaolinite, Kspar=K-feldspar, monz=monzonite, py=pyrite, qtz=quartz, ser=sericite.

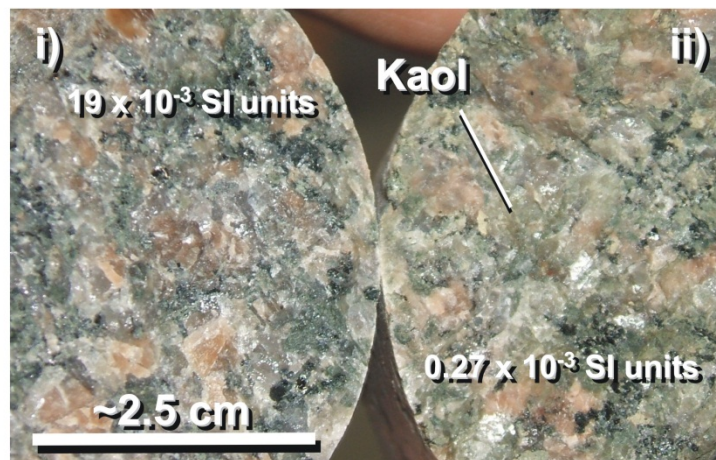


Figure 2.5. Comparison of least-altered Endako quartz monzonite (i), with weakly kaolinite (kaol)-altered Endako quartz monzonite (ii). The susceptibility drops significantly between samples, from 19×10^{-3} SI units (least-altered sample on left) to 0.27×10^{-3} SI units (weakly kaolinite-altered sample on right).

The destruction of magnetite associated with the alteration and mineralization of the EQM host rocks results in low susceptibility values. The Koenigsberger ratio is much higher for the altered samples (from 0.46 to 3.18, geometric averages, Appendix 8) suggesting that the alteration selectively removes the large less magnetically stable magnetite grains. The use of magnetic data, magnetic susceptibility data, and related models, may highlight potentially prospective hydrothermally altered areas within monzonite in this region.

Magnetic surveys have been useful in outlining the contact between the low susceptibility Casey granite and the EQM. Modelling magnetic susceptibility distributions in the subsurface via magnetic inversion could help to further define the 3D geometry of this important contact.

2.3.3. Density and Porosity

It is difficult to discriminate between least-altered and altered Endako quartz monzonite (EQM) samples in the Endako deposit area based on density, due to the overlap in ranges of density data (Figure 2.6).

From histograms, alteration has no apparent effect on density. Densities are generally under 2.7 g/cm^3 , consistent with other intrusive rocks from the BC porphyry deposit sample suite from this study. Casey granite samples have slightly lower densities. Post-mineral basalt dikes have average values only marginally higher than monzonite and granite densities. Their low densities relative to other basaltic rocks sampled during this study, could be due to their plagioclase-rich compositions.

Porosities range up to nearly 5% for Endako samples, with phyllic (quartz+sericite+pyrite) and argillic (kaolinite)-altered samples having the highest porosities. Porosity of least-altered EQM averages less than 1%.

There is a clear trend between porosity and density data collected from Endako samples (Figure 2.7). This sample suite is dominated by rocks from a single intrusive unit, making it easier to compare and interpret trends in physical property data. The increase in porosity of Endako samples is linked to intensity of alteration. Alteration of monzonitic and granitic rocks at Endako causes the rocks to become more friable, resulting in a mass loss and subsequent decrease in density.

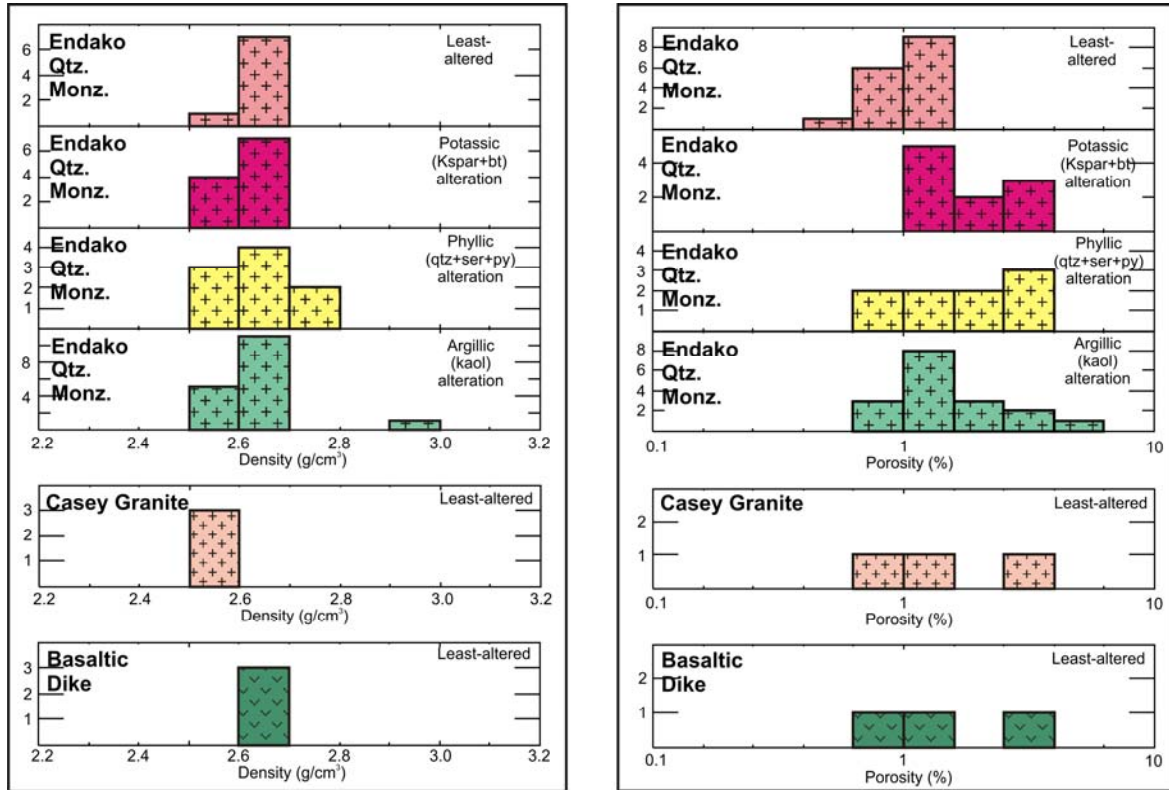


Figure 2.6. Density and porosity data from the Endako deposit. Abbreviations: bt=biotite, kaol=kaolinite, Kspar=K-feldspar, monz=monzonite, py=pyrite, qtz=quartz, ser=sericite.

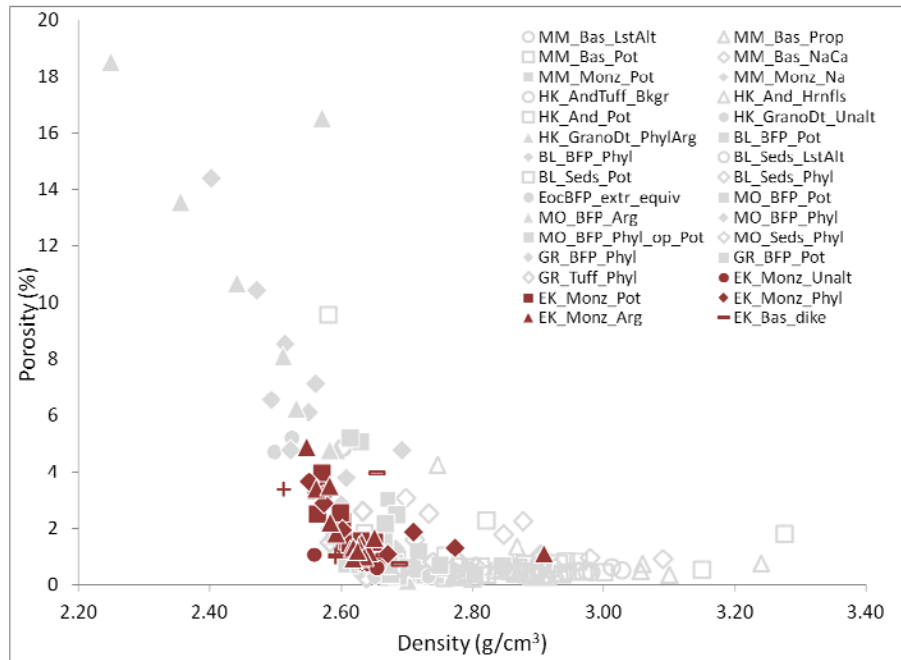


Figure 2.7. Density versus porosity data for all porphyry samples from this study. Endako samples are highlighted in red. There is a clear trend of decreasing densities with increasing porosities which is linked to an increase in alteration intensity. Deposit abbreviations: BL=Bell, EK=Endako, GR=Granisle, HK=Huckleberry, MM=Mount Milligan, MO=Morrison. Rock type abbreviations: And=Andesite, Bas=basalt, BFP=biotite-feldspar porphyry, EocBFP_extr_equiv=Eocene biotite-feldspar porphyry extrusive equivalent, Gran=granite, GranoDt=granodiorite, Monz=monzonite, Seds=sedimentary rocks. Alteration assemblage abbreviations: Arg=argillic, Bkgr=background, Hrnfls=hornfels, LstAlt=least-altered, Na=sodic, NaCa=sodic-calcic, Phyl=phyllic, Phyl_op_Pot=potassic with overprinting phyllic alteration, Pot=potassic, Prop=propylitic, Unalt=unaltered.

2.3.4. Resistivity Data and Deposit Scale Conductivity Data

Least-altered Endako quartz monzonite samples are relatively resistive with resistivity always >1000 Ohm-m (Figure 2.8). Resistivity decreases with alteration; altered EQM samples have resistivities ranging down to 252 Ohm-m, and the geometric average drops from 7600 to 1800 Ohm-m. Two least-altered Casey granite samples have moderate to high resistivities surpassing 24000 Ohm-m. Post-mineral basalt dikes are relatively low resistivity, a consequence of higher porosities which may be related to the presence of amygdules.

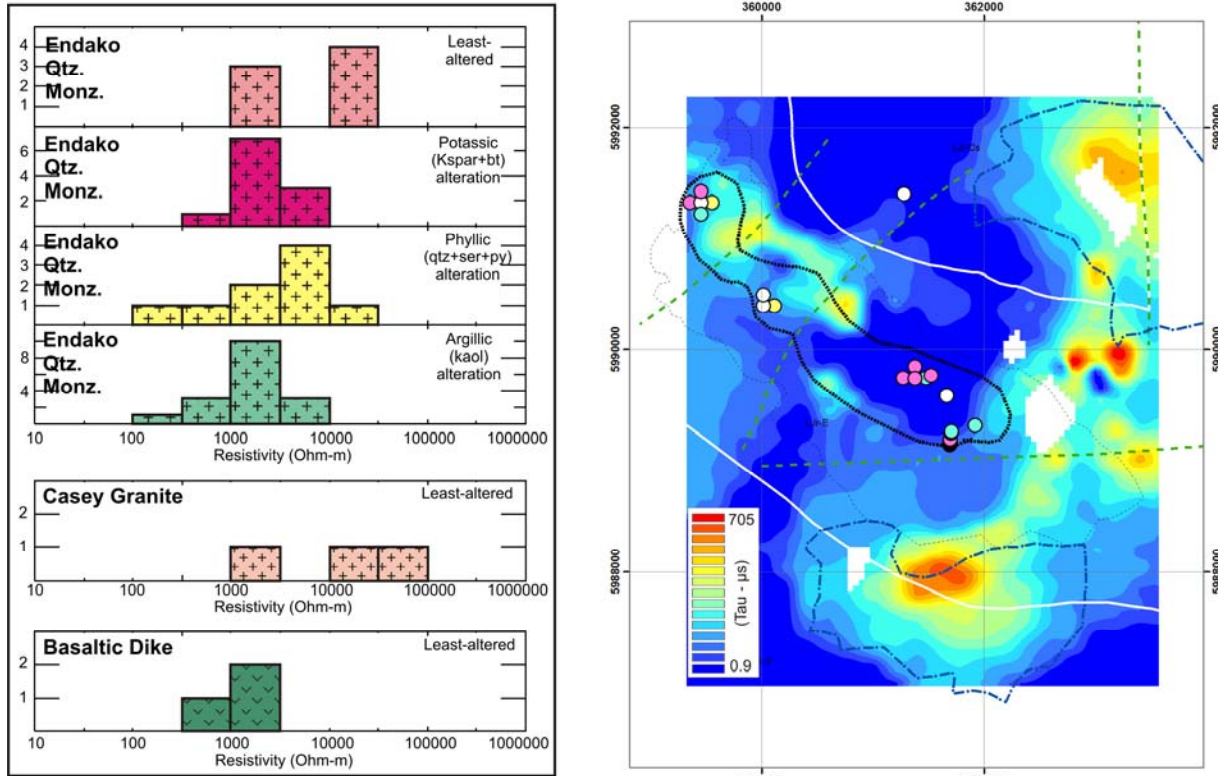


Figure 2.8. Resistivity data from the Endako deposit, and late time Tau map from AeroTEM data (Aeroquest Surveys, 2009) collected over the Endako deposit. Abbreviations: bt=biotite, kaol=kaolinite, Kspar=K-feldspar, monz=monzonite, py=pyrite, qtz=quartz, ser=sericite.

The lower resistivities (higher conductivities) associated with altered EQM samples could be related in part to mineralogy. Higher conductivities might be attributed to the presence of pyrite in samples altered to phyllic quartz+sericite+pyrite assemblages. However, pyrite contents from collected samples are not particularly high, with the most pyrite-rich sample containing only 3.5% pyrite. The presence of clays which are semi-conductors could also lower resistivity.

A potentially more influential variable in lowering resistivities of EQM samples is porosity. Higher porosities and higher groundwater content of the friable clay-altered rocks likely play the most important role in lowering resistivity in the EQM sample suite. This relationship is illustrated in a plot of resistivity versus porosity (Figure 2.9). A distinct negative correlation is present, with least-altered samples characterized by low porosities and high resistivities, and altered samples having high porosities and lower resistivities.

Some conductivity anomalies within Endako airborne electromagnetic data (Aeroquest Surveys, 2009) may be explained by the aforementioned alteration-porosity relationships. To visualize subsurface

conductivity, Tau, reflecting EM response decay time, is calculated from EM data. High Tau values indicate the presence of conductors within the subsurface (Aeroquest Surveys, 2009). Referring to the late time Tau map for the Endako area (Figure 2.8), it is apparent that some of the conductivity highs in the east are in fact related to interference from mine features and infrastructure. An anomaly over the northwestern Endako open pit however, corresponds to the most strongly clay-altered rocks within the mine as depicted on the Endako alteration map (Figure 2.3). Anomalies related to tailings and culture may be removed, and true geologic anomalies within the subsurface may be better differentiated through constrained geophysical inversion modelling.

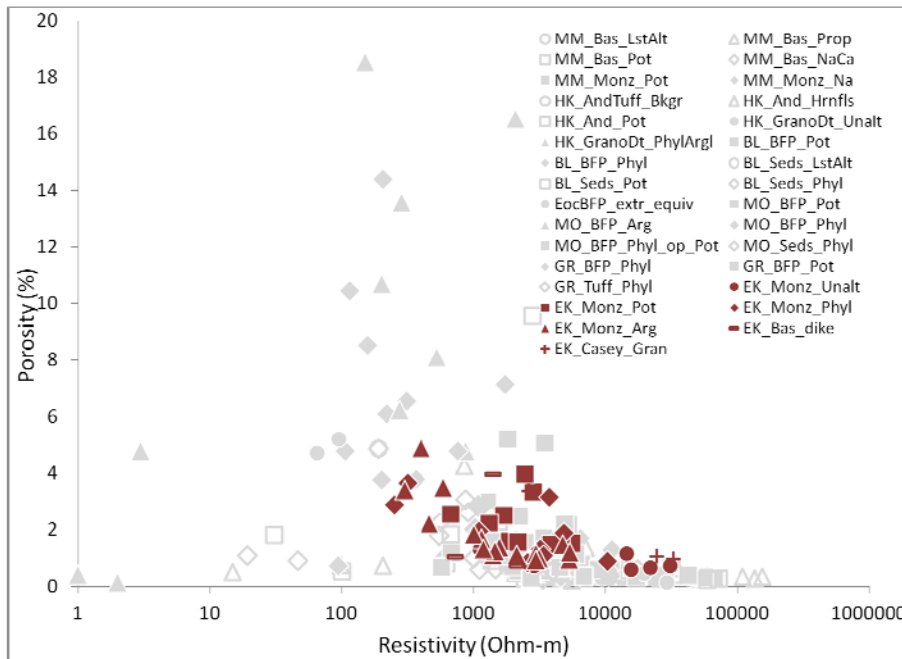


Figure 2.9. Resistivity versus porosity data for all porphyry samples from this study. Endako samples are highlighted in red. Deposit abbreviations: BL=Bell, EK=Endako, GR=Granisle, HK=Huckleberry, MM=Mount Milligan, MO=Morrison. Rock type abbreviations: And=Andesite, Bas=basalt, BFP=biotite-feldspar porphyry, EocBFP_extr_equiv=Eocene biotite-feldspar porphyry extrusive equivalent, Gran=granite, GranoDt=granodiorite, Monz=monzonite, Sed=sedimentary rocks. Alteration assemblage abbreviations: Arg=argillic, Bkgr=background, Hrnfls=hornfels, LstAlt=least-altered, Na=sodic, NaCa=sodic-calcic, Phyl=phyllic, Phyl_op_Pot=potassic with overprinting phyllic alteration, Pot=potassic, Prop=propylitic, Unalt=unaltered.

On a resistivity versus density plot (Figure 2.10), Endako samples plot along a positive trend with resistivity and density increasing as a function of decreasing porosities. This trend contrasts with that existing for Mount Milligan samples where low porosities and increased sulphide abundances decrease resistivity, while maintaining or increasing density.

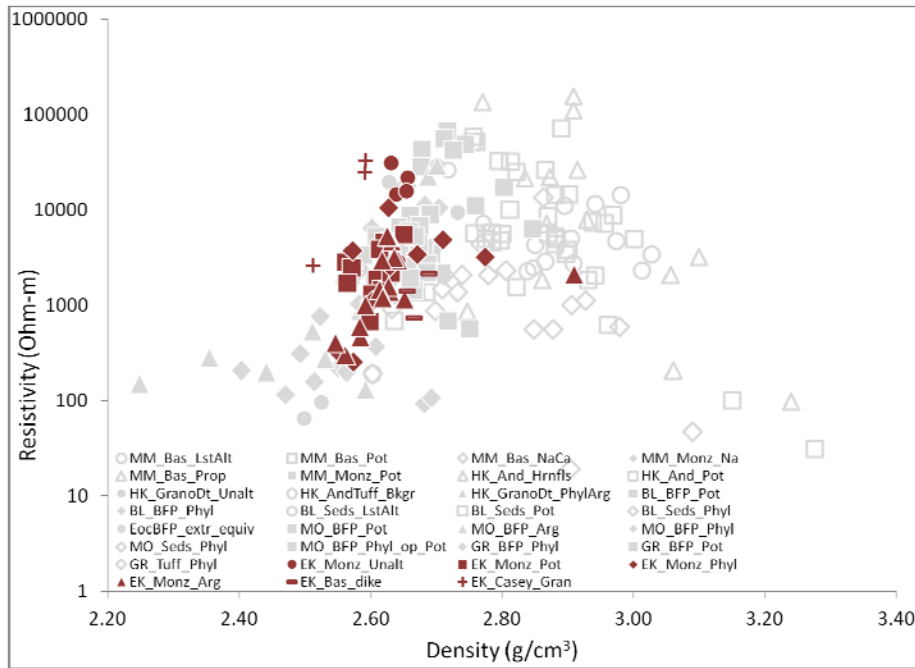


Figure 2.10. Resistivity versus density data for all porphyry samples from this study. Endako samples are highlighted in red. Deposit abbreviations: BL=Bell, EK=Endako, GR=Granisle, HK=Huckleberry, MM=Mount Milligan, MO=Morrison. Rock type abbreviations: And=Andesite, Bas=basalt, BFP=biotite-feldspar porphyry, EocBFP_extr_equiv=Eocene biotite-feldspar porphyry extrusive equivalent, Gran=granite, GranoDt=granodiorite, Monz=monzonite, Seds=sedimentary rocks. Alteration assemblage abbreviations: Arg=argillic, Bkgr=background, Hrnfls=hornfels, LstAlt=least-altered, Na=sodic, NaCa=sodic-calcic, Phyl=phyllic, Phyl_op_Pot=potassic with overprinting phyllic alteration, Pot=potassic, Prop=propylitic, Unalt=unaltered.

2.4. References

- Aeroquest Surveys (2009): Report on a helicopter-borne AeroTEM system electromagnetic & magnetic survey; Geoscience BC, Report 2009-6, 28 p.
- Bysouth, G.D. and Wong, G.Y. (1995): The Endako molybdenum mine, central British Columbia: an update; *in* Porphyry Deposits of the North western Cordillera of North America, T.G. Schroeter (ed.), Canadian Institute of Mining, Metallurgy and Petroleum, Special Volume 46, p. 697–703.
- Kimura, E.T, Bysouth, G.D. and Drummond, A.D. (1976): Endako; *in* Porphyry deposits of the Canadian Cordillera, A. Sutherland Brown (ed.), Canadian Institute of Mining and Engineering, Special Volume 15, p. 444–454.
- Massey, N.W.D, MacIntyre, D.G., Desjardins, P.J. and Cooney, R.T. (2005): Digital geology map of British Columbia: whole province; B.C. Ministry of Energy and Mines, Geofile 2005-1, URL <<http://www.empr.gov.bc.ca/Mining/Geoscience/PublicationsCatalogue/GeoFiles/Pages/2005-1.aspx>> [November 2007].
- Natural Resources Canada (2004): Canadian aeromagnetic data base, Continental Geoscience Division, Geological Survey of Canada, Earth Sciences Sector, Natural Resources Canada, Geoscience Data Repository, URL <<http://gdrdap.agg.nrcan.gc.ca/geodap/home/Default.aspx?lang=e>> [March 2011].
- Selby, D., Nesbitt, B.E., Muehlenbachs, K. and Prochaska, W. (2000): Hydrothermal alteration and fluid chemistry of the Endako porphyry molybdenum deposit, British Columbia; *Economic Geology*, v. 95, p. 183–202.
- Villeneuve, M, Whalen, J.B., Anderson, R.G. and Struik, L.C. (2001): The Endako batholith: episodic plutonism culminating in formation of the Endako porphyry molybdenite deposit, north-central British Columbia; *Economic Geology*, v. 96, p. 171–196.

Appendix 3. Huckleberry

3.1. Regional Geology and Magnetic Data

3.1.1. Regional Geologic Setting

The Huckleberry deposit occurs within the Stikine Terrane of west-central British Columbia. The underlying geology (Figure 3.1) is dominated by Early to Middle Jurassic volcanic, volcanoclastic, and sedimentary rocks of the Telkwa and Smithers formations of the Hazelton Group (Jackson and Illerbrun, 1995). These sequences are overlain by volcanic and sedimentary rocks of the Cretaceous Kasalka and Skeena Groups. Jurassic and Cretaceous stratigraphy is intruded by plutons related to the Late Cretaceous Bulkley plutonic suite.

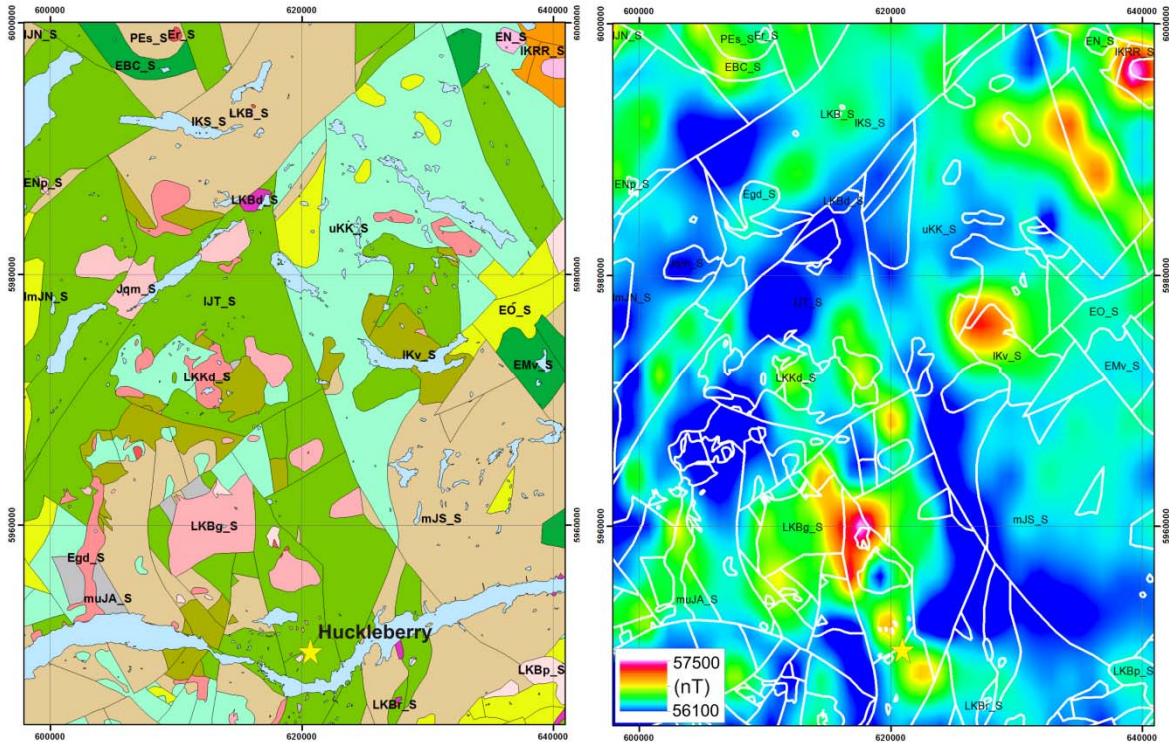

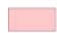




Figure 3.1. Regional geological setting for the Huckleberry porphyry copper deposit (Massey et al., 2005), and regional total magnetic intensity data from Geoscience BC's QUEST-West project (Aeroquest Surveys, 2009).





Regional Geology of the Huckleberry Deposit

Legend



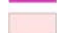
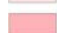
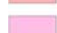
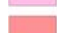
Eocene Intrusive Rocks

-  EN_S - Nanika Plutonic Suite intrusive rocks, undivided
-  ENp_S - Nanika Plutonic Suite quartz monzonitic intrusive rocks
-  Egd_S - Boundary Stock granodioritic intrusive rocks
-  Er_S - Unnamed high level quartz phyric, felsitic intrusive rocks

Paleocene to Eocene

-  EO_S - Ootsa Lake Group rhyolite, felsic volcanic rocks
-  EBC_S - Endako Group - Buck Creek Formation basaltic volcanic rocks
-  EMv_S - Endako Group basaltic volcanic rocks
-  PEs_S - Unnamed undivided sedimentary rocks



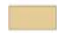

Late Cretaceous Intrusive Rocks

-  LKBr_S - Bulkley Plutonic Suite high level quartz phyric, felsitic intrusive rocks
-  LKBd_S - Bulkley Plutonic Suite dioritic intrusive rocks
-  LKBp_S - Bulkley Plutonic Suite feldspar porphyritic intrusive rocks
-  LKBg_S - Bulkley Plutonic Suite quartz dioritic intrusive rocks
-  LKB_S - Bulkley Plutonic Suite intrusive rocks, undivided
-  LKKd_S - Kasalka Plutonic Suite granodioritic intrusive rocks

Late Cretaceous

-  Kasalka Group
-  uKK_S - Kasalka Group andesitic volcanic rocks



Early Cretaceous

-  Skeena Group
-  IKv_S - Skeena Group - Mt. Ney Volcanics undivided volcanic rocks
-  IKS_S - Skeena Group undivided sedimentary rocks
-  IKRR_S - Skeena Group - Red Rose Formation coarse clastic sedimentary rocks

Middle to Late Jurassic

-  Bowser Lake Group
-  muJA_S - Bowser Lake Group - Ashman Formation mudstone, siltstone, shale fine clastic sedimentary rocks

Early and Middle Jurassic

-  Hazelton Group
-  mJS_S - Hazelton Group - Smithers Formation undivided sedimentary rocks
-  ImJN_S - Hazelton Group - Nanika Volcanics rhyolite, felsic volcanic rocks
-  IJN_S - Hazelton Group - Nilkitkwa Formation undivided sedimentary rocks
-  IJT_S - Hazelton Group - Telkwa Formation calc-alkaline volcanic rocks

Mesozoic Intrusive Rocks

-  Jqm_S - Unnamed quartz monzonitic intrusive rocks

3.1.2. Regional Magnetic Data.

Regional AeroTEM magnetic data from Geoscience BC's QUEST-West project indicates that the Lower Jurassic Hazelton volcanic rocks in west central BC typically yield a weak magnetic response. This could be due to a magnetite-poor composition, or to being dominated by relatively porous volcanoclastic facies which tend to be more susceptible to hydrothermal alteration. Jurassic and Cretaceous sedimentary units generally lack a magnetic response. Although magnetic anomalies in the region can commonly be correlated to mapped intrusive rocks, not all intrusive phases are magnetic. Other magnetic anomalies might represent unmapped intrusive bodies, or could be indicative of magnetite-rich hornfels similar to that which surrounds granodiorite intrusions within the Huckleberry mine area (Jackson and Illerbrun, 1995).

3.2. Deposit Geology

Hazelton Group volcanic rocks in the Huckleberry deposit area are predominantly andesitic lapilli and crystal tuffs (MacIntyre, 1985). Outside of the mine area, these tuffaceous units are variably altered to hematitic or sericite-chlorite assemblages, the rocks consequently taking on a red or a green color (Marsden and Thorkelson, 1992). The secondary mineral assemblages represent their deposition in alternately subaerial and subaqueous settings. The intrusion of the Bulkley granodiorite led to contact metamorphism and hornfels development in the Hazelton Group volcanic rocks, which resulted in addition of biotite, amphibole, chlorite, magnetite, hematite and pyrite to the host andesite (Jackson and Illerbrun, 1995). Mineralization at Huckleberry occurs in proximity to the Bulkley granodiorite stocks. The Main zone is located on the eastern flank of the western granodiorite stock, and the East zone occurs within and adjacent to the eastern stock (Figure 3.2). The Main Zone Extension sits north of the Main zone, and represents the newest open pit at Huckleberry, where mining is currently being focused.

The geological setting of the Huckleberry deposit is similar to that of Mount Milligan, with mineralization sitting predominantly within volcanic sequences at the margins of porphyritic stocks. The intrusive rocks at Huckleberry, however, are calc-alkalic in nature, as at Endako, and alteration assemblages include sericite and clays, mineral phases that are less common in alkalic systems (Holliday and Cooke, 2007), and occur in limited abundance at Mount Milligan. Distal alteration at Huckleberry is characterized by propylitic chlorite+epidote+pyrite assemblages. Proximal alteration assemblages include biotite, K-feldspar, quartz, amphibole, chlorite and sericite. Granodiorite intrusive rocks are overprinted additionally by sericite+kaolinite alteration. Chalcopyrite-bearing veins in samples collected for this study have K-feldspar, quartz and biotite haloes (Figure 3.3). Sulphide mineralization is predominantly fracture-

hosted. Chalcopyrite and bornite occur in narrow veins and as fracture coatings within andesitic host rocks and, to a lesser degree, within granodiorite intrusions. Lesser molybdenite occurs in thin fractures which appear to postdate chalcopyrite-hosting fractures (James, 1976).

As a result of earlier contact metamorphism, the volcanic rocks within the Huckleberry mine area are extremely silicified and hard. The silicified state of the rock potentially influenced the brittle fracture and vein-controlled nature of mineralization at Huckleberry.

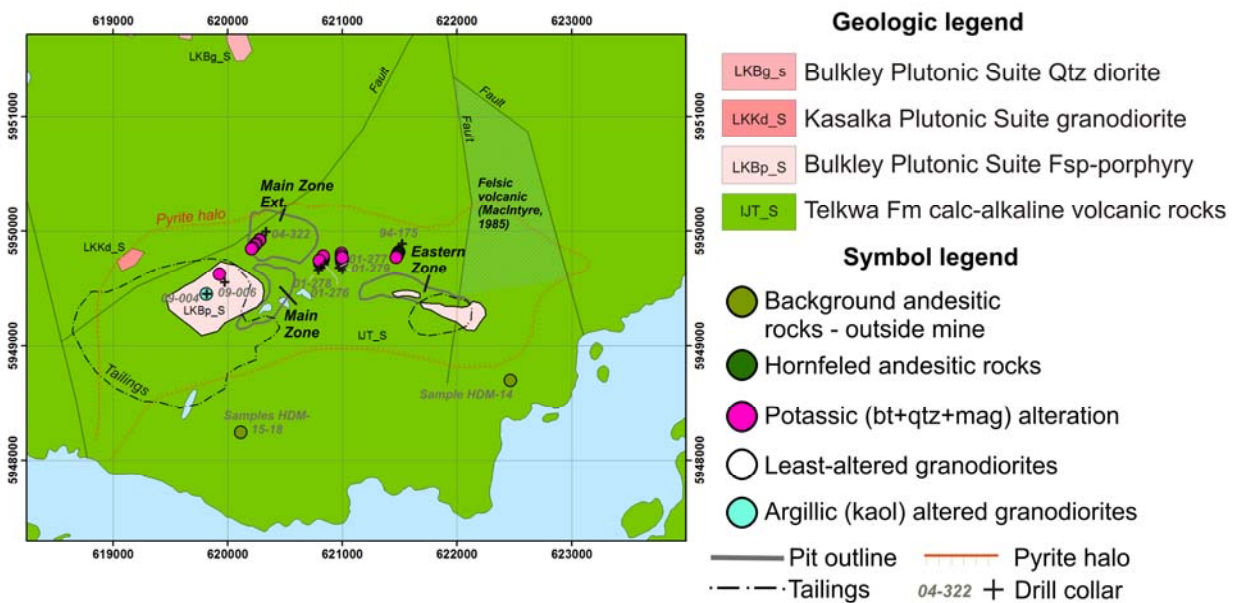


Figure 3.2. Plan-view geology of the Huckleberry mine area (after Massey et al., 2005), showing the three mineralized zones, the Main, East, and Main Extension zones, as well as granodiorite intrusive rocks. Drill core sample locations are projected to surface from depth ('01' drill core series samples are P. Ogryzlo library core). Drill core and hand sample symbols are colored based on alteration.



Figure 3.3. Quartz-chalcopyrite vein with a bleached, K-feldspar+quartz-bearing alteration selvage crosscutting andesitic and granodioritic rocks from the Main zone of the Huckleberry copper deposit.

3.3. Physical Properties of Rocks from the Huckleberry Deposit

3.3.1. Sample Suite

Fifteen andesitic tuff samples were collected from two drillholes on the Huckleberry property: hole 04-322, which intersects moderately mineralized rocks of the Main Extension zone, and hole 94-175, intersecting less mineralized, propylitically-altered rocks just north of the East zone. A handheld KT-9 susceptibility meter was used to collect 189 supplementary magnetic susceptibility measurements along several intervals from each of these two holes.

Only four granodiorite samples were collected from core drilled in 2009; granodiorite is not regularly intersected as most of the mineralization at Huckleberry occurs within the surrounding volcanic rocks. An additional five granite to granodiorite samples were collected from drill core from a 2007 drill program focused on an area 10 km northeast of Huckleberry mine. Drillhole samples (with the exception of samples from 2007 holes) are projected to surface on the map shown in Figure 3.2.

Four hand samples were collected south of the deposit, and represent subaerially and subaqueously deposited andesitic volcanic rocks, and a post-mineral dike from outside the influence of the intrusions and mineralizing system. Another hand sample, collected on the property southeast of the deposit, comes from an outcrop apparently sitting outside the contact metamorphic halo. Two mineralized samples were collected from the Main Extension pit.

A drill core library with representative lithologic units and alteration assemblages from a 2001 drilling program was assembled by former Huckleberry mine geologist Peter Ogryzlo. KT-9 susceptibility measurements were made on library samples from eight drill holes, and this helped to establish an

improved understanding of alteration distribution in the mine area. Susceptibility measurements from 2001 library core samples are projected to the map surface along with other plotted samples in Figure 3.2. These measurements are not included in histograms or plots generated for interpretation, as library core was only examined on site and not sampled for additional physical property or mineralogical analyses.

3.3.2. Magnetic Susceptibility and Deposit Scale Magnetic Data

Magnetic susceptibility data from Huckleberry are displayed in histogram format in Figure 3.4. Andesitic rocks from outside the main mineralized zones have low to moderate susceptibilities ranging up to 56×10^{-3} SI units. Andesitic volcanic rocks hosting granodiorite intrusives were affected by contact metamorphism and converted to hornfels, a process that introduced significant magnetite to the rocks. Magnetic susceptibilities measured from samples collected from hornfelsed rocks are typically $>50 \times 10^{-3}$ SI units and range up to 180×10^{-3} SI units. Within this high-susceptibility zone, susceptibilities can locally decrease slightly where mineralized veins and fractures are associated with potassic quartz+biotite+feldspar alteration selvages. The marginal decrease in susceptibility with alteration is apparent in Figure 3.5 which compares downhole KT-9 susceptibility data measured on the more strongly mineralized 04-322 core, to susceptibility data measured on the generally unmineralized 94-175 core. Magnetite-destructive alteration may be localized to veins and fractures as a result of the poor permeability of the very competent silicified hornfels rocks.

From the small granodiorite sample suite collected, the single least-altered Main zone granodiorite sample is moderately susceptible (28×10^{-3} SI units). Susceptibilities decrease slightly with overprinting sericite and kaolinite alteration.

Magnetic data does not identify Huckleberry mineralized zones as distinct magnetic highs or lows. District scale magnetic data may still be useful however for distinguishing important geological targets. Figure 3.4 shows total magnetic intensity data collected over the Huckleberry deposit. At this scale, the mineralized zones lie generally within magnetic lows, which likely reflect the footprints of the relatively lower susceptibility granodiorites.

The broad magnetic high surrounding the Huckleberry deposit appears to represent the extent of hornfels development. Additional regional background samples are needed to confirm this. If the Telkwa volcanic rocks are normally magnetite-poor, then it may be possible to explore for magnetite-rich hornfels zones within them using magnetic data and inversion modelling. This might help to locate other unexposed Bulkley intrusive rocks in the area and, with subsequent fine-scale geophysics applied, it may be possible to detect variations related to hydrothermal alteration within these metamorphic haloes.

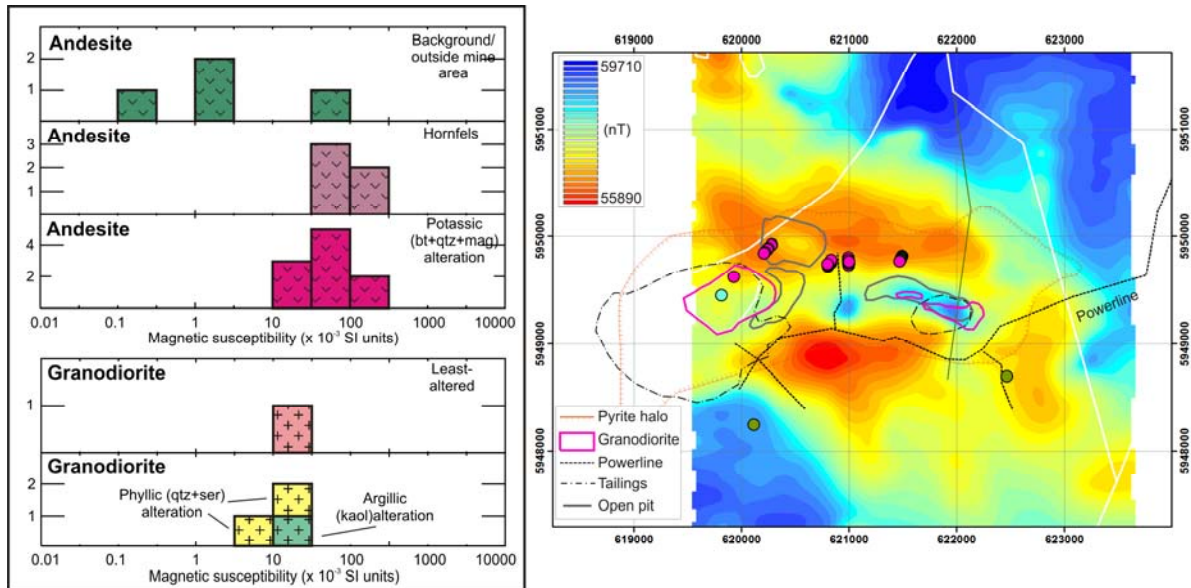


Figure 3.4. Magnetic susceptibility data from andesite and granodiorite samples, and total magnetic intensity data (Aeroquest Surveys, 2009) from the Huckleberry deposit. Abbreviations: bt=biotite, kaol=kaolinite, mag=magnetite, qtz=quartz, ser=sericite.

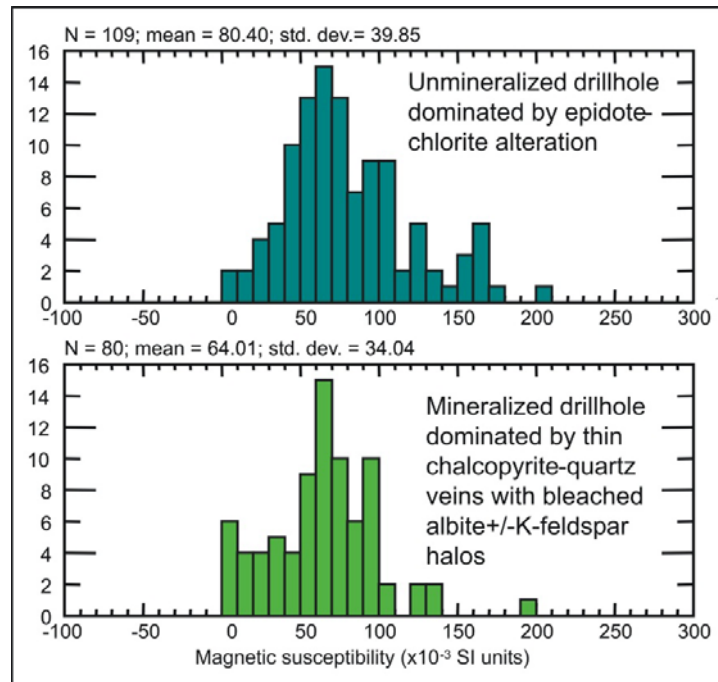


Figure 3.5. Comparison of KT-9 susceptibility measurements taken along poorly mineralized drill core from near the East zone and measurements taken along mineralized drill core from the Main Extension zone of the Huckleberry deposit. A slight decrease in average susceptibility values for mineralized rocks is apparent.

3.3.3. Density and Porosity

Histograms displaying density data for Huckleberry samples (Figure 3.6) show hornfelsed andesite samples have the highest average densities (2.87 g/cm³). Background andesitic tuff samples from outside the region affected by hornfelsing are less dense on average (2.78 g/cm³), which might reflect either a low density mineral assemblage or increased porosity. Potassically-altered samples are also lower density than hornfelsed samples, with decreased values attributed to an overall lower density mineral composition. One anomalously low-density potassically-altered sample is also characterized by an unusually high porosity. There is also one extremely high density potassic-altered andesite (sample HDM-007, not plotted on the histogram) containing 78% sulphide minerals with a density of 4.3 g/cm³.

A slight decrease in average density from andesite samples to granodiorite samples is apparent. As with Mount Milligan samples, this reflects the general increase in quartz and feldspar content. Kaolinite-altered granodiorite has the lowest associated density measurement.

Huckleberry samples have the lowest porosities of the porphyry sample collection, with almost all samples having <1% porosity with the exception of a strongly clay-altered granodiorite and an andesitic tuff sample. The Huckleberry deposit's low porosities and correlated high densities are compared to measurements from other porphyry samples in Figure 3.7.

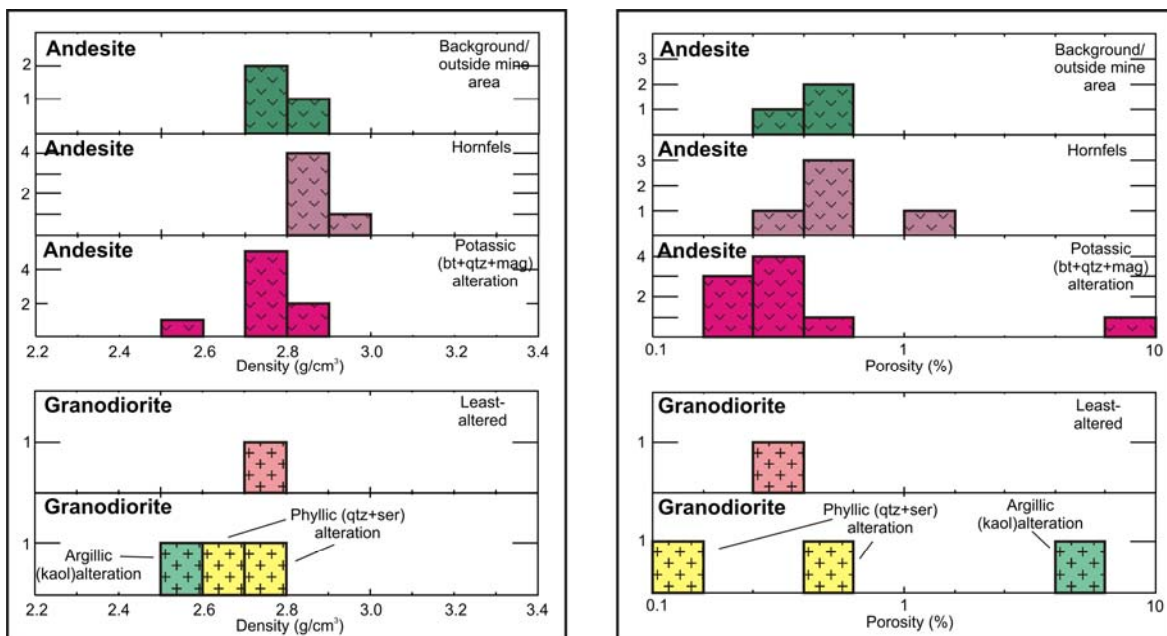


Figure 3.6. Density and porosity data from the Huckleberry deposit. Abbreviations: bt=biotite, kaol=kaolinite, mag=magnetite, qtz=quartz, ser=sericite.

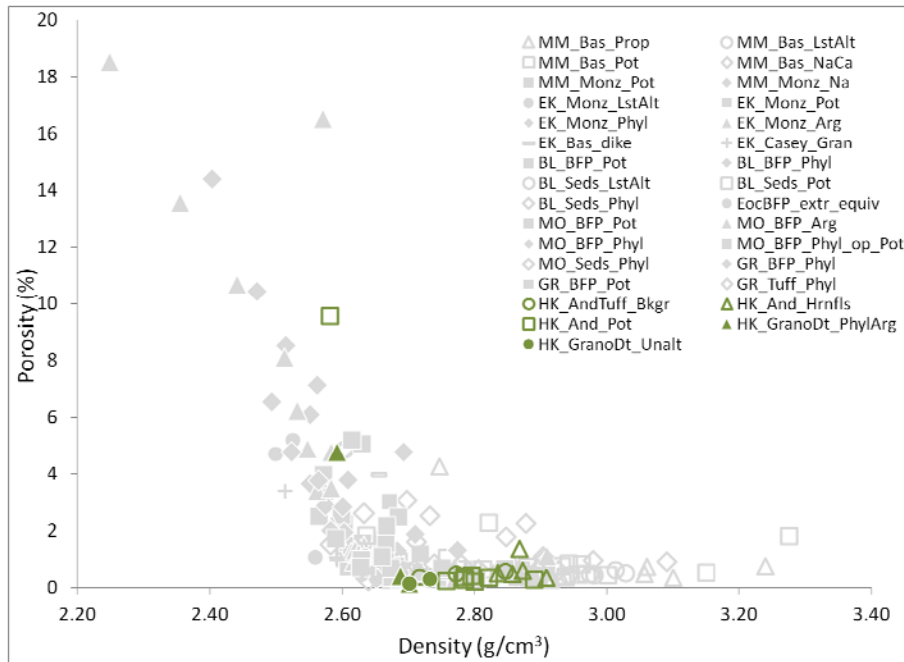


Figure 3.7. Density versus porosity data for all porphyry samples from this study. Huckleberry samples are highlighted in green. Deposit abbreviations: BL=Bell, EK=Endako, GR=Granisle, HK=Huckleberry, MM=Mount Milligan, MO=Morrison. Rock type abbreviations: And=Andesite, Bas=basalt, BFP=biotite-feldspar porphyry, EocBFP_extr_equiv=Eocene biotite-feldspar porphyry extrusive equivalent, Gran=granite, GranoDt=granodiorite, Monz=monzonite, Seds=sedimentary rocks. Alteration assemblage abbreviations: Arg=argillic, Bkgr=background, Hrnfls=hornfels, LstAlt=least-altered, Na=sodic, NaCa=sodic-calcic, Phyl=phyllic, Phyl_op_Pot=potassic with overprinting phyllic alteration, Pot=potassic, Prop=propylitic, Unalt=unaltered.

3.3.4. Resistivity Data and Deposit Scale Conductivity

Samples collected from Huckleberry are highly resistive (Figure 3.8). Hornfelsed and silicified rocks near mineralization are the most resistive samples of the porphyry deposit sample collection. Background andesitic rock samples collected from outside the hornfels zone have lower average resistivities which are likely linked to their marginally higher porosities. Additional regional volcanic rock samples should be collected in order to determine if there is a consistent resistivity contrast between background volcanic rocks and rocks proximal to the ore zone. An altered, and strongly mineralized sample from the Huckleberry pit plots off the lower range of the histogram, with an anomalously low resistivity of 0.23 Ohm-m. This extremely low resistivity measurement is due both to the presence of sulphides in the sample, and the fracture-controlled, connected nature of the sulphides.

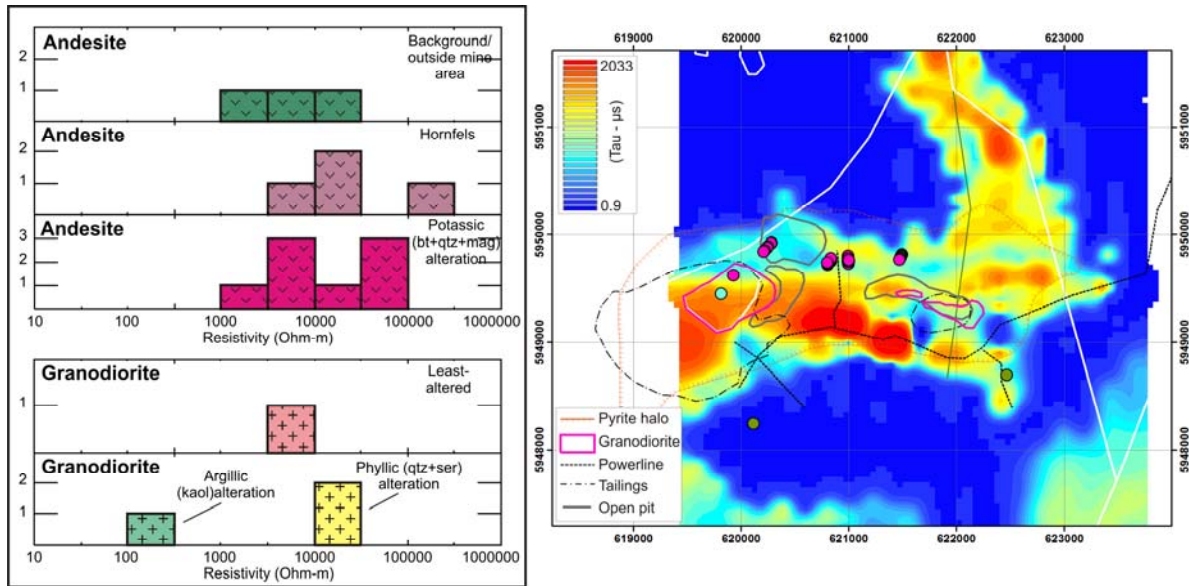


Figure 3.8. Resistivity data from the Huckleberry deposit, and late time Tau map from AeroTEM data (Aeroquest Surveys, 2009) collected over the Huckleberry deposit. Abbreviations: bt=biotite, kaol=kaolinite, mag=magnetite, qtz=quartz, ser=sericite.

Least-altered and phyllic-altered granodiorites have resistivities which fall within the upper and lower resistivity ranges for andesite samples (Figure 3.8). An anomalously low resistivity granodiorite sample is the same kaolinite-altered sample previously noted to have a high porosity. Enhanced porosities may explain reduced resistivities for some of the Huckleberry suite samples, however porosities measured for Huckleberry rocks are low overall compared with porosity data collected from other porphyry suites for this study (Figure 3.9).

Density and resistivity values follow the overall trend for this study, with the low measured porosities of Huckleberry samples leading to some of the highest resistivities observed within the porphyry suite (Figure 3.10). Two high porosity samples have lower resistivities and lower densities. Measurements on additional background volcanic rock samples and granodiorite samples may clarify relationships between resistivity, density, porosity, and mineralization.

AeroTEM late time Tau data (late time decay constant, Aeroquest Surveys, 2009) reveals moderate to high conductivities within mineralized areas (Figure 3.8). Based on the anomalously low resistivity (high conductivity) of a mineralized sample collected from the Huckleberry Main Extension pit (0.23 Ohm-m), and based on the existence of a strongly fracture-controlled sulphide network at Huckleberry, the Huckleberry ore zones are expected to be conductive. As with AeroTEM data collected from over the Endako deposit, however, some of this signal correlates with mine tailings and infrastructure such as

power lines. Constrained EM inversions may provide the means to differentiate between conductive surface features and sulphide-related conductors at depth. Outside the mineralized area, a string of high conductivity anomalies trend northward. These high conductivities correlate with a fault-bounded block of felsic volcanic rocks mapped by MacIntyre (1985).

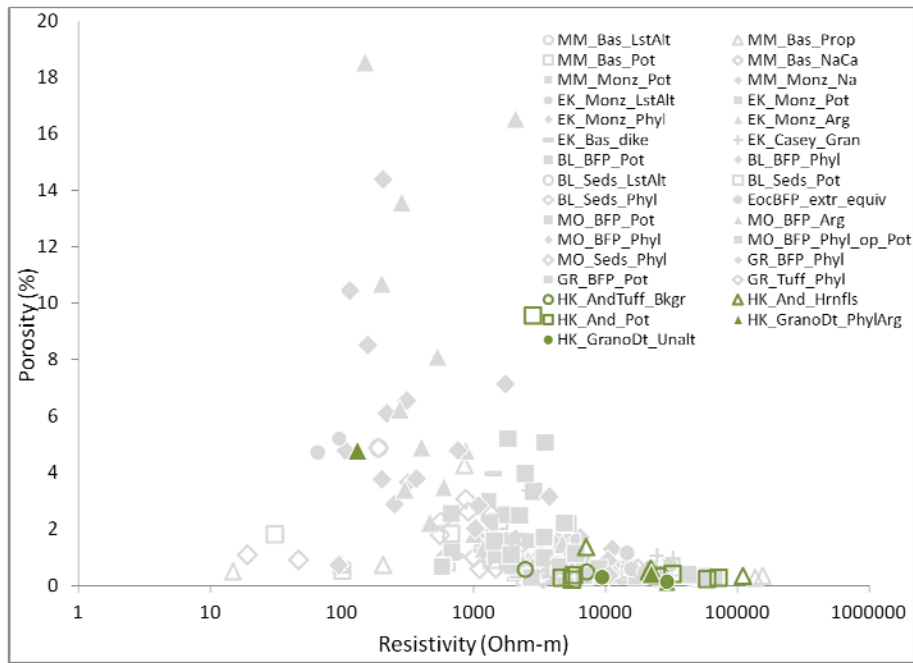


Figure 3.9. Resistivity versus porosity data for all porphyry samples from this study. Huckleberry samples are highlighted in green. Deposit abbreviations: BL=Bell, EK=Endako, GR=Granisle, HK=Huckleberry, MM=Mount Milligan, MO=Morrison. Rock type abbreviations: And=Andesite, Bas=basalt, BFP=biotite-feldspar porphyry, EocBFP_extr_equiv=Eocene biotite-feldspar porphyry extrusive equivalent, Gran=granite, GranoDt=granodiorite, Monz=monzonite, Seds=sedimentary rocks. Alteration assemblage abbreviations: Arg=argillic, Bkgr=background, Hrnfls=hornfels, LstAlt=least-altered, Na=sodic, NaCa=sodic-calcic, Phyl=phyllic, Phyl_op_Pot=potassic with overprinting phyllic alteration, Pot=potassic, Prop=propylitic, Unalt=unaltered.

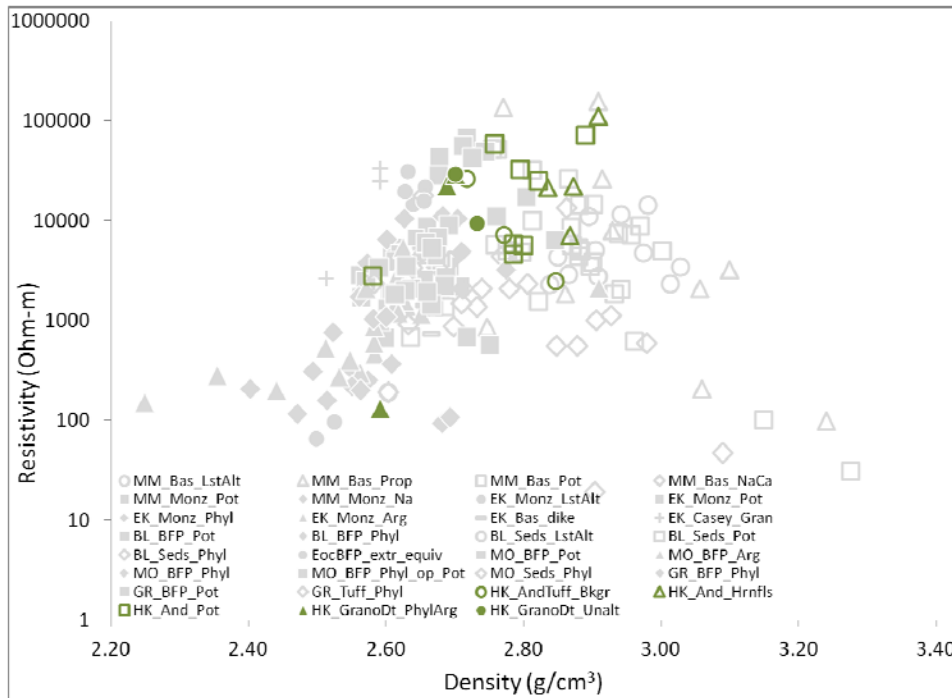


Figure 3.10. Resistivity versus density data for all porphyry samples from this study. Huckleberry samples are highlighted in green. Deposit abbreviations: BL=Bell, EK=Endako, GR=Granisle, HK=Huckleberry, MM=Mount Milligan, MO=Morrison. Rock type abbreviations: And=Andesite, Bas=basalt, BFP=biotite-feldspar porphyry, EocBFP_extr_equiv=Eocene biotite-feldspar porphyry extrusive equivalent, Gran=granite, GranoDt=granodiorite, Monz=monzonite, Seds=sedimentary rocks. Alteration assemblage abbreviations: Arg=argillic, Bkgr=background, Hrnfls=hornfels, LstAlt=least-altered, Na=sodic, NaCa=sodic-calcic, Phyl=phyllic, Phyl_op_Pot=potassic with overprinting phyllic alteration, Pot=potassic, Prop=propylitic, Unalt=unaltered.

3.4. References

- Aeroquest Surveys (2009): Report on a helicopter-borne AeroTEM system electromagnetic & magnetic survey; Geoscience BC, Report 2009-6, 28 p.
- Holliday, J.R. and Cooke, D.R. (2007): Advances in geological models and exploration methods for copper ± gold porphyry deposits; *in*: Proceedings of Exploration 07: Fifth Decennial International Conference on Mineral Exploration, B. Milkereit (ed), p. 791–809.
- Jackson, A. and Illerbrun, K. (1995): Huckleberry porphyry copper deposit, Taitsa Lake district, west central British Columbia; *in* Porphyry Deposits of the Northwestern Cordillera of North America,

T.G. Schroeter (ed.), Canadian Institute of Mining, Metallurgy and Petroleum, Special Volume 46, p. 313–321.

James, D. H. (1976): Huckleberry; *in* Porphyry deposits of the Canadian Cordillera; A. Sutherland Brown (ed.), Canadian Institute of Mining and Engineering, Special Volume 15, p. 284-288.

MacIntyre, D.G. (1985): Geology and mineral deposits of the Tahtsa Lake district, west-central British Columbia: BC Ministry of Energy, Mines and Petroleum Resources, Bulletin 75, 82 p.

Massey, N.W.D, MacIntyre, D.G., Desjardins, P.J. and Cooney, R.T. (2005): Digital geology map of British Columbia: whole province; B.C. Ministry of Energy and Mines, Geofile 2005-1, URL <<http://www.empr.gov.bc.ca/Mining/Geoscience/PublicationsCatalogue/GeoFiles/Pages/2005-1.aspx>> [November 2007].

Marsden, H., and Thorkelson, D.J. (1992): Geology of the Hazelton Volcanic Belt in British Columbia: Implications for the Early to Middle Jurassic evolution of Stikinia; *Tectonics*, v. 11, p.1266-1287.

Appendix 4. Bell

4.1. Regional Geology and Magnetic Data

4.1.1. Regional Geologic Setting

The Bell porphyry copper-gold deposit is one of three porphyry deposits from the Babine Lake area of west-central British Columbia that were investigated during this study.

The Bell, Granisle, and Morrison porphyry copper deposits formed in association with the intrusion of Eocene Babine Igneous Suite biotite-feldspar porphyry (BFP) plugs into Jurassic to Cretaceous volcanic and sedimentary stratigraphy (Figure 4.1). Of the three deposits, the Bell deposit sits highest within the Jurassic to Cretaceous stratigraphy, occurring within the sedimentary Kitsuns Creek Formation of the Lower Cretaceous Skeena Group (MacIntyre, 2001).

The Bell, Granisle, and Morrison deposits are aligned with the northwest-trending Morrison fault and the related Newman fault. Eocene BFP intrusions are interpreted to have intruded into dilational zones within graben structures bound by these faults during a period of Late Cretaceous to Early Tertiary extension (Dirom et al., 1995).

4.1.2. Regional Magnetic Data.

Regionally, magnetic responses reflect distributions of volcanic, volcano-sedimentary, and sedimentary rocks (Figure 4.1). Lithologic units corresponding with noticeable positive magnetic anomalies include Triassic Takla Group, Jurassic Hazelton Group, and Eocene mafic volcanic rocks. Eocene Babine plutonic suite intrusive rocks and Cretaceous dioritic intrusive rocks also appear as magnetic highs. Volcaniclastic and sedimentary units are generally associated with magnetic lows.

4.2. Deposit Geology

The three Babine district porphyry deposits surveyed during Geoscience BC's QUEST-West project, Bell, Granisle, and Morrison, are similar in that mineralization is focused on a central Eocene biotite-feldspar porphyry (BFP), and alteration assemblages reflect 'classic' alteration patterns documented for calc-alkalic porphyry deposits (e.g., Lowell and Gilbert, 1970).

The Bell deposit is related to Eocene BFP and BQFP (biotite-quartz-feldspar porphyry) plugs that were emplaced into argillite sequences and rhyolite domes of the Early Cretaceous Skeena Group (Figure 4.2). The location of the deposit is controlled by the intersection of the northwest-trending Newman fault and a second east-northeast-trending fault (Dirom et al., 1995).

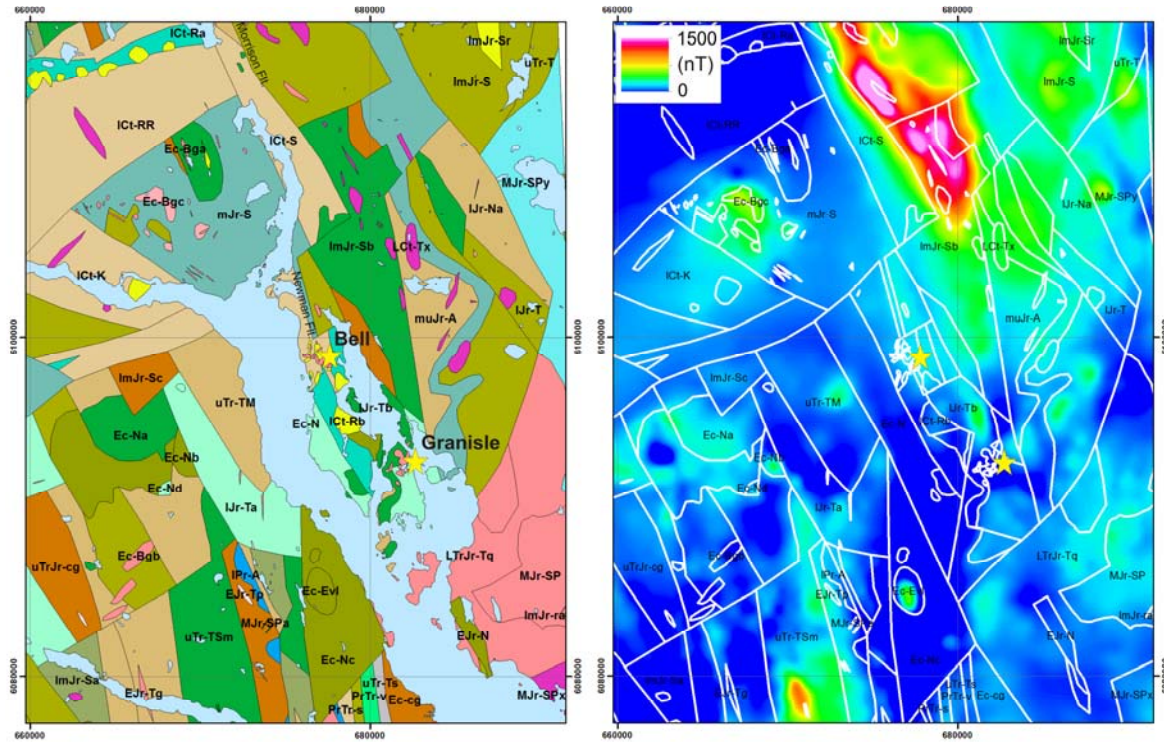


Figure 4.1. Regional geological setting for the Bell and Granisle porphyry copper deposits (Massey et al., 2005), and regional residual total field magnetic data from Natural Resources Canada's Geoscience Data Repository. (Natural Resources Canada, 2004).

Regional Geology of the Bell Deposit

Legend

Eocene

- Ec-Evl - Nechako Plateau Group - Endako Formation coarse volcanoclastic and pyroclastic volcanic rocks
- Ec-N - Nechako Plateau Group - Newman Formation andesitic volcanic rocks
- Ec-Na - Nechako Plateau Group - Newman Formation - Porphyritic Flows Member basaltic volcanic rocks
- Ec-Nb - Nechako Plateau Group - Newman Formation - Breccia Member coarse volcanoclastic and pyroclastic volcanic rocks
- Ec-Nc - Nechako Plateau Group - Newman Formation - Lahar Member coarse volcanoclastic and pyroclastic volcanic rocks
- Ec-Nd - Nechako Plateau Group - Newman Formation - Mafic Flows Member andesitic volcanic rocks
- Ec-cg - Nechako Plateau Group - Newman Formation - Basal Conglomerate Member conglomerate, coarse clastic sedimentary rocks

Eocene Babine Intrusions

- Ec-Bga - Babine Plutonic Suite - Biotite-Quartz-Feldspar Porphyritic Phase granodioritic intrusive rocks
- Ec-Bgb - Babine Plutonic Suite - Biotite-Feldspar Porphyritic Phase granodioritic intrusive rocks
- Ec-Bgc - Babine Plutonic Suite - Quartz Diorite to Granodiorite Phase quartz dioritic intrusive rocks

Lower to Upper Cretaceous

Skeena Group

- LCt-Tx - Unnamed dioritic intrusive rocks
- ICt-S - Skeena Group undivided sedimentary rocks
- ICt-RR - Skeena Group - Red Rose Formation undivided sedimentary rocks
- ICt-Ra - Skeena Group - Rocky Ridge Formation - Subvolcanic Rhyolite Domes alkaline volcanic rocks
- ICt-Rb - Skeena Group - Rocky Ridge Formation - Subvolcanic Rhyolite Domes rhyolite, felsic volcanic rocks
- ICt-K - Skeena Group - Kitsuns Creek Formation undivided sedimentary rocks

Middle to Upper Jurassic

Bowser Lake Group

- muJr-A - Bowser Lake Group - Ashman Formation argillite, greywacke, wacke, conglomerate turbidites

Early to Middle Jurassic

Spike Peak Intrusive Suite

- MJr-SP - Spike Peak Intrusive Suite - Quartz Monzonite Phase granodioritic intrusive rocks
- MJr-SPa - Spike Peak Intrusive Suite diabase, basaltic intrusive rocks
- MJr-SPy - Spike Peak Intrusive Suite syenitic to monzonitic intrusive rocks
- MJr-SPx - Spike Peak Intrusive Suite dioritic intrusive rocks





Lower to Middle Jurassic

Hazelton Group

-  mJr-S - Hazelton Group - Smithers Formation marine sedimentary and volcanic rocks
-  ImJr-Sr - Hazelton Group - Saddle Hill Formation - Subvolcanic Rhyolite Domes rhyolite, felsic volcanic rocks
-  ImJr-S - Hazelton Group - Saddle Hill Formation undivided volcanic rocks
-  ImJr-Sa - Hazelton Group - Saddle Hill Formation - Intermediate Volcanic Member volcanoclastic rocks
-  ImJr-Sb - Hazelton Group - Saddle Hill Formation - Mafic Submarine Volcanic Member basaltic volcanic rocks
-  ImJr-Sc - Hazelton Group - Saddle Hill Formation - Volcanoclastic-Sedimentary Member conglomerate, coarse clastic sedimentary rocks
-  ImJr-ra - Hazelton Group coarse volcanoclastic and pyroclastic volcanic rocks
-  IJr-Na - Hazelton Group - Nilkitkwa Formation argillite, greywacke, wacke, conglomerate turbidites
-  IJr-Ta - Hazelton Group - Telkwa Formation - Felsic to Intermediate Volcanic Member andesitic volcanic rocks
-  IJr-Tb - Hazelton Group - Telkwa Formation - Mafic Volcanic Member basaltic volcanic rocks
-  IJr-T - Hazelton Group - Telkwa Formation undivided volcanic rocks

Late Triassic to Early Jurassic

Topley Intrusive Suite





-  EJr-N - Topley Plutonic Suite - Nose Bay Intrusive Breccia coarse volcanoclastic and pyroclastic volcanic rocks
-  EJr-Tp - Topley Intrusive Suite - Megacrystic Porphyry Dykes feldspar porphyritic intrusive rocks
-  EJr-Tg - Topley Intrusive Suite - Porphyritic Phase granodioritic intrusive rocks
-  LTrJr-Tq - Topley Intrusive Suite - Granodiorite to Monzonite Phase granodioritic intrusive rocks

Upper Triassic to Jurassic


-  uTrJr-cg - Unnamed conglomerate, coarse clastic sedimentary rocks

Upper Triassic

Takla Group


-  uTr-T - Takla Group undivided volcanic rocks
-  uTr-TM - Takla Group - Moosevale Formation argillite, greywacke, wacke, conglomerate turbidites
-  uTr-TSm - Takla Group - Savage Mountain Formation basaltic volcanic rocks
-  uTr-Ts - Takla Group - Dewar Formation mudstone, siltstone, shale fine clastic sedimentary rocks

Permian to Triassic

-  PrTr-s - Deformed Asitka or Takla Groups - Metasedimentary Rocks undivided sedimentary rocks
-  PrTr-v - Deformed Asitka or Takla Groups - Metavolcanic Rocks greenstone, greenschist metamorphic rocks

Lower Permian

Asitka Group

-  IPr-A - Asitka Group limestone, marble, calcareous sedimentary rocks

Eocene Newman Formation volcanic rocks, considered to be extrusive equivalents of Eocene BFP, have been mapped at several locations along the Newman Peninsula and on the western shore of Babine Lake. These units are dacitic to andesitic in composition. Sampling these rocks provides an opportunity to investigate BFP compositions outside the influence of overprinting hydrothermal alteration and mineralization.

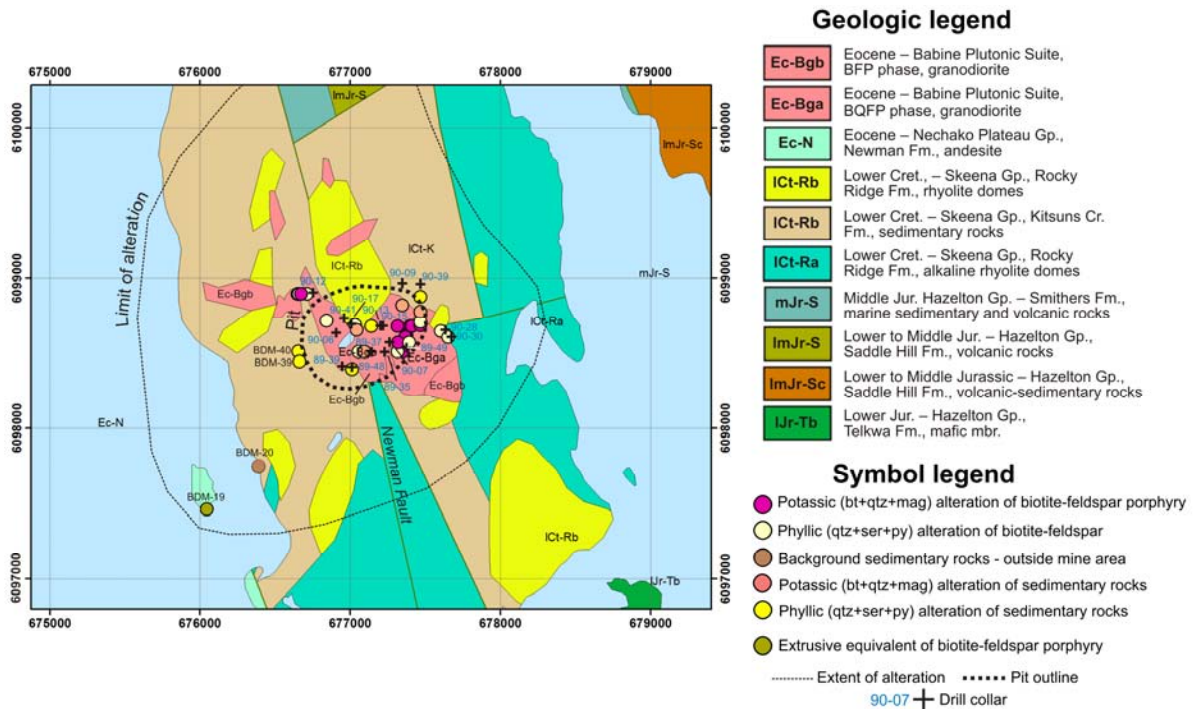


Figure 4.2. Map of the Bell deposit area geology (Massey et al., 2005), showing pit outline (dotted line) and limit of alteration (after Dirom et al., 1995), as well as location of hand samples collected from the perimeter of the open pit and from the margins of the alteration halo (labelled with BDM prefix). Drill core sample locations are projected to surface from depth. Drill core and hand sample symbols are colored based on alteration.

Hydrothermal alteration of the rocks hosting the Bell deposit led to the formation of a potassic biotite+quartz+magnetite alteration core surrounded by a distal propylitic alteration. Later sericite+carbonate and quartz+sericite+pyrite (phyllic) alteration overprints the earlier potassic assemblage. A quartz+sericite+pyrite stockwork fringes the central BFP intrusive and represents an important alteration phase due to its association with high Cu grades. At Bell, rocks altered to quartz+sericite+pyrite contain 50% of the ore. Grades tend to decrease toward the biotite+qtz+magnetite–altered core of the intrusion. Results from isotope studies at Bell suggests a leaching of Cu from the potassic zone occurred in association with later magmatic-hydrothermal fluid boiling and modification through mixing with meteoric waters (Dirom et al., 1995). The Bell deposit is associated with an extensive, greater than 1100 m wide pyrite halo, the footprint of which may be enhanced where it overprints pyrite-bearing Cretaceous argillite units.

4.2. Physical Properties of Rocks from the Bell Deposit

4.2.1. Sample Suite

Twenty-eight drill core samples were collected from an archived drill core library on the past-producing Bell deposit mine site. Pieces of whole and split drill core from 25 core boxes representing 25 drillholes from a 1989–1990 drill program were additionally measured for magnetic susceptibility. Most of the drill core samples are from within the core of the mineralized system and are affected by either phyllic or potassic alteration. For graphical representation, samples are grouped based on whether they are predominantly potassically-altered or phyllic-altered though many phyllic samples show indications of being previously altered to biotite+qtz+magnetite assemblages and most potassic samples have some degree of overprinting phyllic alteration.

Several magnetic susceptibility measurements were made on outcrop and on hand samples collected from the Bell deposit site. Hand samples included two very strongly phyllic-altered sedimentary samples, a chlorite-altered tuff from the perimeter of the Bell pit, and a weakly carbonate-sericite-altered sedimentary sample from the outer margin of the documented pyrite halo. Also collected were four samples of weak to moderate quartz-sericite-carbonate-altered andesitic to dacitic volcanic rock from nearby Newman Island, and from the southern Newman Peninsula and Bear Island (latter two sample sites not shown on Bell location map). Newman Island volcanic rocks are considered to be extrusive equivalents of BFP intrusive rocks. These samples were collected to gain an understanding of least-altered BFP mineral assemblages and physical properties. Locations of hand sample and outcrop measurement sites, and projected drill core samples are shown in Figure 4.2 and are colored based on the predominant alteration assemblage.

4.2.2. Magnetic Susceptibility and Deposit Scale Magnetic Data

Four samples represent extrusive equivalents of Eocene BFP (Figure 4.3). These dacitic to andesitic samples have low to moderate susceptibilities with a geometric average of 4.46×10^{-3} SI units. Two moderately high susceptibility samples from Newman Island appear to contain both primary magnetite (larger, disseminated grains), and secondary magnetite (fine disseminated grains). Two lower susceptibility Eocene volcanic samples from the southern Newman Peninsula and from Bear Island are weakly sericite+carbonate-altered.

Magnetic susceptibility ranges for potassic and phyllic samples from Bell are distinct (Figure 4.3). Potassically-altered BFP yields high susceptibilities generally $>20 \times 10^{-3}$ SI units, whereas quartz+sericite+pyrite-altered BFP samples are associated with consistently low susceptibilities on average $<1 \times 10^{-3}$ SI units. The overprinting phyllic alteration results in magnetite destruction. One phyllic sample with a higher susceptibility measurement of 25×10^{-3} SI units is from drill core derived from beneath the current pit, from deeper levels within the porphyry deposit (294 m downhole). From petrography, this sample appears to have been previously strongly potassically-altered.

The argillite sample collected from the distal southwest margin of the mapped alteration halo, considered to be the least altered argillite sample collected, has a low susceptibility (0.28×10^{-3} SI units). Four potassically-altered sedimentary samples, with varying degrees of overprinting phyllic alteration, have low susceptibilities with most measurements $<1 \times 10^{-3}$ SI units. The potassically-altered sedimentary samples do not appear to yield as high susceptibilities as potassically-altered BFP at Bell. This might be explained by a lack of Fe in the original argillite host which likely limits the formation of magnetite. Phyllic-altered sedimentary rock samples have consistently low susceptibilities with a geometric average of 0.38×10^{-3} SI units.

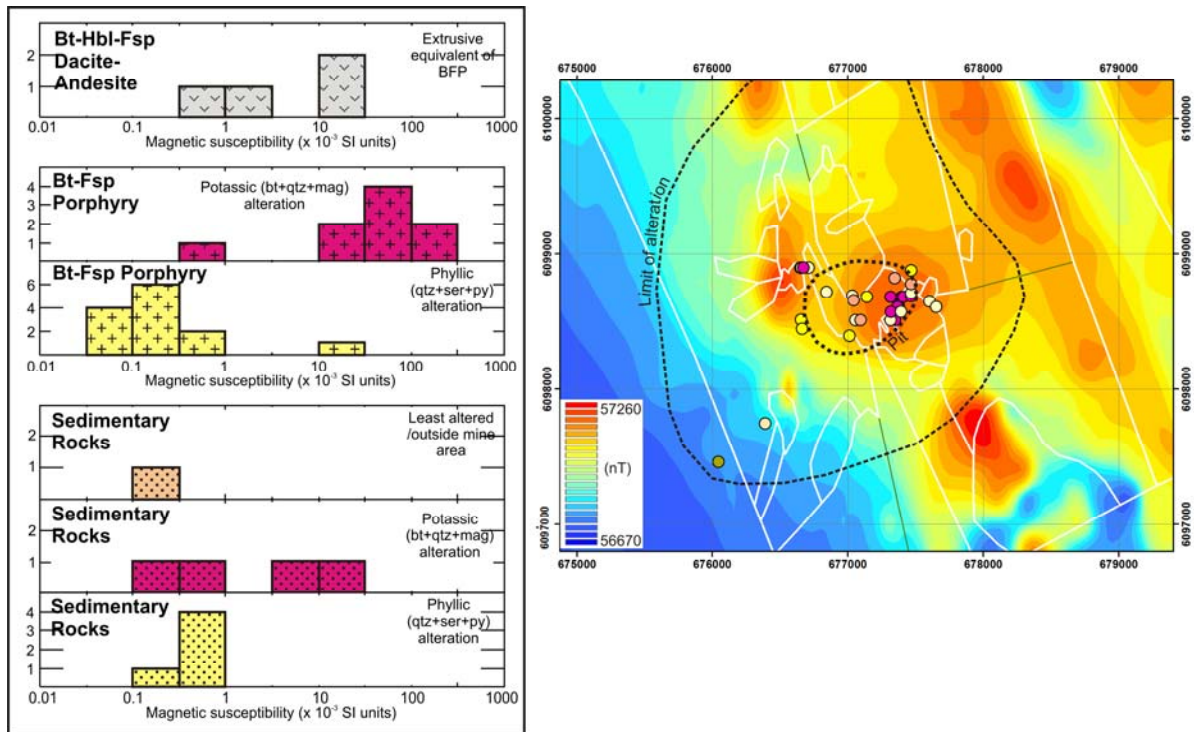


Figure 4.3. Histogram showing magnetic-susceptibility data for variably altered intrusive and sedimentary rock samples from the Bell deposit, and total magnetic intensity data (Aeroquest Surveys, 2009) from the Bell deposit. Abbreviations: BFP=biotite-feldspar porphyry, bt=biotite; fsp=feldspar, hbl=hornblende; mag=magnetite, py=pyrite, qtz=quartz, ser=sericite.

Airborne magnetic data suggests Skeena Group sedimentary rocks and rhyolite domes are weakly magnetic to nonmagnetic, contrasting with variably magnetic Cretaceous volcanic rocks in fault contact to the east (Figure 4.3). Eocene BFP intrusive rocks form clear positive magnetic anomalies within the non-magnetic sedimentary package. Surface and drill core samples are shown on the magnetic map colored based on alteration, with potassically-altered samples colored pink, and phyllic-altered samples colored yellow. The open pit is centered over the boundary between phyllic and potassic alteration zones, near the edge of a magnetic high. Potassic biotite+quartz+magnetite-altered samples align well with the magnetic anomaly marking the contact between mapped BFP and BQFP units. Another biotite+quartz+magnetite-altered sample aligns with a magnetic high northwest of the pit.

4.2.3. Density and Porosity

The sample suite from the Bell deposit is characterized by low densities since it contains predominantly felsic intrusive and sedimentary rocks. Almost all samples from the suite fall below 2.7 g/cm^3 (Figure

4.4). Average densities of potassically-altered BFP samples are slightly increased relative to compositionally similar Eocene extrusive rocks due to their generally lower porosities. Phyllic-altered BFP samples have the lowest average densities of the Bell sample suite, with values as low as 2.40 g/cm³.

Density trends for sedimentary samples differ from BFP sample trends, in that density increases rather than decreases with both potassic and phyllic alteration. Alteration of argillite (least-altered sample density of 2.60 g/cm³) to potassic and phyllic assemblages (averaging 2.66 and 2.77 g/cm³, respectively) may have led to a relative reduction in porosity. This is in contrast to the typical increases in porosity accompanying phyllic alteration of other rocks sampled during this study.

The highest density samples from Bell are those with the lowest porosities, and a general overall trend of increasing density with decreasing porosity supports a relationship between these two properties (Figure 4.5). The highest porosities of the porphyry sample collection are from the Bell deposit, with up to 14% porosity measured from phyllic-altered BFP samples. As data from Endako and Huckleberry samples have previously indicated, phyllic alteration tends to weaken the rock and create friability, enhancing porosity.

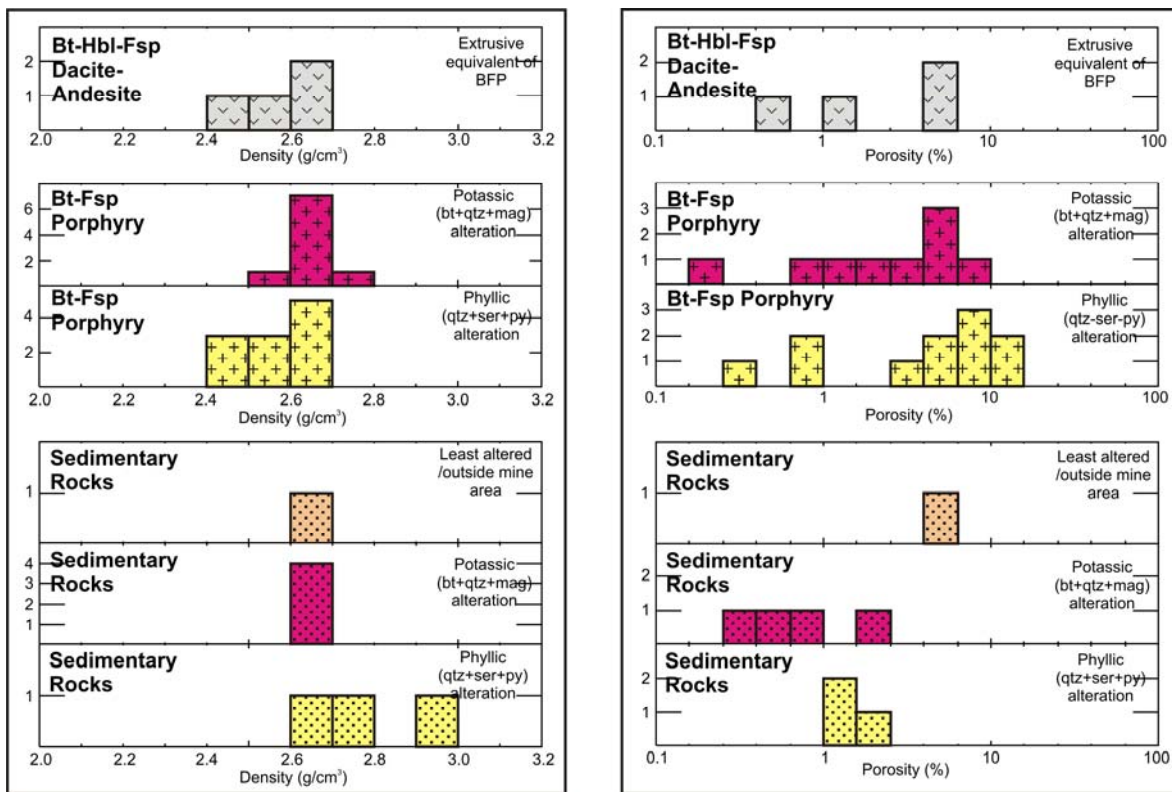


Figure 4.4. Density and porosity data from the Bell deposit. Abbreviations: BFP=biotite-feldspar porphyry, bt=biotite; fsp=feldspar, hbl=hornblende; mag=magnetite, py=pyrite, qtz=quartz, ser=sericite.

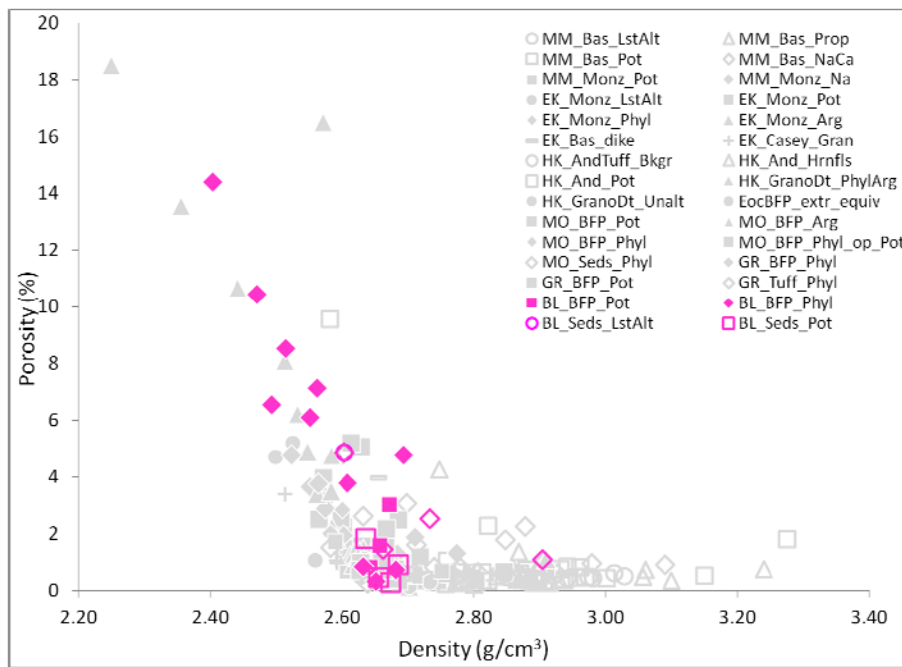


Figure 4.5. Density versus porosity data for all porphyry samples from this study. Bell samples are highlighted in magenta. Deposit abbreviations: BL=Bell, EK=Endako, GR=Granisle, HK=Huckleberry, MM=Mount Milligan, MO=Morrison. Rock type abbreviations: And=Andesite, Bas=basalt, BFP=biotite-feldspar porphyry, EocBFP Extr_equiv=Eocene biotite-feldspar porphyry extrusive equivalent, Gran=granite, GranoDt=granodiorite, Monz=monzonite, Seds=sedimentary rocks. Alteration assemblage abbreviations: Arg=argillic, Bkgr=background, Hrnfls=hornfels, LstAlt=least-altered, Na=sodic, NaCa=sodic-calcic, Phyl=phyllic, Phyl_op_Pot=potassic with overprinting phyllic alteration, Pot=potassic, Prop=propylitic, Unalt=unaltered.

4.2.4. Resistivity Data and Deposit Scale Conductivity Data

Eocene biotite-feldspar phyrlic dacite to andesite samples (extrusive equivalent to BFP intrusive rocks) span the range of recorded resistivities (Figure 4.6), with values reflecting variable sample porosities. Two low resistivity samples are associated with high porosities, while two samples with higher resistivities have low porosities.

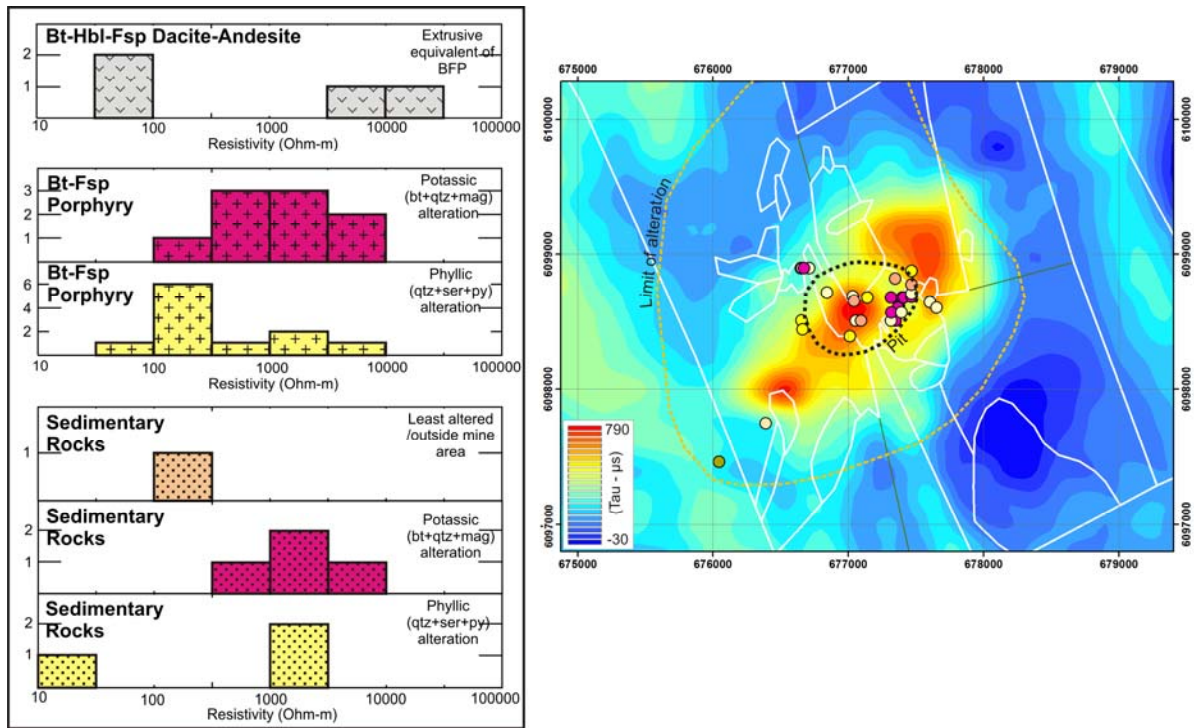


Figure 4.6. Resistivity data from the Bell deposit, and late time Tau map from AeroTEM data (Aeroquest Surveys, 2009) collected over the Bell deposit. Abbreviations: BFP=biotite-feldspar porphyry, bt=biotite, hbl=hornblende; fsp=feldspar, mag=magnetite, py=pyrite, qtz=quartz, ser=sericite.

Potassically-altered BFP samples collected from the Bell deposit are relatively coherent rocks and have moderate to high resistivities on average compared to phyllic samples. Most samples have resistivities greater than 400 Ohm-m, with values ranging up to 7000 Ohm-m (Figure 4.6).

Phyllic-altered BFP samples from Bell are associated with some of the lowest resistivities measured for the BC porphyry deposit sample suite with most samples having resistivities less than 400 Ohm-m. The higher resistivity phyllic-altered BFP samples show evidence of previous potassic alteration and have comparatively low porosities (<1%).

Altered sedimentary rock samples from Bell are relatively resistive compared to the least-altered argillite sample. High densities and low porosities support the interpretation that alteration may have annealed original porosity in these particular rocks, which would limit fluid infiltration and result in increased resistivities.

As expected, the Bell deposit samples define a clear trend on a plot of resistivity versus porosity (Figure 4.7). Porosity, however, may not represent the exclusive control on resistivity at Bell. It is possible that the fracture-controlled sulphides occurring within mineralized rocks play a role in lowering resistivities. Appendix 7 addresses this, and elaborates on relationships between alteration, sulphides, and electrical resistivity data.

On a graph of resistivity versus density (Figure 4.8) Bell samples plot predominantly along a previously defined trend representing density and resistivity decreases linked to increases in porosity. A few samples fall off this trend and are characterized by relatively moderate to high densities and low resistivities (high conductivities). One sedimentary sample is particularly conductive, its conductivity not explained by lower porosities in this case, but by the presence of nearly 10% vein-controlled and disseminated sulphides.

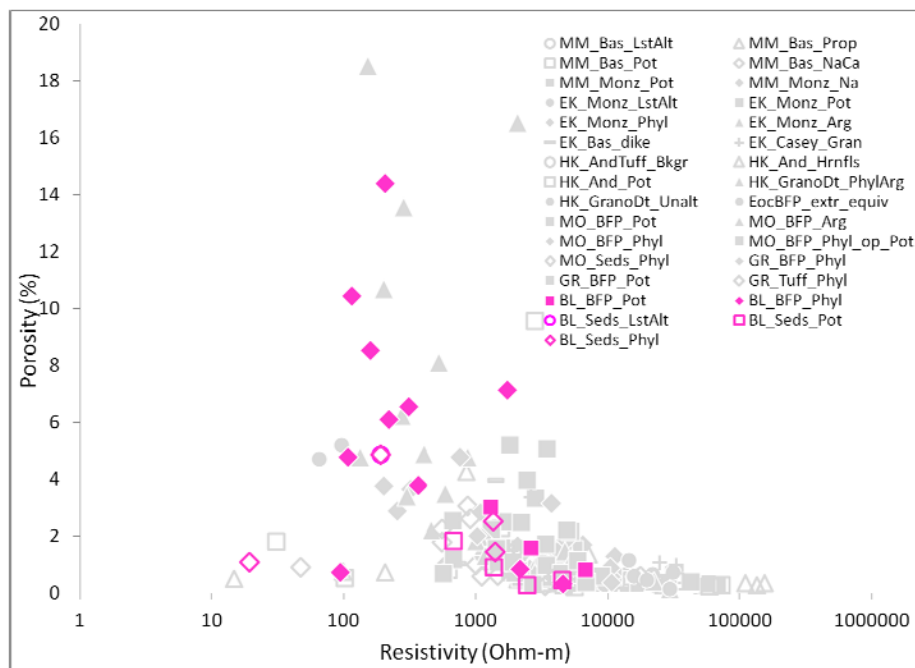


Figure 4.7. Resistivity versus porosity data for all porphyry samples from this study. Bell samples are highlighted in magenta. Deposit abbreviations: BL=Bell, EK=Endako, GR=Granisle, HK=Huckleberry, MM=Mount Milligan, MO=Morrison. Rock type abbreviations: And=Andesite, Bas=basalt, BFP=biotite-feldspar porphyry, EocBFP Extr Equiv=Eocene biotite-feldspar porphyry extrusive equivalent, Gran=granite, GranoDt=granodiorite, Monz=monzonite, Seds=sedimentary rocks. Alteration assemblage abbreviations: Arg=argillic, Bkgr=background, Hrnfls=hornfels, LstAlt=least-altered, Na=sodic, NaCa=sodic-calcic, Phyl=phyllic, Phyl Op Pot=potassic with overprinting phyllic alteration, Pot=potassic, Prop=propylitic, Unalt=unaltered.

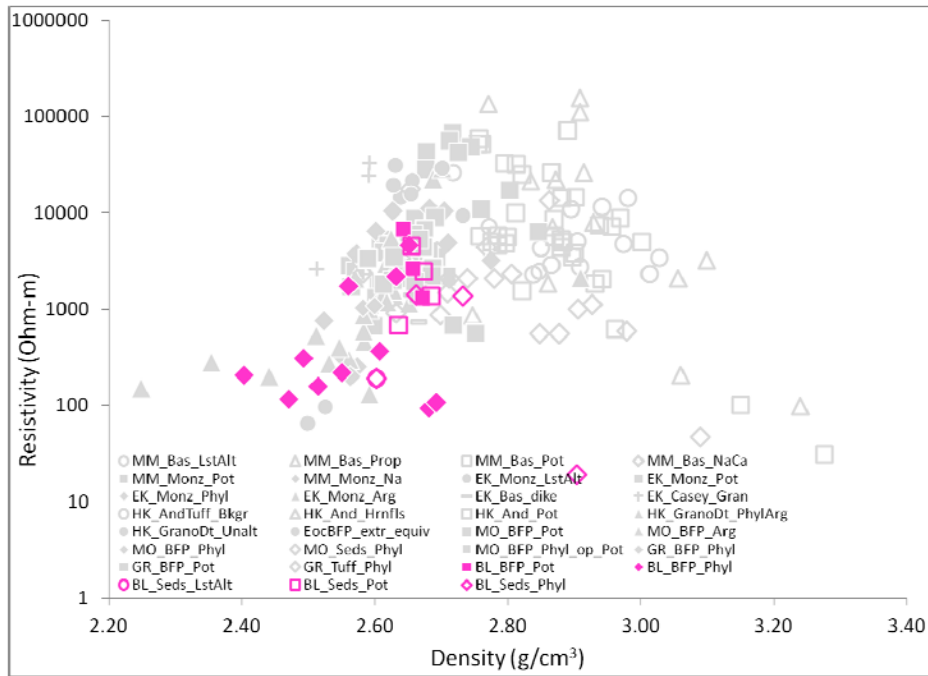


Figure 4.8. Resistivity versus density data for all porphyry samples from this study. Bell samples are highlighted in magenta. Deposit abbreviations: BL=Bell, EK=Endako, GR=Granisle, HK=Huckleberry, MM=Mount Milligan, MO=Morrison. Rock type abbreviations: And=Andesite, Bas=basalt, BFP=biotite-feldspar porphyry, EocBFP Extr Equiv=Eocene biotite-feldspar porphyry extrusive equivalent, Gran=granite, GranoDt=granodiorite, Monz=monzonite, SedS=sedimentary rocks. Alteration assemblage abbreviations: Arg=argillic, Bkgr=background, Hrnfls=hornfels, LstAlt=least-altered, Na=sodic, NaCa=sodic-calcic, Phyl=phyllic, Phyl_op_Pot=potassic with overprinting phyllic alteration, Pot=potassic, Prop=propylitic, Unalt=unaltered.

Three linked high conductivity anomalies trending northeast through the Bell deposit are indicated in the late time Tau (late time decay constant, Aeroquest Surveys, 2009) data (Figure 4.6). Phyllic-altered rock samples (yellow colored samples) collected from drill core, bearing variable amounts of sulphides, correlate with a centralized high conductivity anomaly. An adjacent conductivity anomaly to the northeast overlaps with phyllic-altered samples, further supporting a relationship between conductivity and phyllic alteration. The southwest conductivity anomaly was not tested during this study. Potassically-altered samples sit in resistive areas between conductivity highs. High conductivity anomalies associated with the Bell deposit stand out within the generally resistive sedimentary, volcanic, and intrusive background rocks.

4.4. References

- Aeroquest Surveys (2009): Report on a helicopter-borne AeroTEM system electromagnetic & magnetic survey; Geoscience BC, Report 2009-6, 28 p.
- Dirom, G.E., Dittrick, M.P., McArthur, D.R., Ogryzlo, P.L., Pardoe A.J. and Stothart P.G. (1995): Bell and Granisle porphyry copper-gold mines, Babine region, west-central British Columbia; in Porphyry Deposits of the Northwestern Cordillera of North America, T.G. Schroeter (ed.), Canadian Institute of Mining, Metallurgy and Petroleum, Special Volume 46, p. 256–289.
- Lowell, J.D. and Guilbert, J.M. (1970): Lateral and vertical alteration-mineralization zoning in porphyry ore deposits; *Economic Geology*, v. 65, p. 373-408.
- MacIntyre, D. (2001): Geological Compilation Map Babine Porphyry Copper District Central British Columbia (NTS93L/9, 93M/1,2E,7E,8); BC Ministry of Energy, Mines and Petroleum Resources, Open File 2001-3, scale 1:1 000 000.
- Massey, N.W.D, MacIntyre, D.G., Desjardins, P.J. and Cooney, R.T. (2005): Digital geology map of British Columbia: whole province; B.C. Ministry of Energy and Mines, Geofile 2005-1, URL <<http://www.empr.gov.bc.ca/Mining/Geoscience/PublicationsCatalogue/GeoFiles/Pages/2005-1.aspx>> [November 2007].
- Natural Resources Canada (2004): Canadian aeromagnetic data base, Continental Geoscience Division, Geological Survey of Canada, Earth Sciences Sector, Natural Resources Canada, Geoscience Data Repository, URL <<http://gdrdap.agg.nrcan.gc.ca/geodap/home/Default.aspx?lang=e>> [March 2011].

Appendix 5. Granisle

5.1. Regional Geology and Magnetic Data

5.1.1. Regional Geologic Setting.

Figure 5.1 is equivalent to Figure 4.1 presented in Appendix 4, and shows the location of both Bell and Granisle deposits on geologic and residual total field magnetic maps. The Granisle deposit occurs on Macdonald Island southeast of the Bell deposit, and sits in the lowest stratigraphic position of the three Babine porphyry deposits studied. It is hosted within mafic volcanic rocks from the Telkwa Formation of the Lower Jurassic Hazelton Group. Like the Bell deposit, the Granisle deposit formed in association with the intrusion of Eocene biotite-feldspar porphyry (Figure 5.1). The hosting BFP intrusions are interpreted to be focused along a zone of dilation occurring between two transverse faults (Dirom et al., 1995).

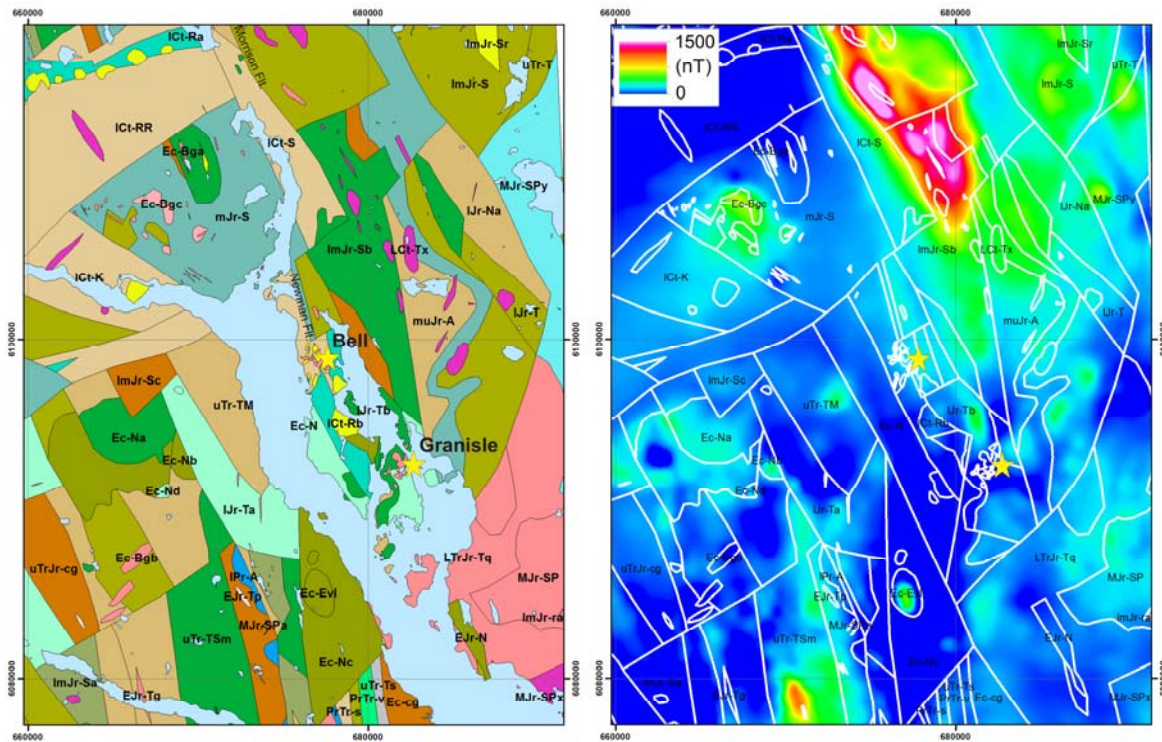


Figure 5.1. Regional geological setting for the Bell and Granisle porphyry copper deposits (Massey et al., 2005), and regional residual total field magnetic data from Natural Resources Canada's Geoscience Data Repository (Natural Resources Canada, 2004).




Regional Geology of the Granisle Deposit

Legend

Eocene







-  Ec-Evl - Nechako Plateau Group - Endako Formation coarse volcanoclastic and pyroclastic volcanic rocks
-  Ec-N - Nechako Plateau Group - Newman Formation andesitic volcanic rocks
-  Ec-Na - Nechako Plateau Group - Newman Formation - Porphyritic Flows Member basaltic volcanic rocks
-  Ec-Nb - Nechako Plateau Group - Newman Formation - Breccia Member coarse volcanoclastic and pyroclastic volcanic rocks
-  Ec-Nc - Nechako Plateau Group - Newman Formation - Lahar Member coarse volcanoclastic and pyroclastic volcanic rocks
-  Ec-Nd - Nechako Plateau Group - Newman Formation - Mafic Flows Member andesitic volcanic rocks
-  Ec-cg - Nechako Plateau Group - Newman Formation - Basal Conglomerate Member conglomerate, coarse clastic sedimentary rocks

Eocene Babine Intrusions

-  Ec-Bga - Babine Plutonic Suite - Biotite-Quartz-Feldspar Porphyritic Phase granodioritic intrusive rocks
-  Ec-Bgb - Babine Plutonic Suite - Biotite-Feldspar Porphyritic Phase granodioritic intrusive rocks
-  Ec-Bgc - Babine Plutonic Suite - Quartz Diorite to Granodiorite Phase quartz dioritic intrusive rocks

Lower to Upper Cretaceous

Skeena Group

-  LCt-Tx - Unnamed dioritic intrusive rocks
-  ICt-S - Skeena Group undivided sedimentary rocks
-  ICt-RR - Skeena Group - Red Rose Formation undivided sedimentary rocks
-  ICt-Ra - Skeena Group - Rocky Ridge Formation - Subvolcanic Rhyolite Domes alkaline volcanic rocks
-  ICt-Rb - Skeena Group - Rocky Ridge Formation - Subvolcanic Rhyolite Domes rhyolite, felsic volcanic rocks
-  ICt-K - Skeena Group - Kitsuns Creek Formation undivided sedimentary rocks





Middle to Upper Jurassic

Bowser Lake Group

-  muJr-A - Bowser Lake Group - Ashman Formation argillite, greywacke, wacke, conglomerate turbidites

Early to Middle Jurassic

Spike Peak Intrusive Suite

-  MJr-SP - Spike Peak Intrusive Suite - Quartz Monzonite Phase granodioritic intrusive rocks
-  MJr-SPa - Spike Peak Intrusive Suite diabase, basaltic intrusive rocks
-  MJr-SPy - Spike Peak Intrusive Suite syenitic to monzonitic intrusive rocks
-  MJr-SPx - Spike Peak Intrusive Suite dioritic intrusive rocks



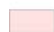
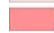
Lower to Middle Jurassic

Hazelton Group

-  mJr-S - Hazelton Group - Smithers Formation marine sedimentary and volcanic rocks
-  ImJr-Sr - Hazelton Group - Saddle Hill Formation - Subvolcanic Rhyolite Domes rhyolite, felsic volcanic rocks
-  ImJr-S - Hazelton Group - Saddle Hill Formation undivided volcanic rocks
-  ImJr-Sa - Hazelton Group - Saddle Hill Formation - Intermediate Volcanic Member volcanoclastic rocks
-  ImJr-Sb - Hazelton Group - Saddle Hill Formation - Mafic Submarine Volcanic Member basaltic volcanic rocks
-  ImJr-Sc - Hazelton Group - Saddle Hill Formation - Volcanoclastic-Sedimentary Member conglomerate, coarse clastic sedimentary rocks
-  ImJr-ra - Hazelton Group coarse volcanoclastic and pyroclastic volcanic rocks
-  IJr-Na - Hazelton Group - Nilkitkwa Formation argillite, greywacke, wacke, conglomerate turbidites
-  IJr-Ta - Hazelton Group - Telkwa Formation - Felsic to Intermediate Volcanic Member andesitic volcanic rocks
-  IJr-Tb - Hazelton Group - Telkwa Formation - Mafic Volcanic Member basaltic volcanic rocks
-  IJr-T - Hazelton Group - Telkwa Formation undivided volcanic rocks

Late Triassic to Early Jurassic

Topley Intrusive Suite





-  EJr-N - Topley Plutonic Suite - Nose Bay Intrusive Breccia coarse volcanoclastic and pyroclastic volcanic rocks
-  EJr-Tp - Topley Intrusive Suite - Megacrystic Porphyry Dykes feldspar porphyritic intrusive rocks
-  EJr-Tg - Topley Intrusive Suite - Porphyritic Phase granodioritic intrusive rocks
-  LTrJr-Tq - Topley Intrusive Suite - Granodiorite to Monzonite Phase granodioritic intrusive rocks

Upper Triassic to Jurassic

-  uTrJr-cg - Unnamed conglomerate, coarse clastic sedimentary rocks

Upper Triassic

Takla Group


-  uTr-T - Takla Group undivided volcanic rocks
-  uTr-TM - Takla Group - Moosevale Formation argillite, greywacke, wacke, conglomerate turbidites
-  uTr-TSm - Takla Group - Savage Mountain Formation basaltic volcanic rocks
-  uTr-Ts - Takla Group - Dewar Formation mudstone, siltstone, shale fine clastic sedimentary rocks

Permian to Triassic

-  PrTr-s - Deformed Asitka or Takla Groups - Metasedimentary Rocks undivided sedimentary rocks
-  PrTr-v - Deformed Asitka or Takla Groups - Metavolcanic Rocks greenstone, greenschist metamorphic rocks

Lower Permian

Asitka Group

-  IPr-A - Asitka Group limestone, marble, calcareous sedimentary rocks

5.1.2. Regional Magnetic Data.

Magnetic data show Triassic Takla Group, Jurassic Hazelton Group, and Eocene mafic volcanic rocks corresponding spatially to magnetic highs (Figure 5.1). Eocene Babine plutonic suite intrusive rocks and Cretaceous dioritic intrusions also appear as magnetic highs. Magnetic lows correlate with volcanoclastic and sedimentary units.

5.2. Deposit Geology

Mineralization at Granisle is spatially correlated with two Eocene porphyritic intrusive bodies, a quartz-diorite microporphyry and a biotite-feldspar-phyrlic intrusive that were emplaced into Early Jurassic Hazelton Group volcanic and volcanoclastic rocks (Figure 5.2).

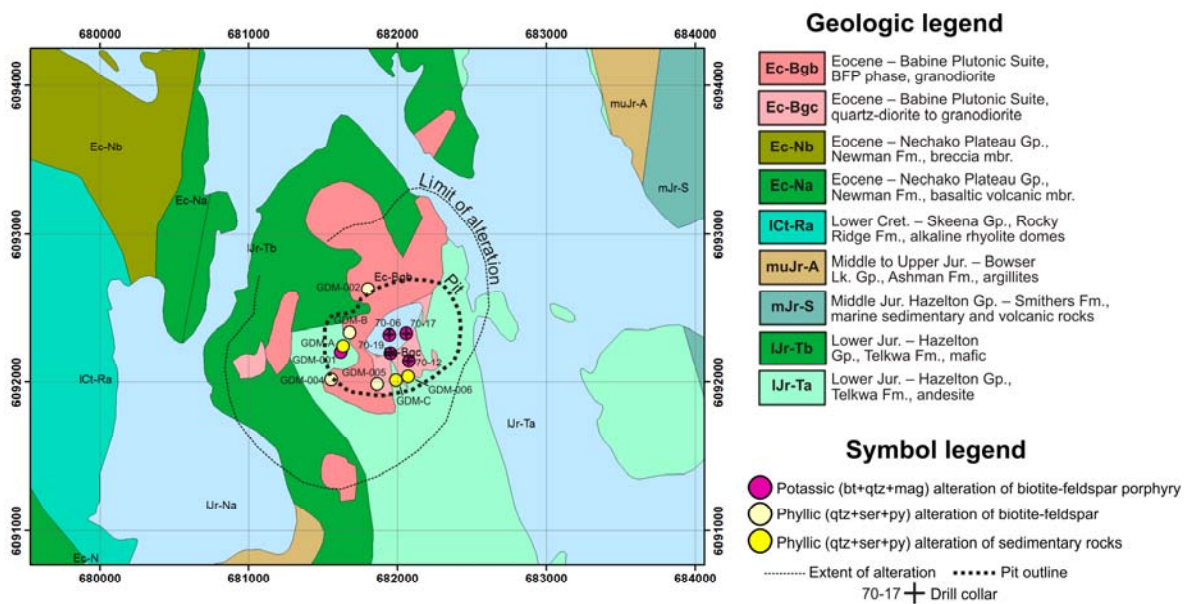


Figure 5.2. Map of the Granisle deposit area geology (Massey et al., 2005), showing pit outline (dotted line) and limit of alteration (after Dirom et al., 1995), as well as location of hand samples collected from the perimeter of the open pit (labelled with GDM prefix). Drill core sample locations are projected to surface from depth. Drill core and hand sample symbols are colored based on alteration.

Potassic biotite+quartz+magnetite alteration occurs at the core of the Granisle porphyry system. A later phyllic (carbonate+sericite+quartz+pyrite) alteration overprint occurs at the fringes of the deposit and most of the volcanic and intrusive rocks sampled from the upper walls of the pit for this study are extensively altered to this assemblage. The majority of Cu ore is hosted in potassically-altered quartz-diorite and BFP intrusive rocks. Pyrite, chalcopyrite, and bornite are the dominant sulphides, which occur within veins and veinlets, and also as disseminated grains. Phyllic alteration is associated with low Cu grades and the affected rocks were considered waste for the mining operations (Dirom et al., 1995).

5.2. Physical Properties of Rocks from the Granisle Deposit

5.2.1. Sample Suite

Of the three Babine district deposits investigated, the Granisle sample suite contains the fewest number of samples. Although there was drill core existing at the past-producing mine site, the core storage racks were partially collapsed, much of the core was unlabeled or depth markers were missing, and time spent at the site was limited. For this study, eight drill core samples were collected from vertically drilled core. Three of the drillholes have no location information and are therefore not plotted on maps presented here. Six hand samples were collected from the perimeter of the Granisle pit. Three outcrop susceptibility measurements from the Granisle pit were used in addition to hand samples to augment the Granisle magnetic susceptibility dataset. Hand samples, outcrop measurements and projected downhole samples are plotted on the geological map of the Granisle area in Figure 5.2, and are colored based on alteration. Several dike samples are plotted on the geologic map, but are omitted from histograms.

5.2.2. Magnetic Susceptibility and Deposit Scale Magnetic Data

Figure 5.3 compiles magnetic susceptibility data for intrusive and volcanic rocks from Granisle. Potassically-altered biotite-feldspar porphyry and quartz-diorite microporphyry samples fall into a higher susceptibility range; combined BFP and microporphyry samples have a geometric average of 26.6×10^{-3} SI units. These relatively high susceptibilities are linked to the formation of secondary magnetite as a product of potassic alteration. Phyllic BFP samples have lower susceptibilities with a geometric average of 0.44×10^{-3} SI units.

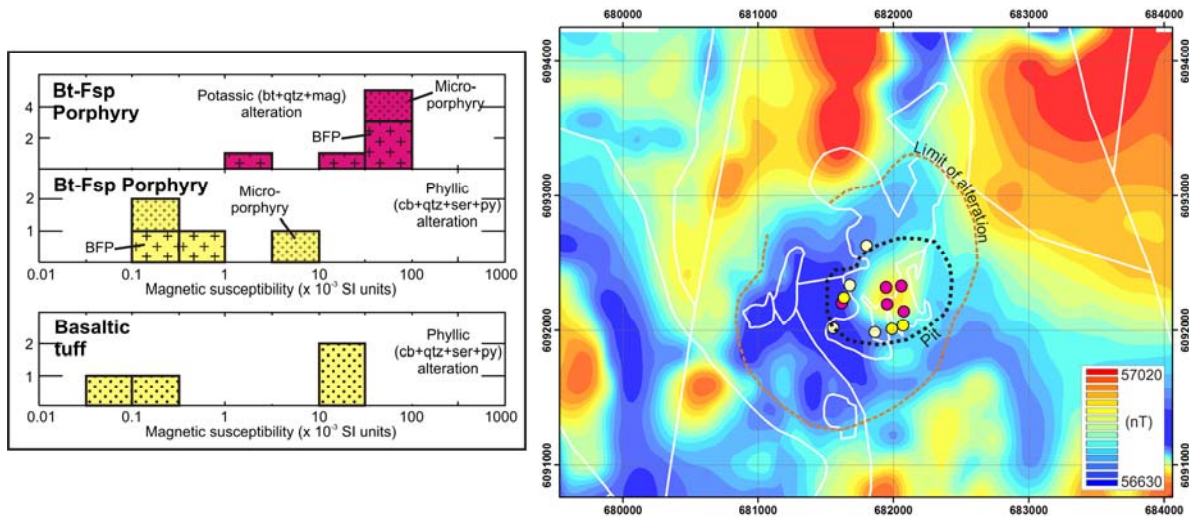


Figure 5.3. Histograms showing magnetic susceptibility data for variably altered intrusive (top) and volcanic (bottom) rock samples from the Granisle deposit, and total magnetic intensity data (Aeroquest Surveys, 2009) collected over the deposit. Abbreviations: BFP= biotite-feldspar porphyry; bt=biotite, cb=carbonate, fsp=feldspar, mag=magnetite, py=pyrite, qtz=quartz, ser=sericite.

No strongly potassically-altered basaltic tuff samples were collected. Two phyllic-altered mafic volcanic rocks from the pit have low susceptibilities with a geometric average of 0.14×10^{-3} SI units, whereas two phyllic-altered mafic volcanic samples collected from drill core have higher susceptibilities with a geometric average of 18.9×10^{-3} SI units. The two drill core samples are derived from core extracted from near the center of the porphyry deposit and appear to contain residual magnetite from an early-stage magnetite-bearing potassic alteration assemblage.

On the Granisle magnetic map (AeroTEM total magnetic intensity data, Aeroquest Surveys, 2009) samples are plotted and colored by alteration. Based on susceptibility measurements collected from drill core, the local magnetic high over the Granisle pit, at the contact between the quartz diorite microporphyry and the BFP intrusion, (Figure 5.3) correlates with potassic alteration of the intrusive rocks. The magnetic low surrounding the deposit is attributed to strong overprinting carbonate+sericite+quartz+pyrite alteration that caused the destruction of primary and/or secondary magnetite within peripheral volcanic and intrusive rocks. Volcanic units outside of the extent of mapped alteration have a stronger magnetic signature in comparison.

5.2.3. Density and Porosity

Phyllic-altered BFP samples have lower densities than potassically-altered BFP samples (Figure 5.4). Decreases in density are attributed to both a change in mineralogy (alteration of higher density to lower density minerals), and an increase in porosity similar to trends observed at the Bell deposit. Mafic volcanic tuff samples have higher measured densities than Granisle BFP samples.

Porosities of Granisle samples reach up to just over 5%. Potassic BFP samples have a lower average porosity than phyllic-altered BFP samples. On a plot of density versus porosity (Figure 5.5), Granisle samples follow the same negative correlation trend seen for Endako samples, whereby increased porosity coincides with lower density.

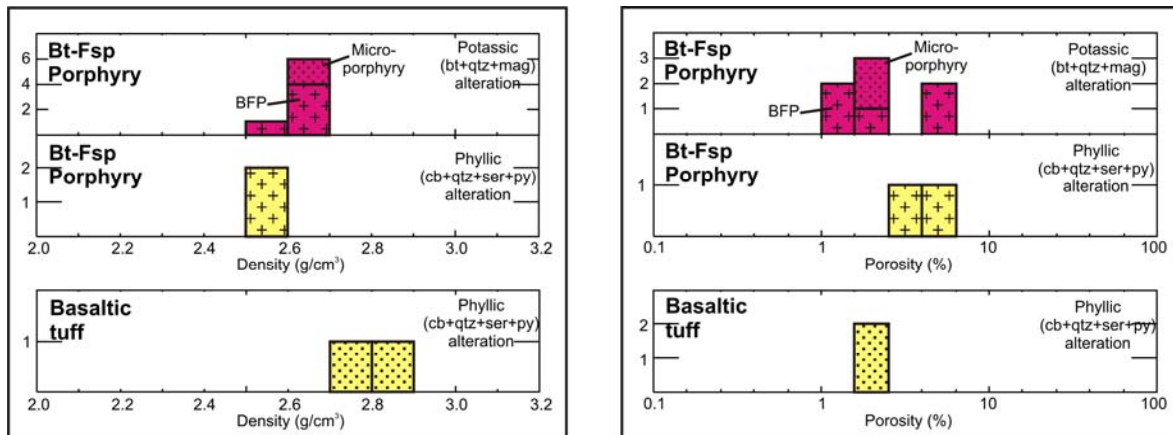


Figure 5.4. Density and porosity data from the Granisle deposit. Abbreviations: BFP= biotite-feldspar porphyry; bt=biotite, cb=carbonate, fsp=feldspar, mag=magnetite, py=pyrite, qtz=quartz, ser=sericite.

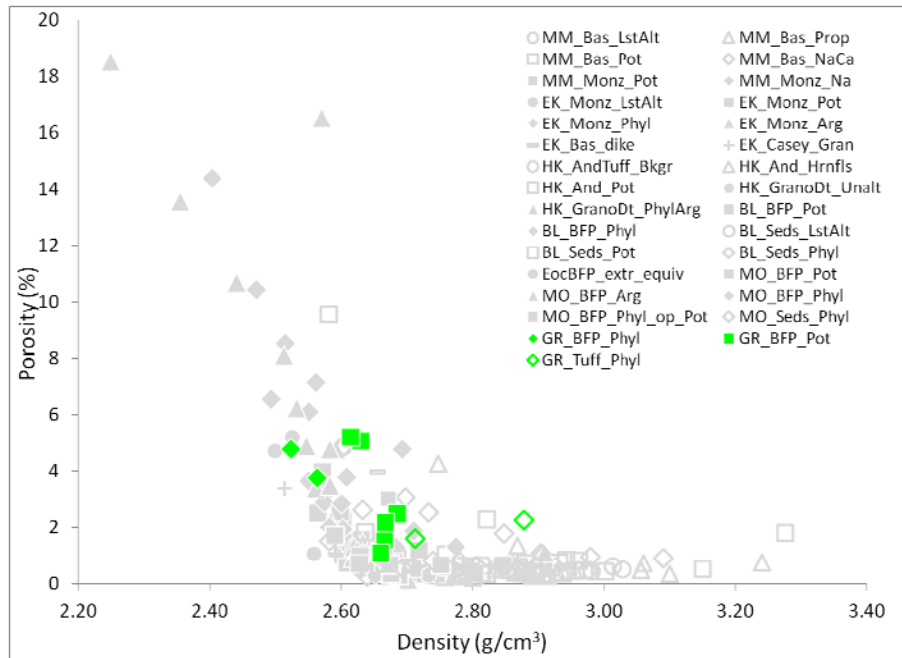


Figure 5.5. Density versus porosity data for all porphyry samples from this study. Granisle samples are highlighted in light green. Deposit abbreviations: BL=Bell, EK=Endako, GR=Granisle, HK=Huckleberry, MM=Mount Milligan, MO=Morrison. Rock type abbreviations: And=Andesite, Bas=basalt, BFP=biotite-feldspar porphyry, EocBFP Extr_equiv=Eocene biotite-feldspar porphyry extrusive equivalent, Gran=granite, GranoDt=granodiorite, Monz=monzonite, Seds=sedimentary rocks. Alteration assemblage abbreviations: Arg=argillic, Bkgr=background, Hrnfls=hornfels, LstAlt=least-altered, Na=sodic, NaCa=sodic-calcic, Phyl=phyllic, Phyl_op_Pot=potassic with overprinting phyllic alteration, Pot=potassic, Prop=propylitic, Unalt=unaltered.

5.2.4. Resistivity Data and Deposit Scale Conductivity

At Granisle, the more coherent, potassically-altered BFP samples have high resistivities relative to the generally more porous phyllic-altered BFP samples (Figure 5.6). Phyllic-altered tuffaceous basalt yielded resistivity measurements intermediate between potassic- and phyllic-altered BFP.

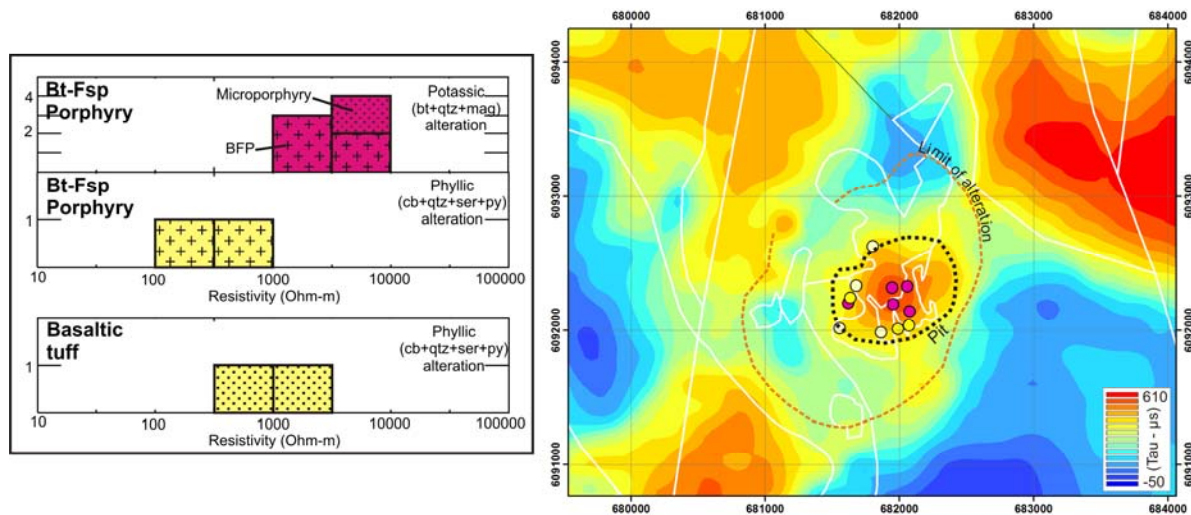


Figure 5.6. Resistivity data from the Granisle deposit, and late time Tau map from AeroTEM data (Aeroquest Surveys, 2009) collected over the Granisle deposit. Abbreviations: BFP= biotite-feldspar porphyry; bt=biotite, cb=carbonate, fsp=feldspar, mag=magnetite, py=pyrite, qtz=quartz, ser=sericite.

On a plot of resistivity versus porosity (Figure 5.7), Granisle samples plot along the negative correlation trend previously defined by other porphyry deposit samples analysed during this study. There is, however, less of a strongly defined linear trend for this suite of limited samples.

The Granisle deposit samples are plotted on a resistivity versus density plot (Figure 5.8). The samples plot predominantly within the lower density and resistivity ranges of a trend defined by other porphyry samples representing correlated decreases in density and resistivity caused by increased porosities.

The AeroTEM late time Tau data, reflecting EM response decay time (Aeroquest Surveys, 2009), show considerable variations in subsurface conductivity (Figure 5.6). Based on sample data and observed alteration assemblages, the conductivity high correlating with the Granisle pit area could be caused by high porosities related to phyllic alteration, but may also be enhanced by the presence of sulphide minerals. Conductivities might also be increased due to the presence of clay minerals deposited on the floor of the flooded open pit. Most volcanic and intrusive rocks mapped just beyond the mine area are resistive by comparison. Conductivity highs in the northeast quarter of the AeroTEM survey area are interpreted to reflect porous Jurassic Smithers Formation and Ashman Formation sedimentary rocks, and highs in the northwest correlate with Eocene breccia. Some alignment of conductivity anomalies with mapped faults is expressed in the late time Tau data. The presence of the adjacent Babine Lake might also influence the conductivity signal.

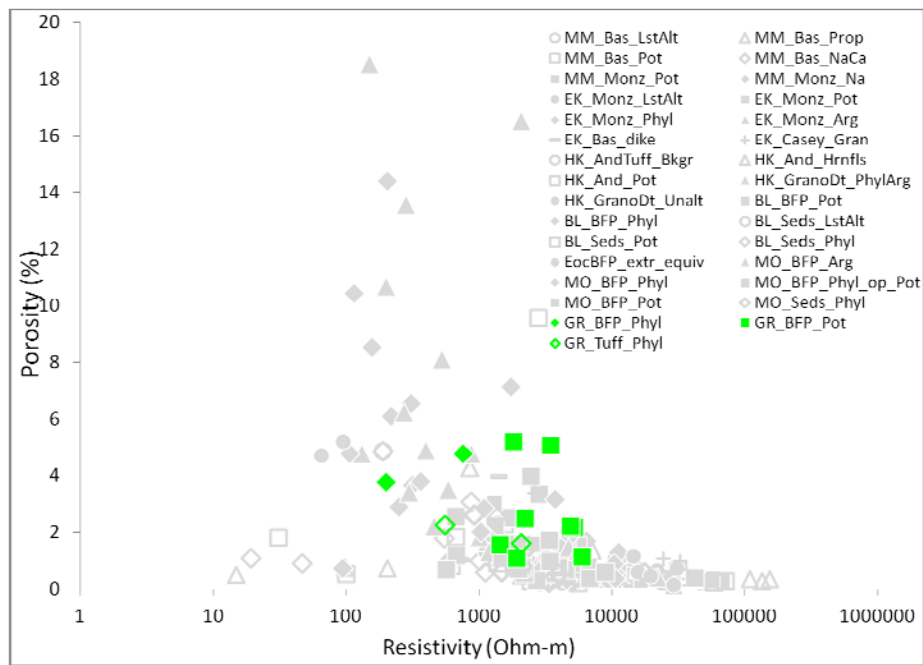


Figure 5.7. Resistivity versus porosity data for all porphyry samples from this study. Granisle samples are highlighted in light green. Deposit abbreviations: BL=Bell, EK=Endako, GR=Granisle, HK=Huckleberry, MM=Mount Milligan, MO=Morrison. Rock type abbreviations: And=Andesite, Bas=basalt, BFP=biotite-feldspar porphyry, EocBFP Extr_equiv=Eocene biotite-feldspar porphyry extrusive equivalent, Gran=granite, GranoDt=granodiorite, Monz=monzonite, Seds=sedimentary rocks. Alteration assemblage abbreviations: Arg=argillic, Bkgr=background, Hrnfls=hornfels, LstAlt=least-altered, Na=sodic, NaCa=sodic-calcic, Phyl=phyllic, Phyl_op_Pot=potassic with overprinting phyllic alteration, Pot=potassic, Prop=propylitic, Unalt=unaltered.

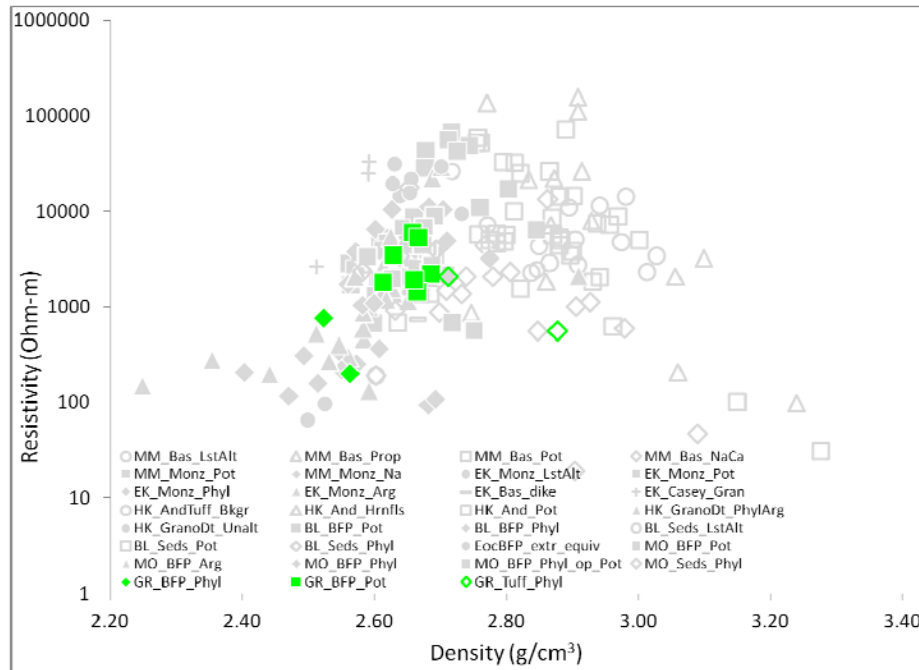


Figure 5.8. Resistivity versus density data for all porphyry samples from this study. Granisle samples are highlighted in light green. Deposit abbreviations: BL=Bell, EK=Endako, GR=Granisle, HK=Huckleberry, MM=Mount Milligan, MO=Morrison. Rock type abbreviations: And=Andesite, Bas=basalt, BFP=biotite-feldspar porphyry, EocBFP Extr Equiv=Eocene biotite-feldspar porphyry extrusive equivalent, Gran=granite, GranoDt=granodiorite, Monz=monzonite, Sed=sedimentary rocks. Alteration assemblage abbreviations: Arg=argillic, Bkgr=background, Hrnf=hornfels, LstAlt=least-altered, Na=sodic, NaCa=sodic-calcic, Phyl=phyllic, Phyl Op Pot=potassic with overprinting phyllic alteration, Pot=potassic, Prop=propylitic, Unalt=unaltered.

5.4. References

- Aeroquest Surveys (2009): Report on a helicopter-borne AeroTEM system electromagnetic & magnetic survey; Geoscience BC, Report 2009-6, 28 p.
- Dirom, G.E., Dittrick, M.P., McArthur, D.R., Ogryzlo, P.L., Pardoe A.J. and Stothart P.G. (1995): Bell and Granisle porphyry copper-gold mines, Babine region, west-central British Columbia; in Porphyry Deposits of the Northwestern Cordillera of North America, T.G. Schroeter (ed.), Canadian Institute of Mining, Metallurgy and Petroleum, Special Volume 46, p. 256–289.
- Massey, N.W.D, MacIntyre, D.G., Desjardins, P.J. and Cooney, R.T. (2005): Digital geology map of British Columbia: whole province; B.C. Ministry of Energy and Mines, Geofile 2005-1, URL

<<http://www.empr.gov.bc.ca/Mining/Geoscience/PublicationsCatalogue/GeoFiles/Pages/2005-1.aspx>> [November 2007].

Natural Resources Canada (2004): Canadian aeromagnetic data base, Continental Geoscience Division, Geological Survey of Canada, Earth Sciences Sector, Natural Resources Canada, Geoscience Data Repository, URL <<http://gdrdap.agg.nrcan.gc.ca/geodap/home/Default.aspx?lang=e>> [March 2011].

Appendix 6. Morrison

6.1. Regional Geology and Magnetic Data

6.1.1. Regional Geologic Setting

The Morrison deposit is located north of the Bell and Granisle deposits at the northern end of Babine Lake, and represents another Eocene biotite-feldspar porphyry (BFP)-related deposit. (Figure 6.1). The deposit occurs within Cretaceous sedimentary stratigraphy which has been down-dropped relative to Jurassic Hazelton Group volcanic stratigraphy sitting to the east. The deposit is aligned along the northwest trend of regional scale structures considered to play an important role in the localization of Babine district porphyry Cu deposits.

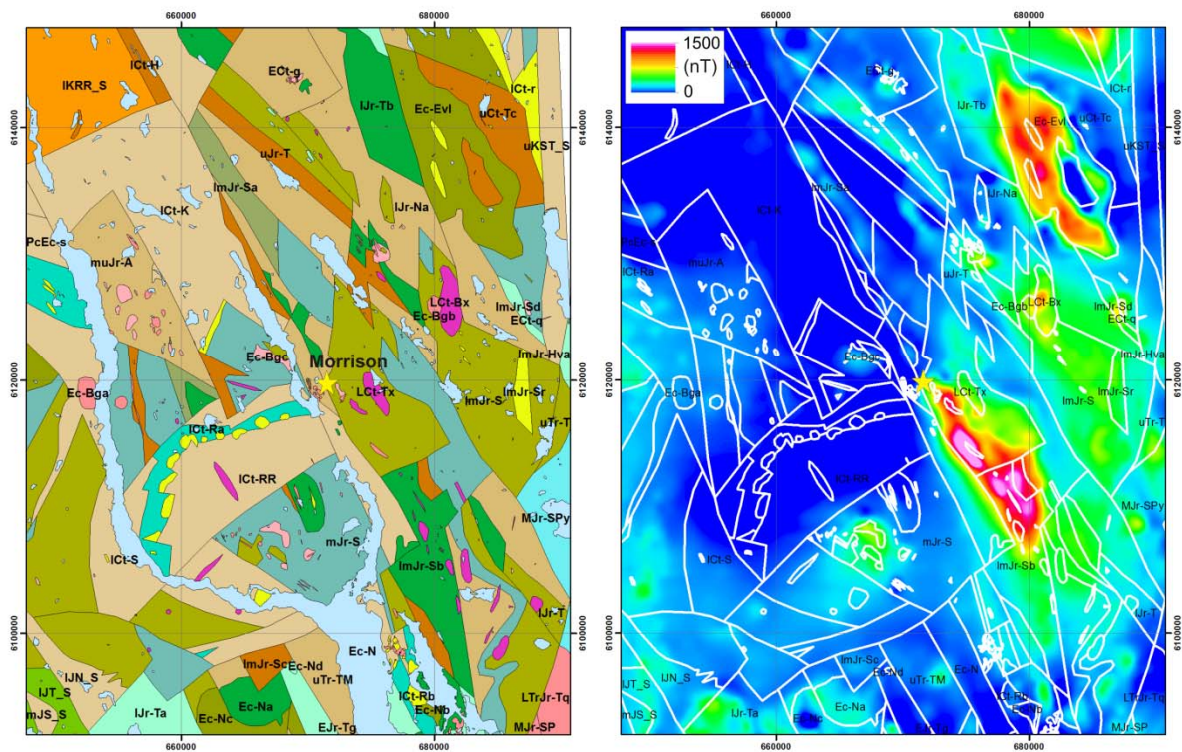


Figure 6.1. Regional geological setting for the Morrison porphyry copper deposit (Massey et al, 2005), and regional residual total field magnetic data Natural Resources Canada's Geoscience Data Repository (Natural Resources Canada, 2004) .

Regional Geology of the Morrison Deposit

Legend

Eocene

- Ec-Evl - Nechako Plateau Group - Endako Formation coarse volcanoclastic and pyroclastic volcanic rocks
- Ec-N - Nechako Plateau Group - Newman Formation andesitic volcanic rocks
- Ec-Na - Nechako Plateau Group - Newman Formation - Porphyritic Flows Member basaltic volcanic rocks
- Ec-Nb - Nechako Plateau Group - Newman Formation - Breccia Member coarse volcanoclastic and pyroclastic volcanic rocks
- Ec-Nc - Nechako Plateau Group - Newman Formation - Lahar Member coarse volcanoclastic and pyroclastic volcanic rocks
- Ec-Nd - Nechako Plateau Group - Newman Formation - Mafic Flows Member andesitic volcanic rocks

Eocene Babine Intrusions

- Ec-Bga - Babine Plutonic Suite - Biotite-Quartz-Feldspar Porphyritic Phase granodioritic intrusive rocks
- Ec-Bgb - Babine Plutonic Suite - Biotite-Feldspar Porphyritic Phase granodioritic intrusive rocks
- Ec-Bgc - Babine Plutonic Suite - Quartz Diorite to Granodiorite Phase quartz dioritic intrusive rocks

Paleocene to Eocene

- PcEc-s - Unnamed undivided sedimentary rocks

Late Cretaceous Bulkley Intrusions

- LCt-Bx - Bulkley Plutonic Suite - Diorite Phase dioritic intrusive rocks

Lower to Upper Cretaceous

Sustut Group

- uKST_S - Sustut Group - Tango Creek Formation undivided sedimentary rocks
- uCt-Tc - Sustut Group - Tango Creek Formation conglomerate, coarse clastic sedimentary rocks

Skeena Group



- LCt-Tx - Unnamed dioritic intrusive rocks
- ICt-S - Skeena Group undivided sedimentary rocks
- ICt-RR - Skeena Group - Red Rose Formation undivided sedimentary rocks
- IKRR_S - Skeena Group - Red Rose Formation coarse clastic sedimentary rocks
- ICt-Ra - Skeena Group - Rocky Ridge Formation - Subvolcanic Rhyolite Domes alkaline volcanic rocks
- ICt-r - Skeena Group - Felsic Volcanics rhyolite, felsic volcanic rocks
- ICt-H - Skeena Group - Hanawald Conglomerate conglomerate, coarse clastic sedimentary rocks
- ICt-K - Skeena Group - Kitsuns Creek Formation undivided sedimentary rocks

Early Cretaceous Intrusive Rocks

- ECt-g - Unnamed granodioritic intrusive rocks
- ECt-q - Wedge Mountain Stock quartz monzonitic to monzogranitic intrusive rocks



Middle to Upper Jurassic

Bowser Lake Group

-  uJr-T - Bowser Lake Group - Trout Creek Formation conglomerate, coarse clastic sedimentary rocks
-  muJr-A - Bowser Lake Group - Ashman Formation argillite, greywacke, wacke, conglomerate turbidites

Early to Middle Jurassic

Spike Peak Intrusive Suite

-  MJr-SP - Spike Peak Intrusive Suite - Quartz Monzonite Phase granodioritic intrusive rocks
-  MJr-SPy - Spike Peak Intrusive Suite syenitic to monzonitic intrusive rocks

Lower to Middle Jurassic

Hazelton Group



-  mJS_S - Hazelton Group - Smithers Formation undivided sedimentary rocks
-  mJr-S - Hazelton Group - Smithers Formation marine sedimentary and volcanic rocks
-  ImJr-Sr - Hazelton Group - Saddle Hill Formation - Subvolcanic Rhyolite Domes rhyolite, felsic volcanic rocks
-  ImJr-S - Hazelton Group - Saddle Hill Formation undivided volcanic rocks
-  ImJr-Sa - Hazelton Group - Saddle Hill Formation - Intermediate Volcanic Member volcanoclastic rocks
-  ImJr-Sb - Hazelton Group - Saddle Hill Formation - Mafic Submarine Volcanic Member basaltic volcanic rocks
-  ImJr-Sc - Hazelton Group - Saddle Hill Formation - Volcanoclastic-Sedimentary Member conglomerate, coarse clastic sedimentary rocks
-  ImJr-Sd - Hazelton Group - Saddle Hill Formation - Megacrystic Porphyry Member andesitic volcanic rocks
-  ImJr-Hva - Hazelton Group andesitic volcanic rocks
-  IJN_S - Hazelton Group - Nilkitkwa Formation undivided sedimentary rocks
-  IJr-Na - Hazelton Group - Nilkitkwa Formation argillite, greywacke, wacke, conglomerate turbidites
-  IJT_S - Hazelton Group - Telkwa Formation calc-alkaline volcanic rocks
-  IJr-Ta - Hazelton Group - Telkwa Formation - Felsic to Intermediate Volcanic Member andesitic volcanic rocks
-  IJr-Tb - Hazelton Group - Telkwa Formation - Mafic Volcanic Member basaltic volcanic rocks
-  IJr-T - Hazelton Group - Telkwa Formation undivided volcanic rocks

Late Triassic to Early Jurassic

Topley Intrusive Suite

-  EJr-Tg - Topley Intrusive Suite - Porphyritic Phase granodioritic intrusive rocks
-  LTrJr-Tq - Topley Intrusive Suite - Granodiorite to Monzonite Phase granodioritic intrusive rocks

Upper Triassic

-  uTr-T - Takla Group undivided volcanic rocks
-  uTr-TM - Takla Group - Moosevale Formation argillite, greywacke, wacke, conglomerate turbidites

6.1.2. Regional Magnetic Data

The Morrison deposit occurs near the eastern edge of a broad magnetic low which marks the extent of Late Jurassic to Early Cretaceous Bowser Lake Group and Cretaceous Skeena Group sedimentary and volcano-sedimentary rocks. To the west, Jurassic Hazelton Group mafic volcanic units are moderately magnetic. Volcaniclastic units tend to be characterized by weaker magnetic signatures. The strongest magnetic responses are correlated with Cretaceous diorite intrusive bodies, and with later onlapping Eocene volcanic sequences.

6.2. Deposit Geology

At the Morrison deposit, mineralization is focused around a central BFP intrusion which is hosted by siltstone and silty argillite units of the Ashman Formation of the Middle to Late Jurassic Bowser Lake Group (Figure 6.2). A north-northwest-trending strike-slip fault, bisects the main BFP intrusive body at Morrison. Eocene porphyritic intrusive rocks are mapped surrounding the central mineralized BFP, some of which are elongate and dike-like, trending north-northwest.

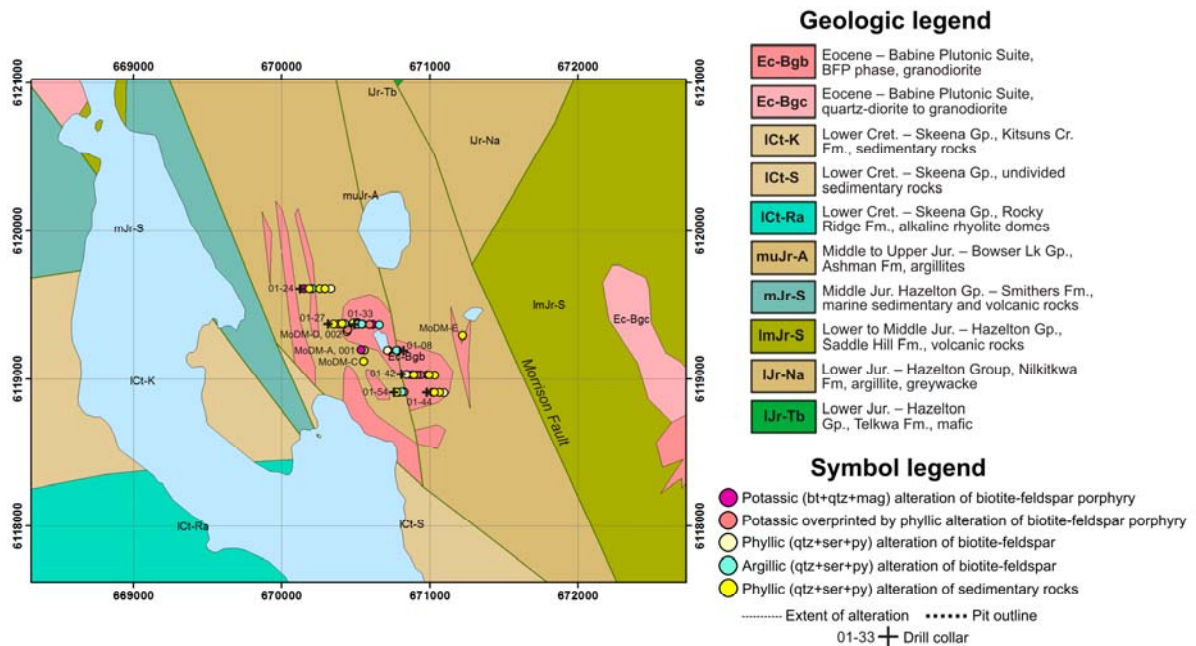


Figure 6.2. Map of Morrison deposit area geology (Massey et al., 2005) showing the location of hand samples and drill core samples collected for this study. The samples are colored based on alteration.

A hydrothermal alteration halo was developed in association with porphyry mineralization at Morrison, and consists of a potassic core of biotite+quartz+magnetite, which grades outward into a propylitic (chlorite+carbonate) alteration zone. Early potassic alteration is overprinted by phyllic (quartz+sericite+pyrite) alteration and eventually by argillic (clay+sericite) alteration, which is locally controlled by late faults (Ogryzlo et al., 1995). Of the Babine district deposits sampled, Morrison appears to have the most intensely developed argillic alteration. Copper mineralization occurs predominantly within and marginal to the potassic biotite+quartz+magnetite alteration zone. Sulphides - chalcopyrite, bornite, and pyrite predominantly - are disseminated as well as vein-hosted.

Regional tectonic events may have dissected and relatively displaced portions of a larger mineralizing system in the Morrison area. The Hearne Hill porphyry Cu prospect is hosted by Jurassic Hazelton Group volcanic rocks which sit in faulted contact with the Bowser Lake sedimentary rocks hosting the Morrison deposit. The Hearne Hill deposit is interpreted to represent the deeper roots of the Morrison deposit (Ogryzlo et al., 1995), the original porphyry deposit having been dismembered as a result of extensional faulting. Later dextral shear shifted the Morrison deposit north of the Hearne Hill deposit.

6.2. Physical Properties of Rocks from the Morrison Deposit

6.2.1. Sample Suite

The majority of physical rock property measurements from the Morrison deposit are derived from samples collected from seven drill cores extracted from different locations on the Morrison property (Figure 6.2). Susceptibility measurements were collected on thirty-nine core samples. Potassic, phyllic, and argillic alteration zones were sampled; propylitically-altered rocks were not encountered in the drillholes examined. Two hand samples were collected from a BFP intrusion outcropping on the deposit site, and additional outcrop susceptibility measurements were made on both BFP and sedimentary rocks.

Samples are grouped for evaluation purposes based on alteration assemblage. Specifically, BFP samples are grouped into potassically-altered, potassic + phyllic-altered, predominantly phyllic-altered, and argillic-altered samples. The sedimentary rock sample suite contains phyllic-altered samples only.

6.2.2. Magnetic Susceptibility and Deposit Scale Magnetic Data

Figure 6.3 shows susceptibility data measured from Morrison BFP and sedimentary samples. Potassically-altered BFP samples, and samples where phyllic alteration has overprinted potassic alteration are the most magnetically susceptible samples. Potassic samples range up to 44×10^{-3} SI units and have a geometric average of 11.2×10^{-3} SI units. Phyllic and argillic alteration of BFP overprints potassic alteration, causing magnetite to break down and susceptibilities to drop significantly. Phyllic samples have a geometric average susceptibility of 0.52×10^{-3} SI units and argillic samples have a geometric average of 0.22×10^{-3} SI units.

Sedimentary rock samples from the Morrison deposit were all collected from the phyllic alteration zone. Since mineralization is focused on the BFP intrusive body, the surrounding sedimentary rocks naturally correlate spatially with the more distal alteration assemblages. Phyllic-altered sedimentary rock samples generally have low susceptibilities, with a geometric average of 0.46×10^{-3} SI units. Two moderately susceptible phyllic-altered sedimentary rock samples (3.27 and 7.36×10^{-3} SI units) represent samples that appear to have been previously altered to potassic assemblages, and were later overprinted.

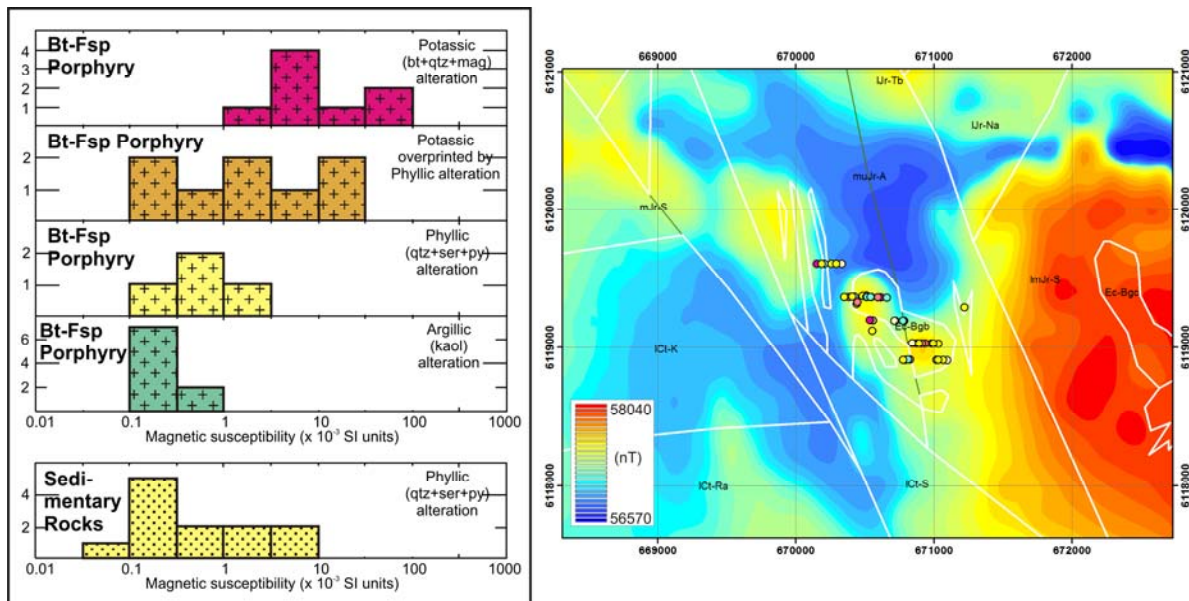


Figure 6.3. Histograms showing magnetic susceptibility data for variably altered intrusive and sedimentary rock samples from the Morrison deposit and total magnetic intensity data (Aeroquest Surveys, 2009) from the Morrison deposit. Abbreviations: bt=biotite, fsp=feldspar, kaol=kaolinite, mag=magnetite, py=pyrite, qtz=quartz, ser=sericite.

Magnetic data collected over the Morrison deposit show local moderate positive magnetic anomalies over the dissected BFP intrusive body, as well as over BFP dikes (Figure 6.3). The centers of local magnetic anomalies coincide with projected locations of potassic-altered drill core samples (colored pink), with phyllic-altered samples (yellow) generally sitting on the flanks of the anomalies. A potassically-altered sample coincides with the edge of a magnetic anomaly to the northwest of the main mineralized area. The anomaly is aligned with mapped north-northwest trending porphyritic dikes. Several argillic-altered drill core samples are projected to sit on or near the later Morrison fault, others however are found sitting within the northwestern portion of the faulted BFP pluton, perhaps representing more local scale faulting not recorded on the geological map. Mapped sedimentary rocks appear to be generally nonmagnetic (Figure 6.3). East of the Morrison deposit, a prominent magnetic high corresponds to mafic volcanic rocks of the Saddle Hill Formation of the Jurassic Hazelton Group.

6.2.3. Density and Porosity

Biotite-feldspar porphyry samples from the Morrison deposit have densities below 2.8 g/cm^3 (Figure 6.4). Potassically-altered BFPs have the highest densities of this sample suite, averaging 2.66 g/cm^3 . Phyllic-altered samples have slightly lower average densities, while argillic samples have significantly lower densities averaging 2.46 g/cm^3 . Argillic samples are particularly low density because of their high porosities, a relationship indicated by the plot in Figure 6.5. With the exception of the seven high porosity argillic-altered BFP samples (from 4-19% porosity), porosities of sampled Morrison rocks are below 3%, with most samples falling below 1%. The overall negative correlation between density and porosity follows the trend established for Bell, Granisle and Endako intrusive samples. Sedimentary samples generally plot along the same trend with the lowest density samples having the highest porosities. Sedimentary rock samples do not attain porosities as high as BFP samples collected from the Morrison deposit.

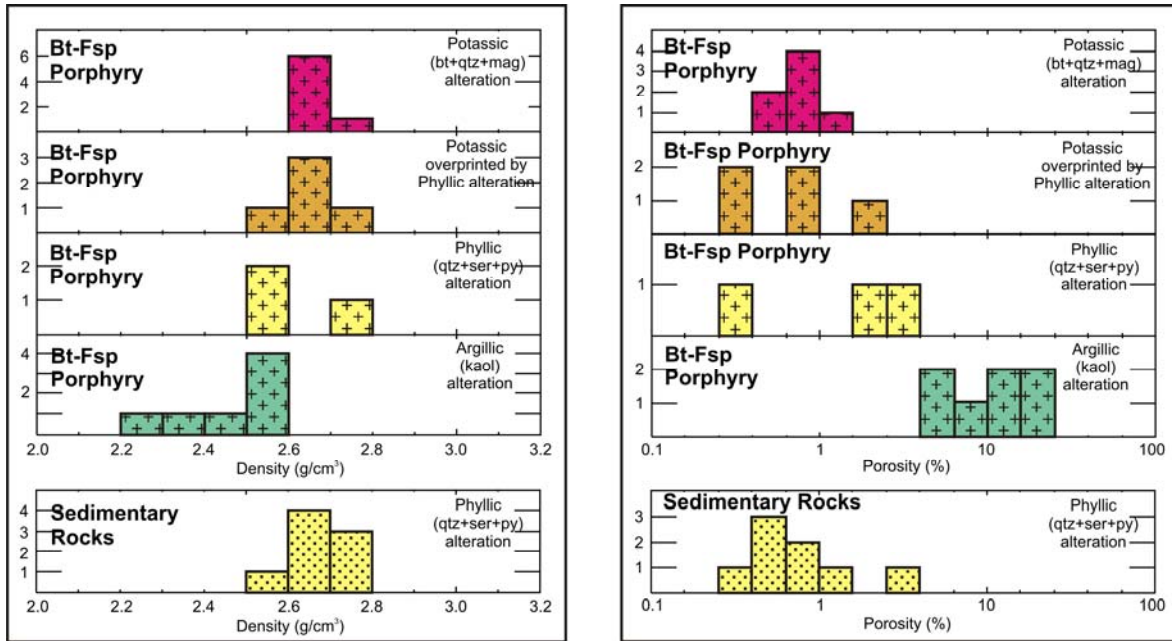


Figure 6.4. Density and porosity data from the Morrison deposit. Abbreviations: bt=biotite, fsp=feldspar, kaol=kaolinite, mag=magnetite, py=pyrite, qtz=quartz, ser=sericite.

6.2.4. Resistivity Data and Deposit Scale Conductivity

Potassically-altered, and potassic + phyllic-altered BFP samples are the most resistive of the Morrison BFP suite, with most samples measured at >1000 Ohm-m (Figure 6.6). Phyllic-altered BFP and sedimentary samples have similar resistivities to potassically-altered BFP. The lowest resistivity samples at Morrison are those BFP samples altered to argillic assemblages, with typical resistivities less than 1000 Ohm-m.

A relationship between porosity and resistivity is clearly indicated in Figure 6.7. The highest porosity samples, specifically a group of argillic-altered samples, have the lowest resistivities. Similar relationships noted at the Bell and Endako deposits, suggested that sericite and kaolinite alteration leads to a break-down of feldspars increasing porosity, promoting infiltration of fluids, and increasing conductivities. The majority of the samples collected from Morrison however have relatively low porosities and correspondingly high resistivities.

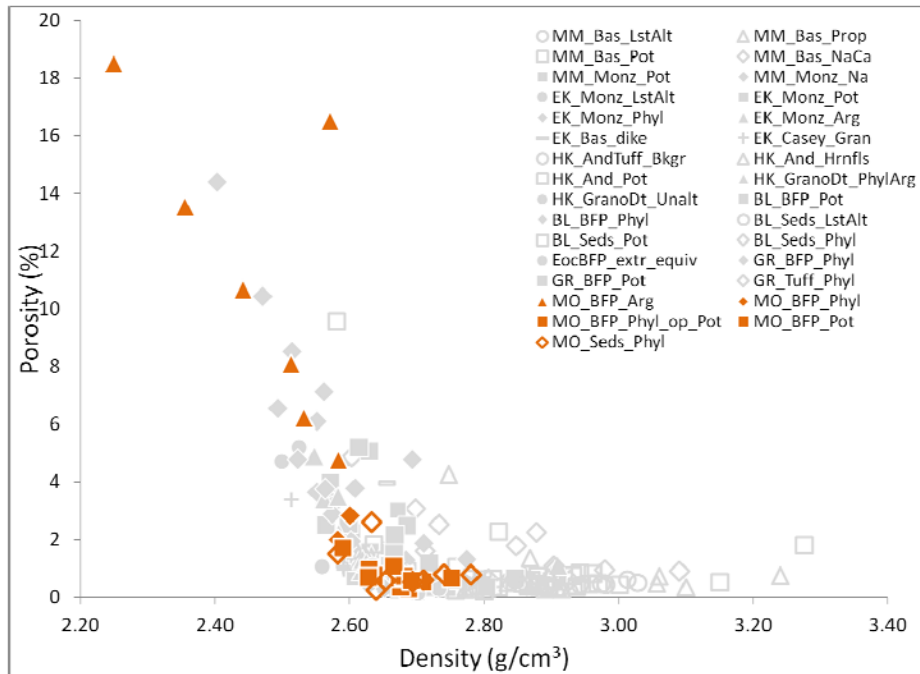


Figure 6.5. Density versus porosity data for all porphyry samples from this study. Morrison samples are highlighted in orange. Deposit abbreviations: BL=Bell, EK=Endako, GR=Granisle, HK=Huckleberry, MM=Mount Milligan, MO=Morrison. Rock type abbreviations: And=Andesite, Bas=basalt, BFP=biotite-feldspar porphyry, EocBFP_extr_equiv=Eocene biotite-feldspar porphyry extrusive equivalent, Gran=granite, GranoDt=granodiorite, Monz=monzonite, Sed=sedimentary rocks. Alteration assemblage abbreviations: Arg=argillic, Bkgr=background, Hrnfls=hornfels, LstAlt=least-altered, Na=sodic, NaCa=sodic-calcic, Phyl=phyllic, Phyl_op_Pot=potassic with overprinting phyllic alteration, Pot=potassic, Prop=propylitic, Unalt=unaltered.

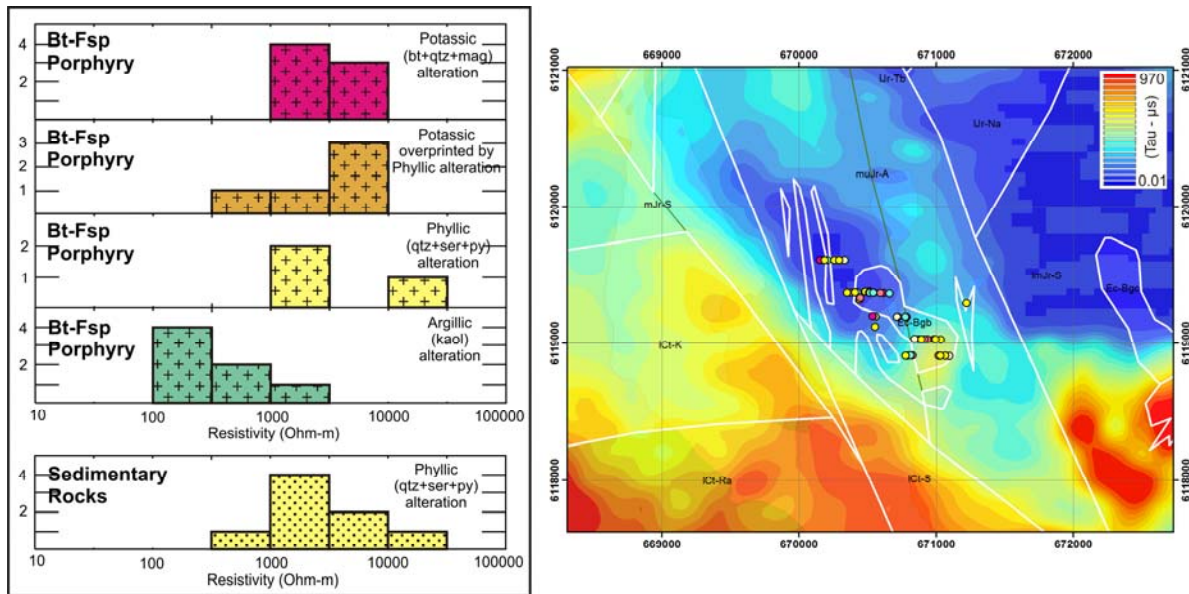


Figure 6.6. Resistivity data from the Morrison deposit, and late time Tau conductivity map from AeroTEM data (Aeroquest Surveys, 2009) collected over the Morrison deposit. Abbreviations: bt=biotite, fsp=feldspar, kaol=kaolinite, mag=magnetite, py=pyrite, qtz=quartz, ser=sericite.

Morrison samples plot along the same trend as Bell and Endako samples on a plot of resistivity versus density (Figure 6.8). High densities and high resistivities characterize low porosity BFP samples, and coinciding low resistivities and low densities are explained by high porosities attributed to clay-rich alteration. In contrast to the Bell sample suite, there are no samples that fall significantly off this trend. One sample has a lower than expected resistivity given its density. This sample is one with a higher abundance of sulphides (4.9% pyrite) than most samples in the suite.

AeroTEM late time Tau data (Figure 6.6) reveals variable conductivity across the Morrison property. The southeastern half of the faulted BFP pluton is characterized by higher conductivities (lower resistivities), and the northwestern half by low conductivities (higher resistivities). This pattern is not explained in resistivity data collected from Morrison samples, with porous and conductive phyllic- and argillic-altered rocks logged as occurring in both zones. The low conductivity zone spans an area between the northern lobe of the central BFP and BFP dikes to the northwest. The anomaly could potentially indicate an unsampled deeper coherent, thus resistive, intrusive body sitting within the otherwise moderately conductive argillite sedimentary package. To the east of the Morrison deposit, mafic volcanic rocks are relatively resistive.

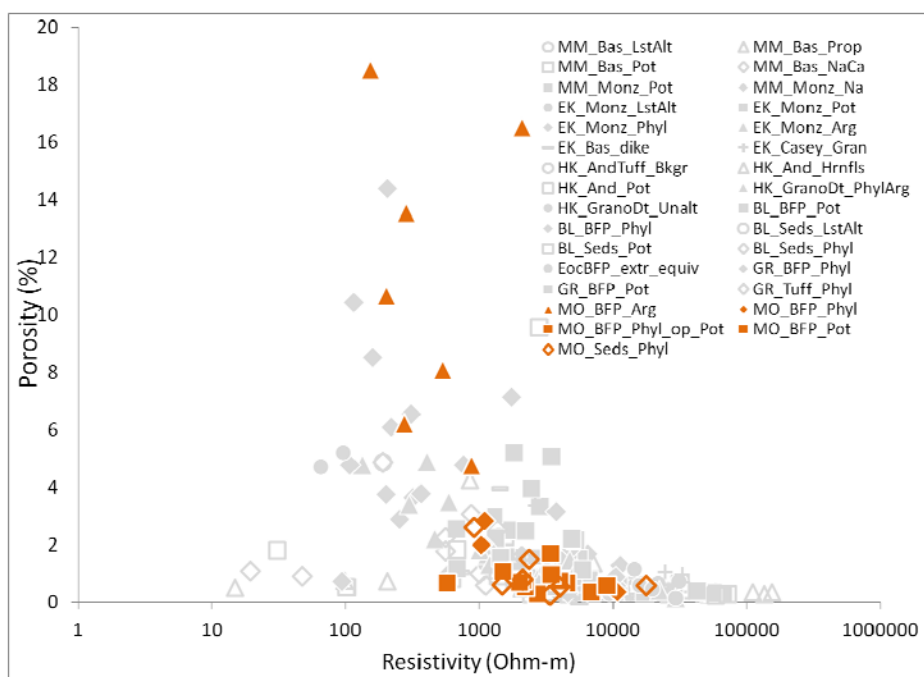


Figure 6.7. Resistivity versus porosity data for all porphyry samples from this study. Morrison samples are highlighted in orange. Deposit abbreviations: BL=Bell, EK=Endako, GR=Granisle, HK=Huckleberry, MM=Mount Milligan, MO=Morrison. Rock type abbreviations: And=Andesite, Bas=basalt, BFP=biotite-feldspar porphyry, EocBFP_extr_equiv=Eocene biotite-feldspar porphyry extrusive equivalent, Gran=granite, GranoDt=granodiorite, Monz=monzonite, SedS=sedimentary rocks. Alteration assemblage abbreviations: Arg=argillic, Bkgr=background, Hrnfls=hornfels, LstAlt=least-altered, Na=sodic, NaCa=sodic-calcic, Phyl=phyllic, Phyl_op_Pot=potassic with overprinting phyllic alteration, Pot=potassic, Prop=propylitic, Unalt=unaltered.

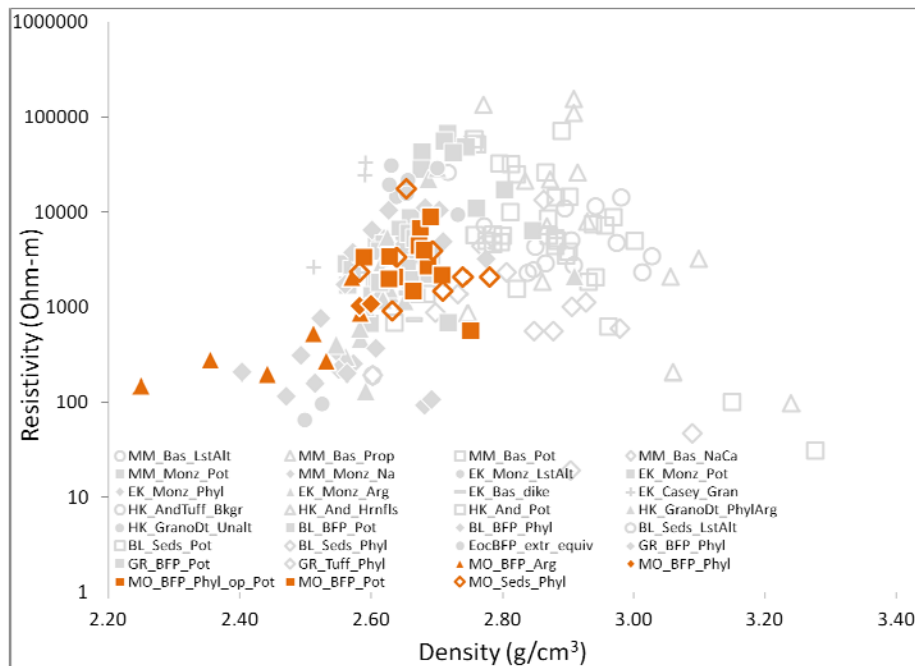


Figure 6.8. Resistivity versus density data for all porphyry samples from this study. Morrison samples are highlighted in orange. Deposit abbreviations: BL=Bell, EK=Endako, GR=Granisle, HK=Huckleberry, MM=Mount Milligan, MO=Morrison. Rock type abbreviations: And=Andesite, Bas=basalt, BFP=biotite-feldspar porphyry, EocBFP Extr_equiv=Eocene biotite-feldspar porphyry extrusive equivalent, Gran=granite, GranoDt=granodiorite, Monz=monzonite, Seds=sedimentary rocks. Alteration assemblage abbreviations: Arg=argillic, Bkgr=background, Hrnfls=hornfels, LstAlt=least-altered, Na=sodic, NaCa=sodic-calcic, Phyl=phyllic, Phyl_op_Pot=potassic with overprinting phyllic alteration, Pot=potassic, Prop=propylitic, Unalt=unaltered.

6.4. References

Aeroquest Surveys (2009): Report on a helicopter-borne AeroTEM system electromagnetic & magnetic survey; Geoscience BC, Report 2009-6, 28 p.

Dirom, G.E., Dittrick, M.P., McArthur, D.R., Ogryzlo, P.L., Pardoe A.J. and Stothart P.G. (1995): Bell and Granisle porphyry copper-gold mines, Babine region, west-central British Columbia; in *Porphyry Deposits of the Northwestern Cordillera of North America*, T.G. Schroeter (ed.), Canadian Institute of Mining, Metallurgy and Petroleum, Special Volume 46, p. 256–289.

Massey, N.W.D, MacIntyre, D.G., Desjardins, P.J. and Cooney, R.T. (2005): Digital geology map of British Columbia: whole province; B.C. Ministry of Energy and Mines, Geofile 2005-1, URL <<http://www.empr.gov.bc.ca/Mining/Geoscience/PublicationsCatalogue/GeoFiles/Pages/2005-1.aspx>> [November 2007].

- Natural Resources Canada (2004): Canadian aeromagnetic data base, Continental Geoscience Division, Geological Survey of Canada, Earth Sciences Sector, Natural Resources Canada, Geoscience Data Repository, URL <<http://gdrdap.agg.nrcan.gc.ca/geodap/home/Default.aspx?lang=e>> [March 2011].
- Ogryzlo, P.L., Dirom G.E. and Stothart P.G. (1995): Morrison-Hearne Hill copper-gold deposits, Babine region, west-central British Columbia; in Porphyry Deposits of the Northwestern Cordillera of North America, T.G. Schroeter (ed.), Canadian Institute of Mining, Metallurgy and Petroleum, Special Volume 46, p. 290–303.

Appendix 7. Deposit-scale Relationships between Metallic Minerals and Electrical Properties

Sulphide minerals are typically the host for Cu, Au, and Mo in porphyry deposit settings. Geophysical methods effective in detecting sulphides, such as DC resistivity, induced polarization (IP), and electromagnetic (EM) methods, are thus frequently applied in exploration for porphyry deposits. The development of a method for predicting sulphide type and abundance from electrical rock properties, like conductivity and chargeability, would further enhance the value of electrical geophysical methods, leading to more effective exploration targeting. There are limited studies exploring sulphide mineral discrimination using electrical data. One older, but relevant, reference is Pelton et al. (1978), which documents differences in complex resistivity measurements between massive sulphides, graphite, magnetite, and pyrrhotite. Prediction of sulphides from electrical data, however, is challenging since numerous variables can affect a rock's electrical properties. As alluded to in previous sections of this report, electrical rock properties can be affected by sulphide texture, grain size, rock texture, and water content. Porosity, for example, was indicated to be an important influence on conductivity at several of the porphyry deposits investigated for this study.

This section highlights some of the correlations existing between sulphide abundance, electrical properties, and other related rock properties measured from BC porphyry deposit samples. This provides a framework for interpretation of deposit-scale conductivity and chargeability anomalies in analogous environments. Data from all of the investigated porphyry deposits are analyzed together here in order to maximize the sample populations.

7.1. Controls on Electrical Resistivity/Conductivity - Sulphide Abundance vs. Porosity

Resistivity was shown to be correlated with sulphide abundance at Mount Milligan. Figure 7.1 shows sulphide (pyrite + chalcopyrite) abundance versus resistivity for all XRD-analyzed porphyry deposit samples from this study. A general trend of decreasing resistivity with increasing sulphide abundance is apparent. The presence of sulphides leads to the rock having a greater capacity to conduct electrical current, thereby lowering resistivities.

A second control on resistivity - porosity - has been referenced in previous sections of this report. Figure 7.2 illustrates this relationship. An increase in porosity, whether due to brecciation or fracturing of a rock, or to increased alteration, allows fluids to infiltrate the rock, lowering its resistivity.

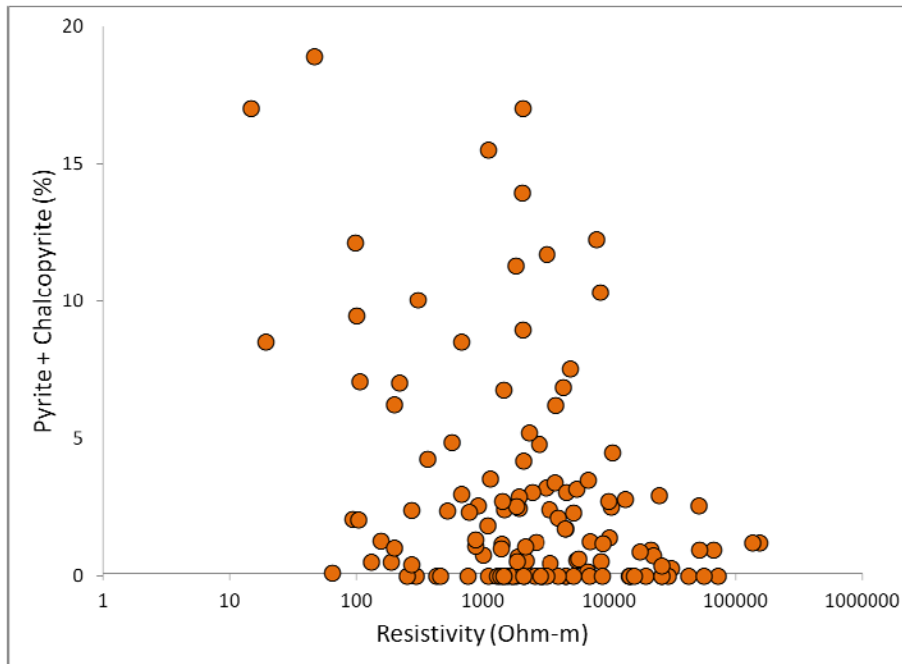


Figure 7.1. Plot of resistivity versus sulphide abundance for samples from all porphyry deposits studied. A general decrease in resistivity with increased pyrite and chalcopyrite abundance is noted. Sulphide abundances determined by XRD Rietveld analysis.

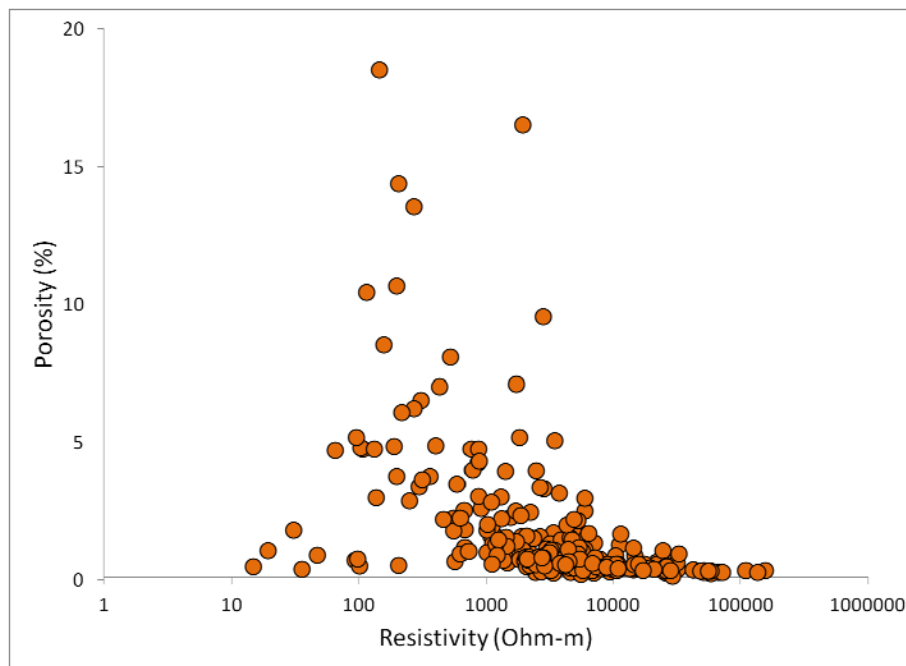


Figure 7.2. Plot of resistivity versus porosity for all porphyry deposit samples from this study. Resistivities generally decrease with increases in porosity.

With multiple factors influencing a rock's resistivity, it is difficult to resolve the overriding control on this electrical property. By considering a third variable, density, primary controls on resistivity may become more evident. Figure 7.3 shows the relationship between density and resistivity for mafic volcanic, intrusive, and sedimentary samples. Similar figures were presented in each of the previous Appendices, but here sulphide abundance is indicated by bubble size. If a decrease in resistivity is accompanied by an increase in density then the presence of sulphides, which are usually significantly more dense than silicate and carbonate minerals, might explain the reduced resistivities. Figure 7.4 demonstrates a general increase in sample density with increases in sulphide abundance.

If low resistivity samples are also characterized by low densities, porosity may be the greater influence on resistivity, as is demonstrated in Figure 7.5. The least dense and resistive samples are consistently higher porosity.

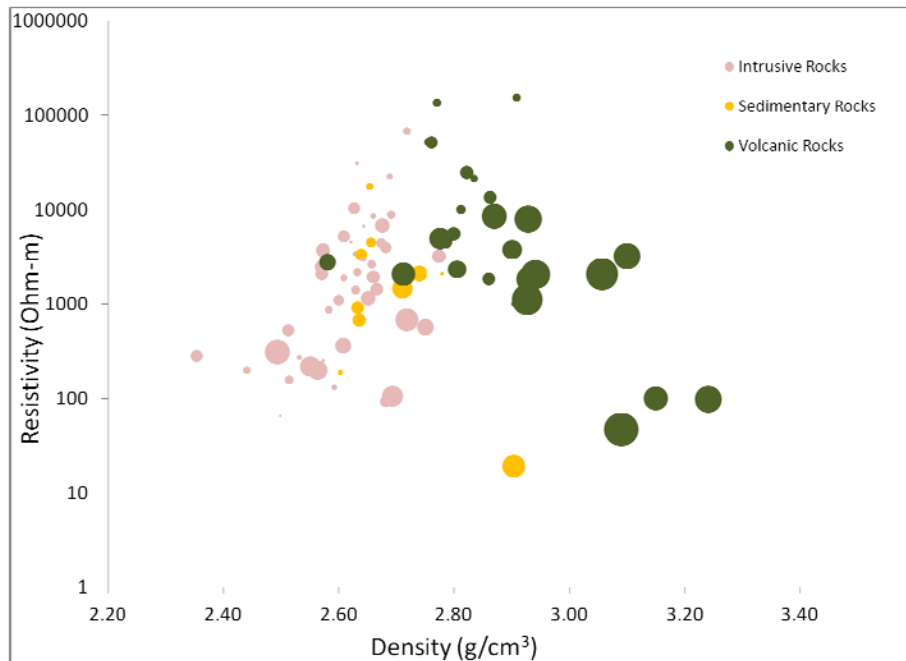


Figure 7.3. Plot of density versus resistivity, with samples colored to represent general lithology, and bubble sizes representing sulphide (pyrite + chalcopyrite) abundance. Samples with increased sulphide abundances have increased densities and decreased resistivities.

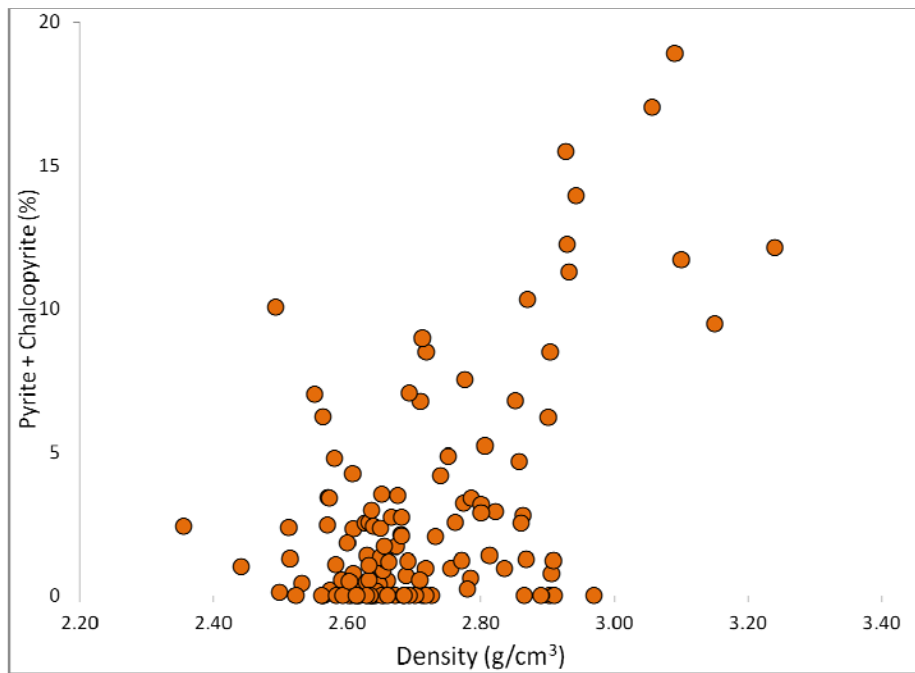


Figure 7.4. Density versus sulphide abundance. A general positive correlation exists between the two variables. Sulphide abundances are determined by XRD Rietveld analysis.

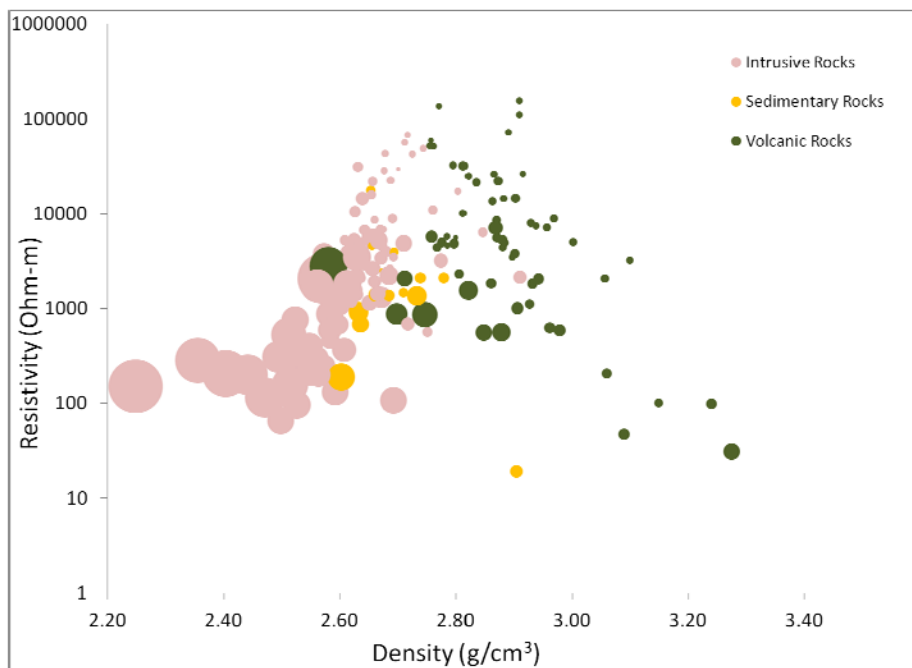


Figure 7.5. Plot of density versus resistivity, with samples colored to represent general lithology, and bubble sizes representing porosity. Samples with increased porosities typically have low densities and resistivities.

7.2. Controls on Electrical Resistivity/Conductivity - Sulphide Distribution

The distribution of sulfides within a rock will affect its resistivity. Electrical conductivity is enhanced when sulphides within the rock are connected through vein and fracture networks. Disseminated sulphides are less effective at conducting an electrical current. The distribution of sulphides therefore may have as significant an influence on rock resistivity as sulphide abundance. To explore these relationships, porphyry samples were grouped based on sulphide occurrence determined visually from drill core and hand samples, and from petrographic analysis. Not all samples were investigated petrographically and very fine-grained sulphides may have been missed in certain cases, thus the categorization of samples is not rigorously applied. Nonetheless some trends emerge. Figure 7.6 demonstrates a weak correlation between sulphide distribution in a sample, and resistivity. Samples with disseminated sulphides sit within a marginally higher range of resistivities. Samples characterized by vein and fracture-controlled sulphides have lower average resistivities. As previously discussed, porosity was determined to strongly influence sample resistivity. To try and compare the duelling effects of sulphide distribution and rock texture on resistivity, the sample symbols plotted in Figure 7.6 are sized according to porosity. From this plot, it is obvious that within each sulphide distribution group, the most conductive samples are those with higher porosities.

An examination of rock texture and mineralogy sheds light on the relationships indicated in the plotted sample data. For the Babine district porphyry deposit samples, phyllic-altered samples containing pyrite in veins had consistently low resistivities, and potassically-altered samples were relatively resistive. Figure 7.7 presents two sets of photomicrographs showing the mineralogical and textural differences between higher resistivity and lower resistivity samples from the Bell deposit. The vein-hosted sulphides in the phyllic-altered sample may be partly responsible for the decreased resistivities recorded. The process of alteration leads to textural changes in the rocks, which also influences resistivity. Potassically-altered samples from the Babine porphyry deposits typically have silicified annealed groundmasses, which may act to inhibit electrical currents. In contrast, phyllic alteration breaks down feldspars and other minerals, increasing permeability to fluids, and subsequently increasing conductivity. The link between phyllic alteration and resistivity is indicated in Figure 7.8, which plots abundance of typical phyllic and argillic alteration assemblage minerals against resistivity.

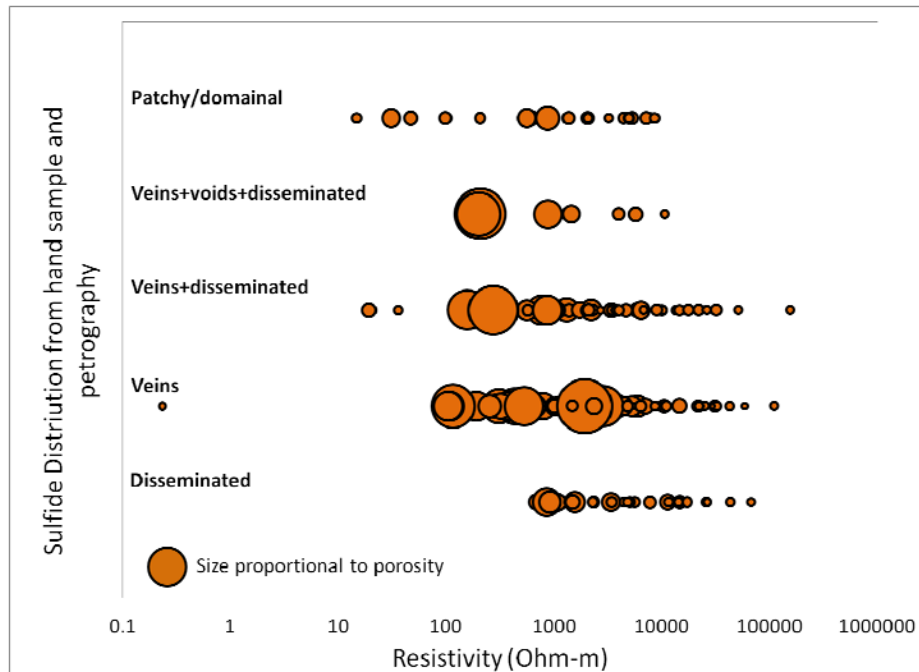


Figure 7.6. Plot showing ranges of resistivity associated with groups of samples subdivided based on the nature of sulphide distribution. Bubble size represents porosity. Higher porosity samples have lower resistivities.

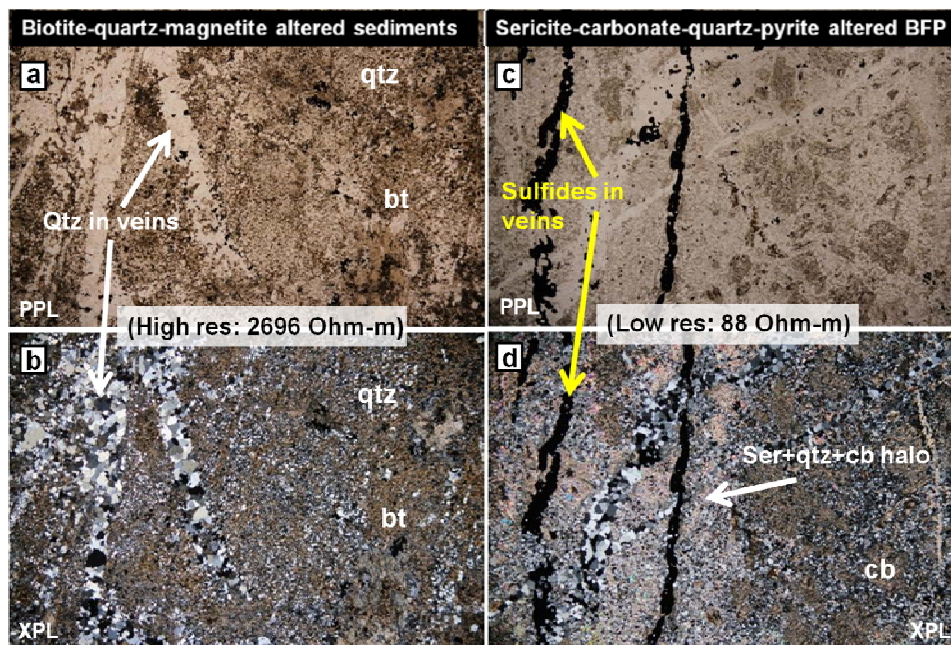


Figure 7.7. Comparison of mineralogy and texture of a high resistivity potassically-altered sedimentary sample with a low resistivity phyllic-altered biotite-feldspar porphyry sample. A combination of higher porosities and the presence of sulphide in veins decreases resistivities. Abbreviations: bt=biotite, cb=carbonate, qtz=quartz, ser=sericite, res=resistivity, PPL=plane-polarized light, XPL=cross-polarized light.

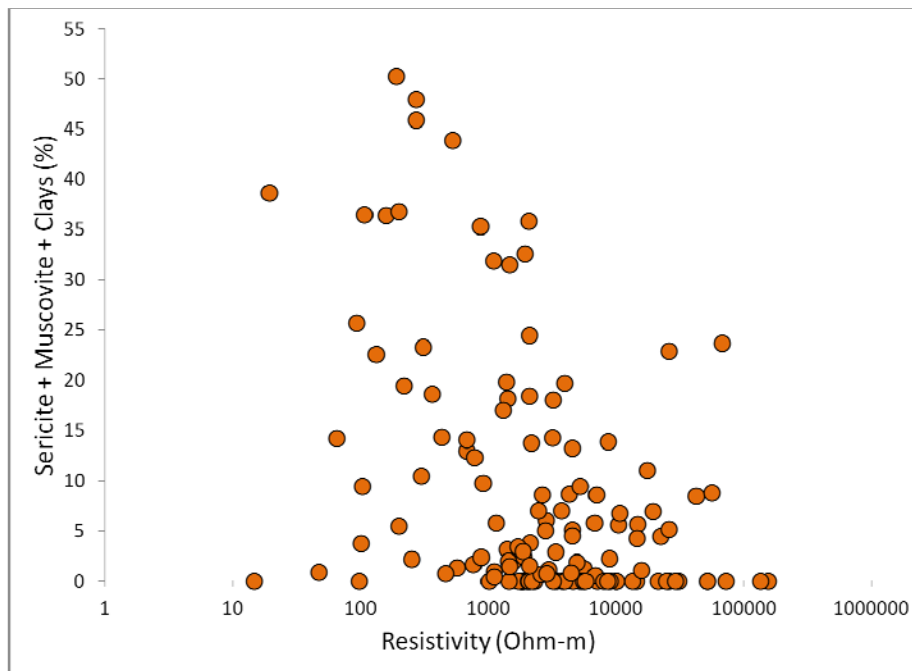


Figure 7.8. Sample resistivity versus abundance of alteration minerals determined by XRD Reitveld analysis. Feldspar and other minerals break down during alteration, increasing porosity and reducing resistivities.

7.3. Controls on Chargeability - Sulphide Abundance and Distribution

Chargeability was modelled from spectral impedance data (Enkin et al., 2012, see Section 2.1 of this report). Chargeability is typically linked to the presence of sulphide minerals which can cause a build-up of electrical charge within a rock (Telford et al., 1990).

A plot of chargeability versus sulphide abundance indicates there is a weak positive correlation between the two variables for the porphyry deposit sample suite (Figure 7.9). Chargeabilities over 1 ms may be related to increased pyrite and chalcopyrite abundances, however, numerous samples above 1 ms are recorded to contain little to no sulphides. The occurrence of metallic oxide minerals, such as magnetite and hematite can also potentially contribute to increases in chargeability. To examine its effect within the investigated porphyry deposit settings, magnetite and hematite abundance is added to sulphide abundance and the total is plotted against chargeability (Figure 7.10). The resulting trend between mineralogy and chargeability is better defined, and it is apparent that the > 1 ms samples that were not recorded to contain sulphide, contain oxide minerals which are likely contributing to increased chargeabilities.

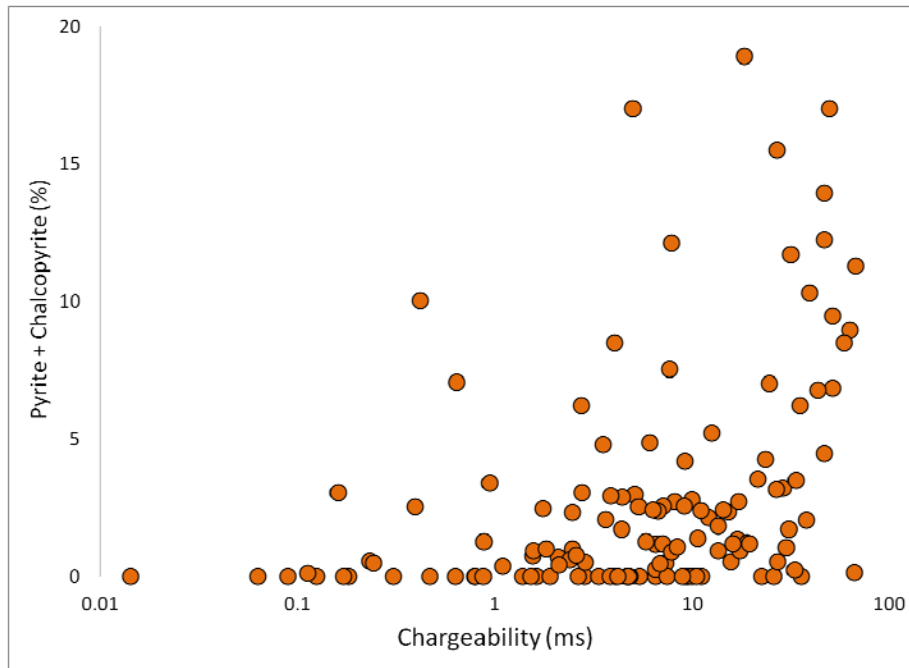


Figure 7.9. Chargeability versus sulphide abundance. A weak correlation between the two variables exists. For samples with very low chargeabilities (<1 ms), very few, or no sulphides are recorded. Sulphide abundances are determined by XRD Rietveld analysis.

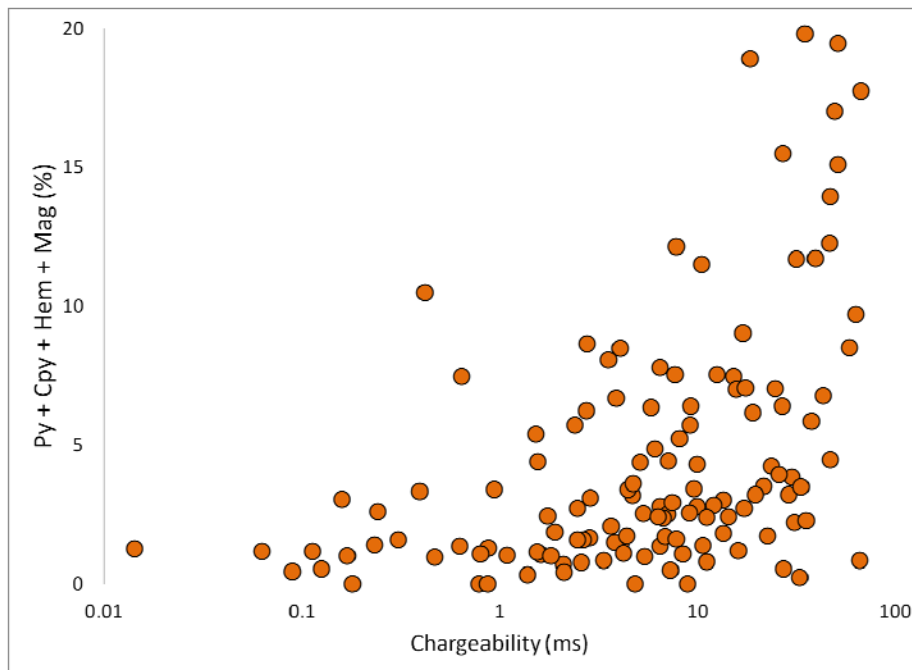


Figure 7.10. Chargeability versus sulphide + magnetite + hematite abundance. A more obvious trend is now apparent between mineralogy and chargeability. For chargeabilities greater than 10 ms, some amount of sulphides and/or oxides can be expected.

Chargeability is related to the surface area of conductive minerals in a rock. For a given concentration of sulphides, a rock hosting disseminated sulphides should in theory be more chargeable than a rock characterized by connected or massive sulphides. To investigate these relationships for the porphyry deposits studied, chargeability is plotted based on sulphide distribution (Figure 7.11). The expected association of higher chargeabilities with disseminated sulphides is not revealed in the plot. Instead the plot indicates a very general trend of increasing chargeability with increased number of distribution modes of sulphides, which perhaps reiterates the previously defined relationship between sulphide abundance and chargeability. The lack of correlation with sulphide distribution here makes sense in light of the previously indicated contribution of oxide minerals to the chargeability of the samples - oxides must be accounted for as well. Figure 7.12 shows reflected light images from sulphide and oxide bearing samples from the BC porphyry deposit sample suite, arranged in order from highest to lowest chargeability. The images in Figure 7.12 support the interpretation that magnetite content influences chargeability. A general decrease in chargeability with decreasing sulphide and oxide abundance is apparent.

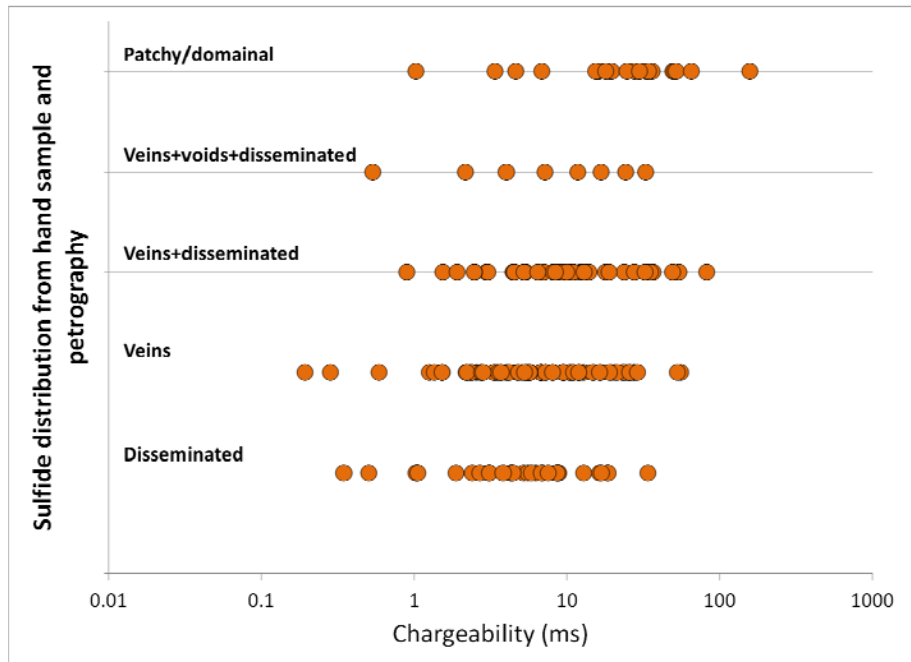


Figure 7.11. Plot showing ranges of chargeability associated with groups of samples subdivided based on the nature of sulphide distribution.

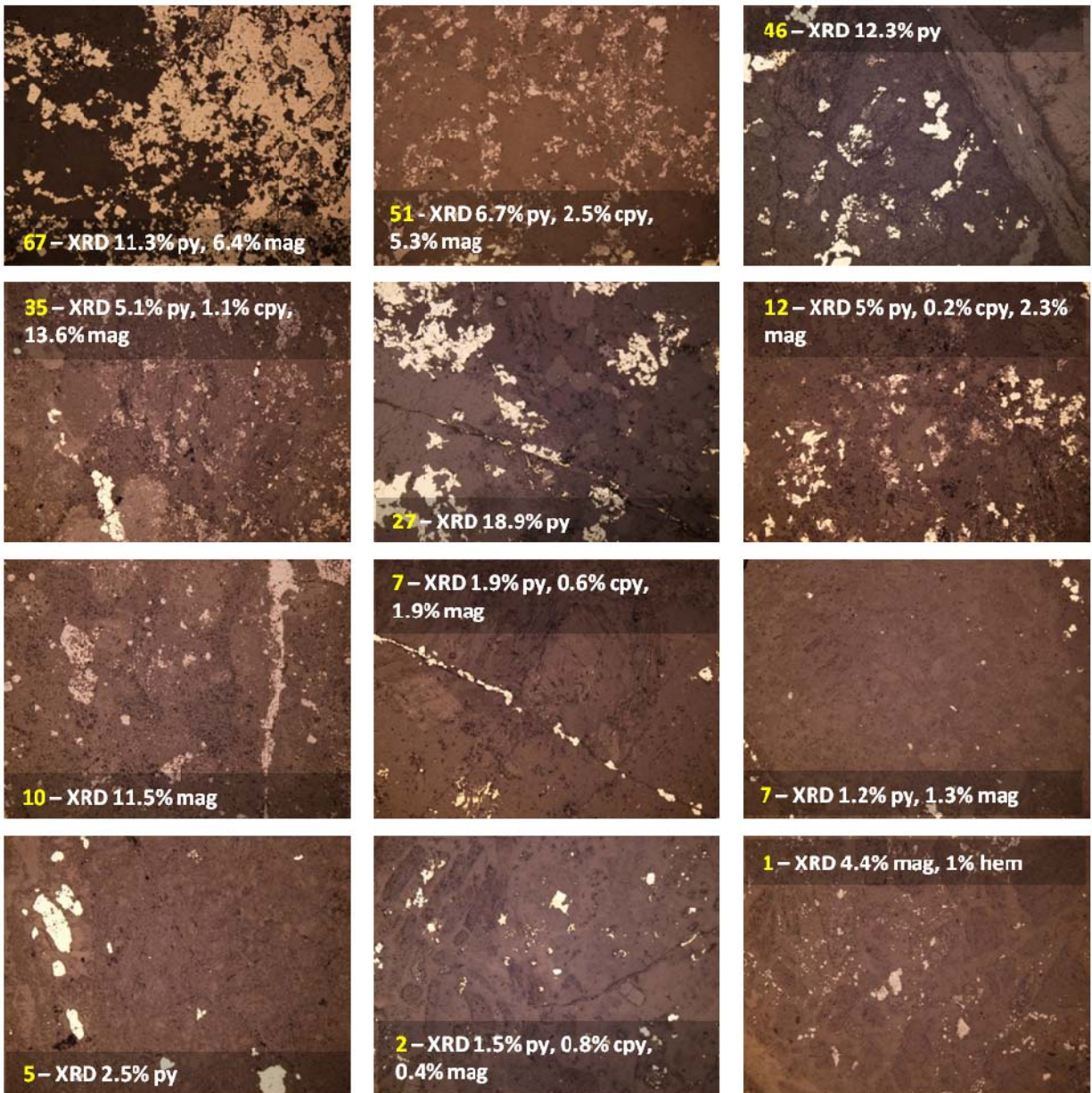


Figure 7.12. Reflected-light photomicrographs of Mount Milligan samples showing distribution of sulphide and oxide minerals and comparing chargeability measurements (in milliseconds, yellow text) with XRD-determined mineral abundances. Abbreviations: cpy=chalcopyrite, hem=hematite, mag=magnetite, py=pyrite.

As earlier stated, sulphide distribution was determined from visual analysis of the samples, and fine-grained sulphides may not have been accurately estimated or characterized. These relationships could be more rigorously investigated by performing image analyses on thin sections or polished sample slabs. A scanning electron microscope or even photo editing software, can be used to locate reflective minerals and may reveal more accurately the nature of sulphide distributions.

7.4. Summary of Resistivity and Chargeability Trends for BC Porphyry Case Study Sites

For the deposits investigated, sample resistivity appears to be most strongly correlated with rock porosity, and less so with sulphide abundance or distribution. Increases in porosity accompanying sericite and/or clay alteration leads to increased fluid content of the rock, which decreases resistivity (increases conductivity). Resistivity is weakly correlated to sulphide abundance and the nature of its distribution (figures 7.1 and 7.6), but the relatively low sulphide abundances typically associated with porphyry deposits could mean that mineralized zones may not cause a prominent conductivity anomaly. Exploration vectors to mineralization, such as faults, breccia zones, and clay-rich alteration however, may still be identifiable as conductors.

Chargeability was indicated to increase with increased sulphide and oxide abundance. Porphyry deposits are often characterized by a disseminated distribution of sulphides and are thus ideally suited to the application of induced polarization methods.

The electrical rock property relationships discussed are best observed at local, or deposit scales. Local variations in sulphide abundances, and in rock texture might not be recognizable within data collected from larger scale electromagnetic or induced polarization surveys but might be indicated in detailed high resolution ground surveys or borehole geophysics data.

7.5. References

- Enkin, R.J., Cowan, D., Tigner J., Severide, A., Gilmour, D., Tkachyk, A., Kilduff, M., Vidal, B., and Baker, J. (2012): Physical property measurements at the GSC Paleomagnetism and Petrophysics Laboratory, including electric impedance spectrum methodology and analysis; Geological Survey of Canada, Open File 7227, 42 p.
- Pelton, W.H., Ward, S.H., Hallof, P.G., Sill, W.R., and Nelson, P.H. (1978): Mineral discrimination and removal of inductive coupling with multifrequency IP; *Geophysics*, v.43, p. 588-609.

Telford, W.M., Geldart, L.P. and Sheriff, R.E. (1990): Applied Geophysics, Second Edition; Cambridge University Press, 770 p.

Appendix 8. Physical Property Data

(Available digitally as an .xls file)

Appendix 9. XRD Mineral Data

(Available digitally as an .xls file)

Appendix 10. Geochemistry

(Available digitally as an .xls file)